COMPARING OPTIMAL AND ACTUAL FOREST ROAD LOCATIONS USING

LEAST-COST ANALYSIS IN ARCGIS

By:

Matthew Guenther

An Undergraduate Thesis Submitted in Partial Fulfillment of the Requirements for the

Degree of Honours Bachelor of Science in Forestry

Faculty of Natural Resources Management

Lakehead University

April 2022

Mr. Ryan Wilkie, MScF   Mr. Alex Bilyk, RPF

Major Advisor   Second Reader

LIBRARY RIGHTS STATEMENT

In presenting this thesis in partial fulfillment of the requirements for the Honours Bachelors of Science in Forestry degree at Lakehead University in Thunder Bay, I agree that the University will make it freely available for inspection.

This thesis is made available by my authority solely for the purpose of private study and may not be copied or reproduced or in whole or in part (Except as permitted by the Copyright Laws) without my written authority.

Signature:

Date: April 20, 2022

A CAUTION TO THE READER

This Honours Bachelor of Science in Forestry thesis has been through a semi-formal process of review and comment by at least two faculty members. It is made available for loan by the Faculty of Natural Resources Management for the purpose of advancing the practice of professional and scientific forestry.

The reader should be aware that opinions and conclusions expressed in this document are those of the student and do not necessarily reflect the opinions of the thesis supervisor, the faculty, or of Lakehead University.

ABSTRACT

Guenther, M.R. 2022. Comparing optimal and actual forest road locations using least-cost analysis in QGIS. Honours Bachelor of Science in Forestry thesis, Faculty of Natural Resources Management, Lakehead University, Thunder Bay, Ontario. 86 + vii pp.

Keywords: Forest Roads, Least-Cost Path Analysis, ArcGIS, QGIS, ArcPy, Ontario.

For the Lakehead Forest licence, west of Thunder Bay, Ontario, a least-cost roads model was built in QGIS using provincial Digital Elevation Model (PDEM) data, and data provided by Greenmantle. A cost-surface was also generated from the PDEM using a script created in the ArcPy module of Python. The model identified the most cost-efficient routes for operational roads within a limited criterion, connecting terminal points in harvested stands to terminal points along primary access roads. The modelled roads were then compared to existing roads mirroring the modelled versions, to analyze whether differences were significant. The network of roads as a whole was significantly different at the 0.05-alpha level, while 41 of 42 individual road pairs were significantly different at the 0.05-alpha level.

iv

CONTENTS

List of Tables.

List of Figures.

ACKNOWLEDGMENTS

1

INTRODUCTION

Forest roads are an essential aspect of the anthropogenic use of forested areas,

primarily allowing for resource extraction activities, but also supporting various

recreational uses (Gucinski 2001). There are economic, ecological, and hydrological

factors and associated trade-offs that must be accounted for when planning a forest road

network (Laschi *et al.* 2016). It is imperative that these factors are correctly accounted in

planning roads networks, as the construction and maintenance of these roads is

recognized to be one of the most economically expensive and ecologically damaging

forest operations (Cahskan 2013). Best practices to minimize the environmental impacts

of roads activities include limiting the width of the roads; use of natural relief; avoidance

of ecologically sensitive areas; avoidance of sensitive slopes, among others (Aguiar *et

al*. 2021).

The Lakehead Forest is comprised of private forest, crown forest, urban areas,

and protected areas, surrounding the city of Thunder Bay, Ontario (Appendix 1). The

forest is approximately 767 square kilometers, with 355 square kilometers of that being

Crown land managed by Greenmantle (Greenmantle Forest Incorporated n.d.).

Using Provincial Digital Elevation Model (PDEM) data from the Government of

Ontario, forest road engineering cost formulas, and harvest scheduling data from

Greenmantle, a road network was generated in QGIS using the Dijkstra algorithm for

least cost path and compared to a real-world road network (QGIS.org 2021). The created

roads mirrored real-world operational or bock roads, with modelled roads constrained to

areas identified by Greenmantle as compatible with forest road construction. The least-

cost path algorithm incorporated sum of the earthworks excavation and fill, road

surfacing and grading, drainage ditch excavation, and culvert installation costs for associated with constructing an operation road within a given area, calculated based on formulas created by Ghajar *et al.* (2013). These road segments were then compared to the actual road segments used as the basis for the created road network.

To quantifiably compare the networks, matching segment locations for actual and modelled roads were randomly selected along all segments of the three road networks were in QGIS (QGIS.org 2021). The distance between the selected points on Greenmantle's road segments and matching the created road segments were measured horizontally, determining the sum of deviations as a proportion of the total road length.

It was expected that there would be no significant differences between the generated road network and the actual road network. If true, this would suggest that the methodology used is sufficient for modelling cost-effective roads in the Lakehead Forest. If the modelled roads were found to be significantly different from the actual roads, then this methodology would be found to not be applicable to real-world road planning.

LITERATURE REVIEW

History of Forest Product Transportation

Planning for cost-effective transportation of harvested wood fibre from a cut block to the mill or purchaser in the boreal forest has been an area of interest in Canada and the United States since the opening first commercial mills in the North American Boreal Forest. In the 19th century, this was often done by floating the logs down streams or rivers from an area near the harvest site to the mill (Brunson 1842; McManus 1919). This method limited the areas where timber could be harvested, while also necessitating the construction of a camp to house the employees while harvesting in a given area (McManus 1919). In 1915, the first known use of a truck in an active logging operation occurred in the state of Washington, with the use of trucks to haul wood becoming commonplace across the Pacific Northwest in the early 1920s (Knapp 1921; Prouty 1985). Although alternative methods continued to be used to transport wood, by 1942 it was recognized that vehicular hauling on roads was the most widely applicable method of transporting harvested volume from roadside landings to the destination (Jones 1942; Hutson 1953).

The majority of early forest roads were constructed as the need arose, with no planning performed beyond the shortest possible segment between the existing road network and the area to be harvested (Harrison 1955). Bryant (1913) stated that the transportation of the forest products from stump to the mill or market represent "75% or more of the total cost" of a given product. Other foresters agreed that more research and effort in planning forest roads was necessary, both from an economic and environmental

point of view (Norcross and Grefe 1931, Jones 1942, Irwin 1947). This led to the first methods of forest road network optimization in the 1930s (Norcross and Grefe 1931).

Optimization in Forest Road Planning

It was in the 1930s that forest planners began researching methods to optimize road networks in forests (Norcross and Grefe 1931; Jones 1942). Early researchers in forest road planning were generally focused on minimizing the costs of construction and transportation based on the length of the road network, with calculations done by hand using paper maps. This was done by drawing travel-time areas on maps based on calculations derived from a set speed of travel along the length of the roads in areas of interest (Norcross and Grefe 1931). Later research was concerned with determining the minimum possible length of roads in a network to access all timber resources in a given area, in order to minimize costs of road construction (Jones 1942). Other research focused on determining a slope gradient value that minimized both the road length and the cost of transportation per unit volume of wood hauled along that segment of road (Harrison 1955).

In the 1950s and the 1960s, the complexity of management objectives in forest road planning and the complexity of the models used to do the planning increased (Sonley 1957; Waelti 1970). The quantity of continuous variables involved in identifying optimal road locations meant many early computer programs were unable to generate an output without a significant amount of work by the user (Burke 1974; Weintraub and Navon 1976). The Timber Access Road program, and Weintraub and Navon's (1976) linear programming method, both sought to simplify the task of roads planning by converting the problem to identifying the least-costly path between two

nodes, where each node represented a known location within the forest (Burke 1974).

These programs were still limited in the scale at which solutions were returned, as well

only considering discrete inputs or outputs (Burke 1974; Weintraub and Navon 1976;

Waelti 1970).

Towards the end of the twentieth century, the increasing computational power of

the hardware available to planners allowed for the creation of increasingly complex

software for road planning (Kallo *et al.* 1986; Murray and Church 1997; Dean 1997;

Murray 1998). These programs used raster files in the form of a grid, where the variables

available to the planner were represented as the values for each cell in the grid,

connecting known start and finish cells through the path determined as least costly based

on the objectives used (Dean 1997; Murray 1998). A computer program capable of

identifying optimal placement of road segments to access multiple target nodes using

digital terrain data in GIS was developed by Dean (1997). This program could analyze

raster grids up to 121 cells by 121 cells (14,500 total cells) at a resolution of 30 meters in

order to determine to most cost-efficient route (Dean 1997; Murray 1998).

Least-Cost Path Analysis and Forest Roads

Least-cost path analysis is a method of quantitative analysis that can aid forest

planners in the optimization of their road networks (Kamarudin et al. 2014). Due to the

large number of variables and management objectives in roads planning, the application

of computational analysis facilitates a cost-effective road network that follows best

practices (Aguiar et al. 2021). This can be accomplished with the application of

Dijkstra's algorithm, an algorithm that determines the path with the lowest cost between

two points on a graph with known, non-negative cost values (Dijkstra 1959, Peterson

and Davie 2012). It is possible to apply this algorithm to a digital elevation model (DEM) raster shapefile in QGIS, determining the optimal road location with slope of the road as the objective variable (Engstrom and Tigerstrom 2017; QGIS.org 2021). As there are factors other than the slope of the terrain that are relevant when determining the most cost-efficient location for a road corridor, the construction of cost-raster for the area of interest is necessary (Engstrom and Tigerstrom 2017). A cost-raster is a spatial dataset, composed of a number of cells of a set size representing a real-world area, where the value stored in each cell is the cost of the activity of interest in the real-world location represented by that cell, such as the time it would take to travel through that cell if time was the cost of interest (Antikainen 2013). The cost-raster can then be 'solved' computationally in the same manner as Dean (1997), whereby the algorithm is given a source cell and an end cell within the cost-raster and then seeks to identify a path of connecting cells the two points of interest having the lowest cumulative travel cost (Antikainen 2013; Dean 1997, Engstrom and Tigerstrom 2017).

ArcGIS is a suite of GIS tools that have been used in many instances to both create and evaluate cost-rasters (Antikainen 2013; Durmaz et al. 2019; Etherington 2011; Yu *et al.* 2003). ArcGIS Pro supports the use of the Python and ArcPy programming languages, allowing for automation and customization of datasets within the software as well as the tools used in the software, allowing the user to automate or customize many of the tools to meet their needs (Etherington 2011; T. Sapic in lecture NRMT-3350, September 17, 2021). This allows for the direct creation of cost-rasters from DEM data, provided that the dollar-value of the costs is known and that some forest resource information is known (Antikainen 2013; Aguiar et al. 2021). QGIS is an

open-source software that supports many of the same functions as ArcGIS Pro, either directly or indirectly through plugins, and is also open source, allowing for the user to develop their own tools for analysis if needed (QGIS.org 2021). There is a Least-Cost Path plugin for QGIS that functions the same as the tool of the same name in ArcGIS Pro, with the added benefit of not requiring the start and end locations to be raster cells (ESRI n.d.(b); FlowMap Group@SESS-PKU 2020).

<u>Forest Planning Policy in Ontario</u>

In Ontario, areas of Crown Forest are divided into Forest Management Units (FMUs), which can be managed by a single forestry company, collectives of forest operators, or other arrangements under Sustainable Forest Licences (SFLs) (OMNR 2014a). The holder of the licence is known as the licensee, and they must meet the obligations that the Ministry of Natural Resources and Forestry sets for their FMU in the relevant landscape guide (OMNR 2014a; OMNR 2014b; OMNRF 2020a). One of these obligations is the creation of a Forest Management Plan (FMP), governed by the requirements set in the Forest Management Planning Manual (FMPM) (OMNRF 2020a). Each FMP covers a period of ten years (With some exceptions) and identifies which stands will be harvested over the next ten years, where the roads constructed to access these stands will be, a rough schedule of when these operations will occur, as well as detailing the when and where other silvicultural, operational, or tending activities will occur (OMNRF 2020a). Within an FMP, road construction operations are detailed in the Annual Work Schedule (AWS) (OMNRF 2020a). The AWS states the timing of road construction, as well as where the road will be constructed (OMNRF 2020a).

Planning the location of forest road corridors well in advance is necessary due to the adverse environmental impacts that have been correlated with forest roads, as well as the legal obligation of the licensee to consult local stakeholders and relevant Indigenous and Metis communities (Nasiri and Askari 2020; Berges et al. 2013; OMNRF 2020a). Adverse environmental effects that have been identified as being caused by the presence of forest roads include increased rates of erosion near water crossings, decreased floristic diversity, and compacting of the soil causing long-term de-vegetation of the roadbed (Nasiri and Askari 2020; Berges et al. 2013; Ramos-Scharron and LeFevor 2018).

In Ontario, the Ontario Ministry of Natural Resources and Forestry (OMNRF) has policies in place to reduce the risks of resource roads causing environmental harm (OMNR 2014a). Resource road construction and maintenance are classified as access operations and are subject to compliance inspections and reports (OMNR 2014a). Regulations applicable to locating routes for resource roads include, but are not limited to: ensuring that the road is adequately drained; traffic safety has been considered (E.g., sightlines, wide right-of-way); any water crossings must follow erosion protection and fish passage regulations; and ensuring all Areas of Concern (AOCs) or other restrictions are followed (OMNR 2014a). In addition to the negative environmental impacts caused by roads, failure to comply with operational restrictions can result in financial, professional, or legal penalties (OMNR 2014a). By ensuring resource road location and construction is in compliance with the applicable restrictions, environmental damage to the forest can be minimized (Nasiri and Askari 2020; OMNR 2014a). If a road is to be constructed through an AOC or other important ecological feature, the AWS must detail how the road design and construction activities will be modified to preserve the features

on site (OMNRF 2020a; OMNR 2010). Roads requiring water crossings require the completion of water crossing documentation in the AWS, as well as an MNRF review and approval of the crossing if all water crossing standards cannot be met in their entirety (OMNRF 2020a).

By performing a least-cost path analysis to connect existing access roads to the stands scheduled for harvest, the forest planner can determine where the road corridor will be located and begin any field planning, water crossing inspection processes, or AOCs deemed necessary. This study will attempt to replicate the real-world restrictions on the placement of road corridors in order to create a scenario with parameters as close as possible to those used to create the actual roads.

Software alternatives to Least Cost Path for Road Planning

There are several software alternatives to Least-Cost Path that have been found to be viable for cost-efficient resource road planning (Kurulak 2019; Durmaz *et al.* 2019; Abdi *et al.* 2009). One alternative is "PEGGER", a program operating within the ArcView GIS software (Rogers and Schiess 2001; Talebi *et al.* 2022). This program works to connect two or more terminal points with multiple routes, with cost values determined by slope and elevation data alone (Abdi *et al.* 2009; Talebi *et al.* 2022). The user then must calculate the other costs associated with forest road construction themselves, and then select the PEGGER route determined to be 'better' than the other routes themselves (Abdi *et al.* 2009). The use of PEGGER for forest road planning has been determined to be best-suited for preliminary identification of road corridors to be validated in the field (Talebi *et al.* 2022; Abdi *et al.* 2009).

An additional software is 'RoadEng'; a program designed primarily for resource road planning (Lepoglavec *et al.* 2011). RoadEng is capable of incorporating many different cost factors, including but not limited to, soil types and depth, hauling and loading costs and parameters, maximum slopes, and minimum curve radii values (Kurulak 2019). This program has been found to be near-equivalent or even surpass the cost-efficiency and distance of roads planned in the field (Kurulak 2019; Lepoglavec *et al.* 2011; Nasiri and Askari 2020). However, by default RoadEng does not automate cost optimization of routes (Softree 2021). An additional software package, "Softree Optimal" must be purchased in order for optimal routes between two points to be identified (Softree 2021).

While RoadEng has been found to obtain results that are feasible to implement, it is worthwhile to explore the viability of using less specialized, less costly software to implement road planning optimization. As a result, a combination of QGIS and ArcGIS Pro were selected as the software to be used (QGIS.org 2021, ESRI 2022).

The Lakehead Forest

The Lakehead Forest Management Unit is located in northwestern Ontario, in the immediate vicinity of Thunder Bay (Greenmantle Forest Incorporated n.d.). Below, Figure 1 displays an overview map of the Lakehead Forest, as well as the location of the forest within Ontario (Greenmantle Forest Incorporated n.d.). As Digital Elevation Model (DEM) data was only available for areas of the Lakehead Forest located to the west and south of Thunder Bay, no areas in the eastern area of the forest were considered. Appendix II shows the specific boundaries of the area that was considered.
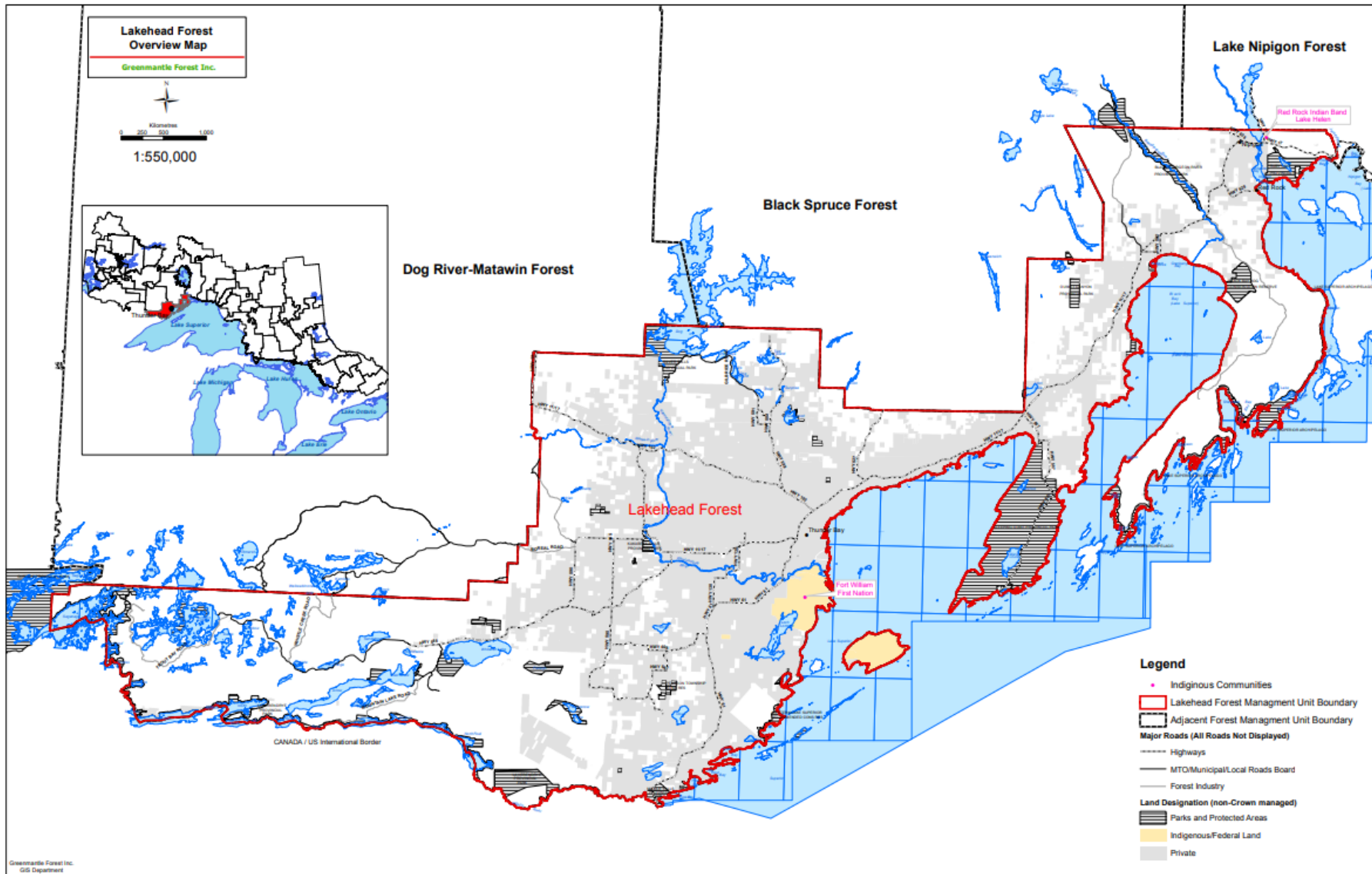
Figure 1. Overview of the Lakehead Forest (Greenmantle Forest Incorporated n.d.).

METHODS AND MATERIALS

<u>Materials</u>

To determine whether the examined road networks were optimal, computational least-cost path analysis was performed to generate a roads network considered to be the optimal roads network (Kamarudin *et al*. 2014; Engstrom and Tigerstrom 2017). The shapefiles used in order to generate this optimal road network are as follows:

1. Ontario Provincial Digital Elevation Model (OMNRF 2019a). This raster dataset represents the true-ground elevation for Ontario with a 30-meter resolution, projected in NDA83/Ontario MNR Lambert (EPSG:3161) (OMNRF 2019a).

2. Ontario Ministry of Natural Resources and Forestry Road Segments (OMNRF 2021). This shapefile is a vector dataset, containing all road segments in Ontario under the jurisdiction of the OMNRF at the time of publication as line segments (OMNRF 2021). The dataset was created in NAD83 with a horizontal accuracy of +/- 10 meters, containing the name of the road (if applicable), a unique numeric identifier of the road segment, the name of the organization responsible for the road, and the class of forest management roads (Primary, Branch, or Operational, if applicable) among other information (OMNRF 2021).

3. Ontario Road Network Segment with Address (OMNRF 2018). This vector dataset contains all roads known to the Ministry of Transportation in Ontario as line segments with associated addresses, road names, the organization responsible for the road, and the class of the road (Highway, Arterial, Municipal, etc.) (OMNRF 2018). This shapefile was created in the NAD83 datum with no set projection (OMNRF 2018).

4. Ontario Hydro Network- Waterbody (OMNRF 2019b). This vector dataset contains polygons representing all natural or man-made bodies of standing or flowing water in Ontario with a horizontal accuracy of +/- 10-meter horizontal accuracy, and a scale of 1:20,000 in the NAD83 datum with no specified projection (OMNRF 2019b).

5. Forest Resources Inventory Packaged Products – Version 2 (OMNRF 2020b). This vector dataset contains the boundaries of all Forest Management Units (FMUs) in Ontario as Polygons, with the name of the FMU, the organization responsible for management of the FMU, and the start and end year of the current management plan for the FMU included (OMNRF 2020b). The file metadata does not mention any datum, projection, or accuracy measurements (OMNRF 2020b).

6. Greenmantle Forest Incorporated: Scheduled harvest block boundaries. Vector dataset containing Polygons marking the boundaries of stands, with the area of the stand and the year harvested indicated (Pers. Comm., P. Brown R.P.F., November 22, 2021).

7. Greenmantle Forest Incorporated: Road segments by year of construction and seasonality. Vector data set containing roads owned by Greenmantle as line features, with the length of the road and the year constructed included (Pers. Comm., P. Brown R.P.F., November 22, 2021).

8. Greenmantle Forest Incorporated: Area of Concern, Birds. Vector dataset containing Areas of Concern related to bird habitat features as Polygons. Included in the attribute table was a column indicating operational restrictions or considerations for

road construction within the Polygon (Pers. Comm., P. Brown R.P.F., November 22, 2021).

9. Greenmantle Forest Incorporated: Area of Concern, Values. Vector dataset containing Areas of Concern related to unspecified landscape features as Polygons. Details on the specifics of the Area of Concern were not included for privacy reasons. Included in the attribute table was a column indicating operational restrictions or considerations for road construction within the Polygon (Pers. Comm., P. Brown R.P.F., November 22, 2021).

10. Greenmantle Forest Incorporated: Area of Concern, Other. Additional vector dataset containing Areas of Concern related to unspecified landscape features as Polygons, with same features as previous (Pers. Comm., P. Brown R.P.F., November 22, 2021).

11. Greenmantle Forest Incorporated: Land Ownership. Vector dataset showing the boundaries of private property within the SFL as Polygons (Pers. Comm., P. Brown R.P.F., November 22, 2021).

12. Greenmantle Forest Incorporated: Reserved Forest. Vector data set showing areas of forest reserved for habitat planning and compliance with patch retention as polygons (Pers. Comm., P. Brown R.P.F., November 22, 2021).

Methods

All the above shapefiles were downloaded from their respective owners and added to a project in QGIS under their original projections (QGIS.org 2021). All shapefiles were then re-projected into NAD83 / UTM zone 16N, which is a subset of the NAD83

projection for the longitudes around Thunder Bay (EPSG:26916) (EPSG n.d.). Once all

of the shapefiles had been re-projected, the 'Selected by query' tool in QGIS was used

on the "Forest Resources Inventory Packaged Products – Version 2" dataset to create a

new dataset containing only the boundary for the Lakehead FMU (OMNRF 2020b;

QGIS.org 2021). The Vector Geometry tool 'Singlepart to Multipart' was then used on

the Lakehead SFL boundary to create a new Polygon, demarcating the boundaries of the

study area, which can be viewed as a map in Appendix II. Once the polygon

representing the boundaries of the study area was created, the Vector Geoprocessing

'Clip' tool was applied to all of the vector shapefiles listed above, with the exception of

the FRI dataset, using each respective vector layer as the 'Input' for the tool and the

study area boundary polygon as the 'Overlay' layer. Additionally, the 'Clip Raster by

Mask Layer' tool was applied to the PDEM layer, with the study area boundary polygon

utilized as the 'Mask' layer. This resulted in a map of the study area containing the

layers listed above, with no data existing outside of the study area.

The area selected as the study area was identified by Phil Brown (Per. Comm., in

phone call Nov. 2021), one of the foresters working for Greenmantle in the Lakehead

Forest, as an area to focus on. By selecting this area, the spatial extent of the dataset was

reduced in order to minimize the complexity of the created cost surfaces, and increase

the efficiency of cost surface and optimize route creations. The focused study area was

selected, as it was identified as an area where there is a high density of roads constructed

in the time frame of interest. Below, Figure 2 shows the study area in red, within the

outline of the Lakehead Forest Unit.

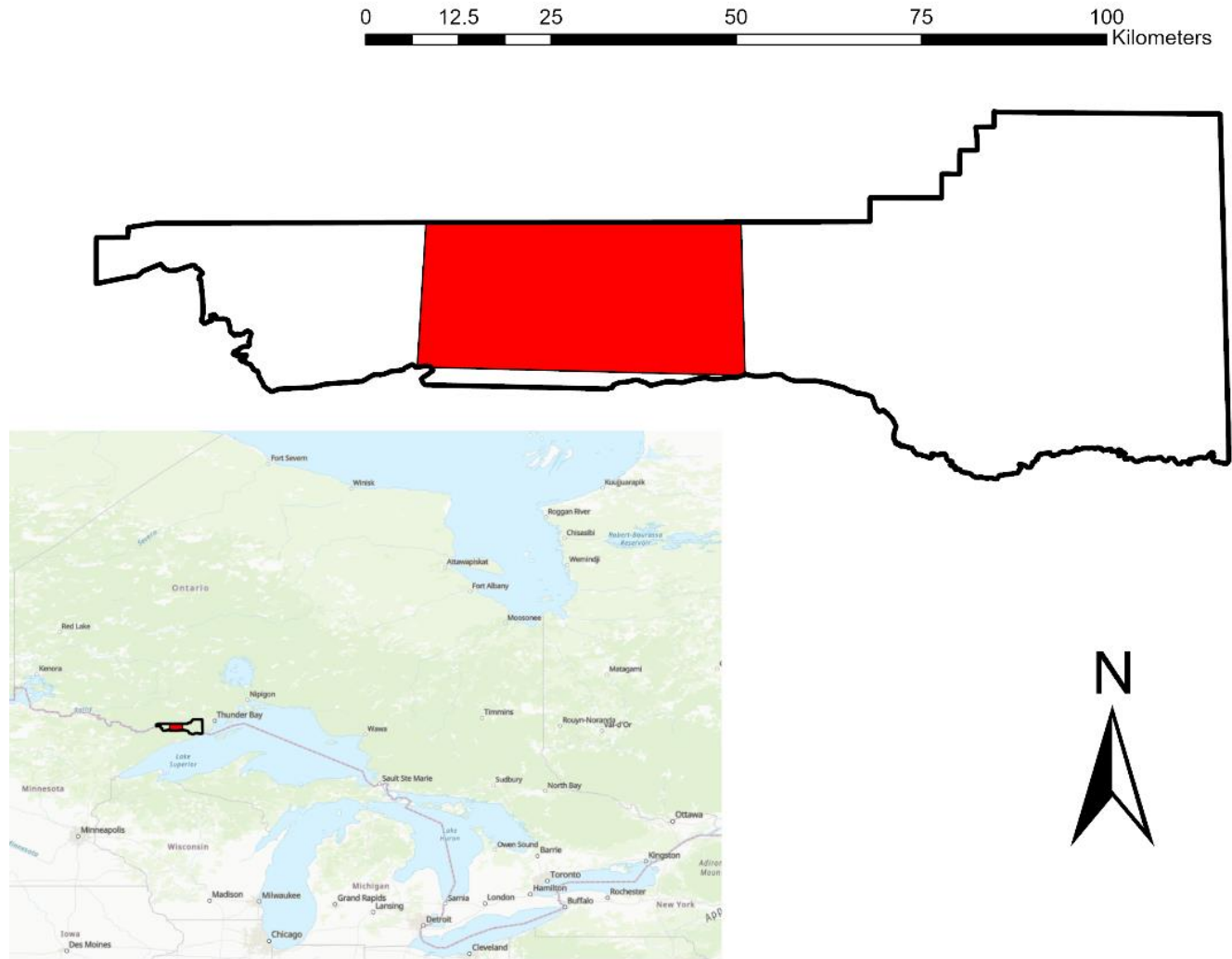# Location of Focused area within the study area

Figure 2. Location of the focused study area within the study area and within Ontario

The next step was to manipulate the data included in each of the above layers to facilitate interpretation of the map. This was done as follows:

1. Ontario Provincial Digital Elevation Model (OMNRF 2019a). Render type was changed from Singleband Gray to Hillside, using multiplicative blending and cubic resampling to display the DEM such that it appears to have three dimensions. A copy of the layer was made and converted into a raster file showing the average slope (%) for each cell in the raster file using ArcGIS Pro (ESRI 2021).

2. Ontario Ministry of Natural Resources and Forestry Road Segments (OMNRF 2021). Using an attribute table query, all road segments under the responsibility of Greenmantle were made into a separate layer ('RESPONSI_1' = 'GFI'). The remaining roads not the responsibility of the OMNRF were removed from the table ('ROAD_AUTHO' =! 'MNRF'). The remaining segments represented the OMNRF managed roads for the SFL and are rendered on the map as black line segments. The Greenmantle roads layer was rendered using conditional formatting, separating the roads visually into Primary, Operational, or Branch roads (FMP_ROAD_C = P; FMP_ROAD_C = B; FMP_ROAD_C = O).

3. Ontario Road Network Segment with Address (OMNRF 2018). No further manipulations were done to this layer.

4. Ontario Hydro Network- Waterbody (OMNRF 2019b). A query was applied to the attribute table to classify the dataset based on the type of waterbody represented by each polygon ('NAME' LIKE 'LAKE' to identify all lakes; 'NAME' LIKE 'RIVER' OR 'NAME' LIKE 'CREEK' to identify all rivers or streams). The

remaining waterbodies not belonging to either of the above groups were rendered as Miscellaneous Hydro Features.

5. Lakehead SFL Boundary, derived from Forest Resources Inventory Packaged Products – Version 2 (OMNRF 2020b). The rendering of this layer was changed from 'Fill' to a 'Simple Line' boundary, such that the outline of the polygon is the only feature visible.

6. Greenmantle Forest Incorporated: Scheduled harvest block boundaries. A query was run on the attribute table to separate the forest stands by year of harvest ('YRDEP' = 2016 OR 'YRDEP' > 2016). The results of this query were 'cut' from the base shapefile and added to a new shapefile indicating only stands harvested post-2016. This year was used here and with several other datasets as the PDEM was dated to 2016, in order to ensure interoperability of datasets.

7. Greenmantle Forest Incorporated: Road segments by year of construction and seasonality. A query was run on the attribute table to separate the roads by year of construction ('YEAR_CONST' = 2016 OR 'YEAR_CONST' > 2016). The results of this query were 'cut' from the base shapefile and added to a new shapefile indicating only roads constructed post-2016. These will be the roads that the generated road network will be compared against.

8. Remaining datasets: For the three AOC datasets, a query was run on the attribute table selecting all Polygons with road construction restrictions of '6- No Roads', '5- Extremely Restrictive'. '4- Justification Required', '3 – Timing Restrictions'. The resulting polygons were cut from their original layer and added to

a new layer representing areas where roads cannot feasibly be located. The datasets containing Ontario Hydrological features, private properties, and forest reserves were also added to this layer.

Below, Figure 3 shows the map project as it existed following the above manipulations. Lakes are shown as light-blue polygons with fill, rivers are shown as dark blue polygons with fill, and miscellaneous water features are shown as light green polygons with fill. Miscellaneous areas with road restrictions are shown in purple, and forest reserve areas are shown in green. Also shown is the PDEM as the base layer, with Greenmantle stands harvested post-2016 shown in as orange polygons.
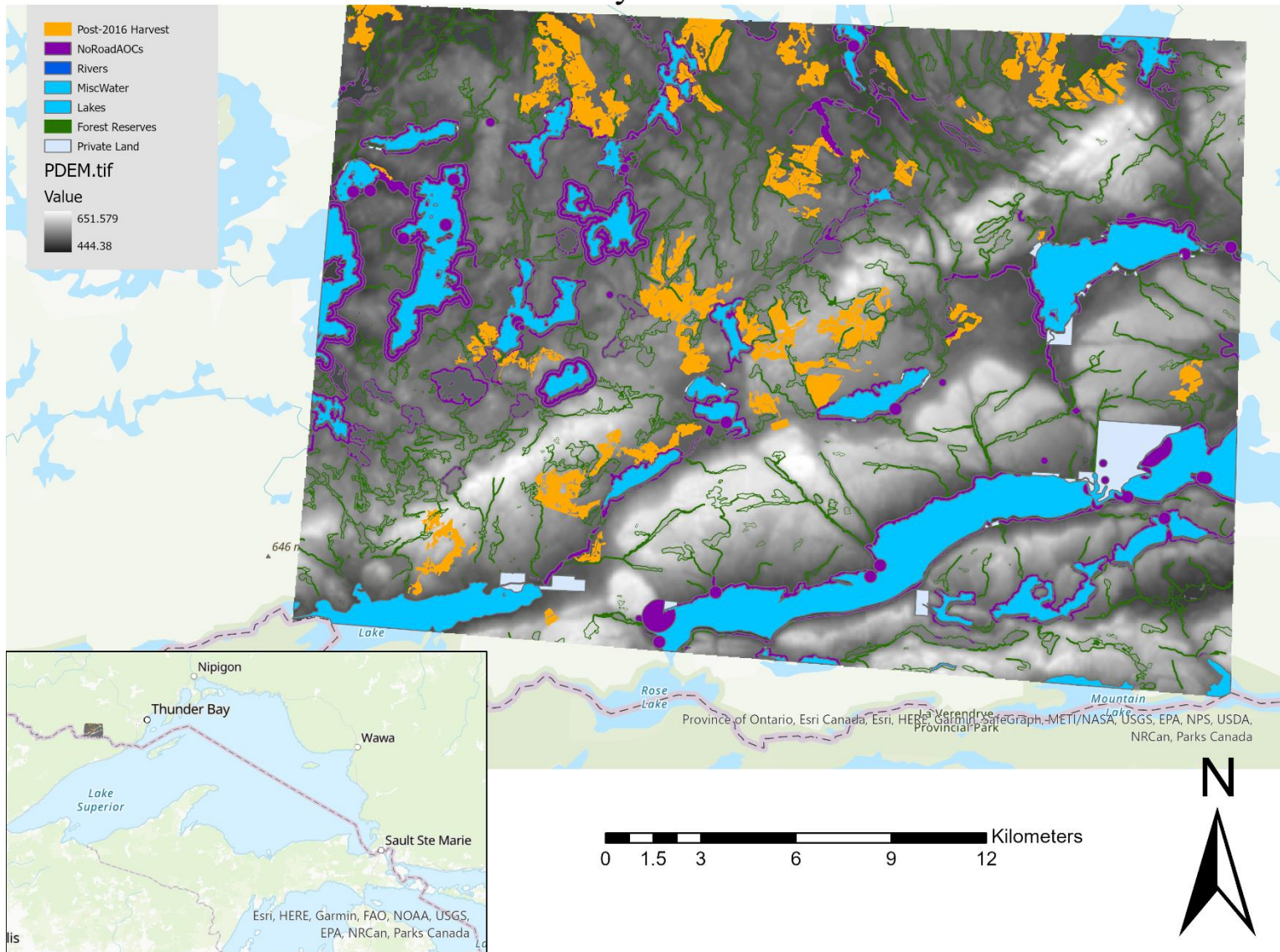
Figure 3. Map of Study Area showing Greenmantle Roads, public roads, waterbodies, and elevation.

Selection of Candidate Roads for Comparison

        Several operations were performed in QGIS to identify candidate roads for comparison (QGIS.org 2021). For all road line features within the study area found in the datasets used, there were a total of 8,009-line features. All roads owned by either the Ministry of Transportation of Ontario (MTO), Local Roads Boards (LRB), and other municipal roads were then removed, removing 3,471-line features. A query was then applied to the attribute table of the shapefile containing the remaining roads, removing roads where 'OWNER' IS NOT 'Greenmantle', removing 1,959-line features. These roads were then clipped to the boundaries of the focused study area (Figure 4, above), which removed 1,993-line features. An additional query was applied to the attribute table, removing all roads where 'AR_YEAR' (Shapefile field storing the year of construction) IS <= 2015 OR 'AR_YEAR' IS 'null'. This query removed all roads constructed prior to 2016, reducing the number of candidate roads to 84 and removing 502-line features. The 'Simplify Line Geometry' tool in QGIS was then used to amalgamate all line features connecting a given cut block to a primary road, provided the line features were connected to one other already (QGIS.org 2021). This removed 35-line features. The final step was to remove all roads with a length of 150 meters or less, in order to ensure sufficient opportunity for differentiation to make comparison meaningful. This left 42 candidate roads. This process is summarized in Table 1, below.

Table 1. Summary of Candidate Road Selection.

Total Number of Road Line Features in FMU:		8,009
Operation Performed	Roads Removed	Candidate Roads Remaining
Removed Roads owned by MTO or MOU	3,471	4,538
Road Owner is Greenmantle	1,959	2,579
Clipped Roads to Study Area	1,993	586
Road constructed pre-2016	502	84
Simplified Line Geometry	35	49
Road Length is at least 150m	7	42

Creation of Cost Rasters

In order to apply Least-Cost Path Analysis to this dataset and identify the optimal

path for road construction, a cost surface must be created (ESRI n.d.(b)). A cost surface

is a continuous raster dataset, where the value of each cell in the raster represents the

unit cost of travelling through that cell (ESRI n.d.(b)). As cost surfaces are specific to

one cost factor (I.e., time or currency) for a specific site, it was necessary to create one

for the focused study area (Figure 3). This was done using within an ArcGIS Pro

geodatabase, using ArcPy code to apply formulas derived from those put forward by

Ghajar et al. (2013) for determining forest road construction (ESRI 2021). These

formulae were based on a cross-section of a typical forest road seen in Figure 4, below,
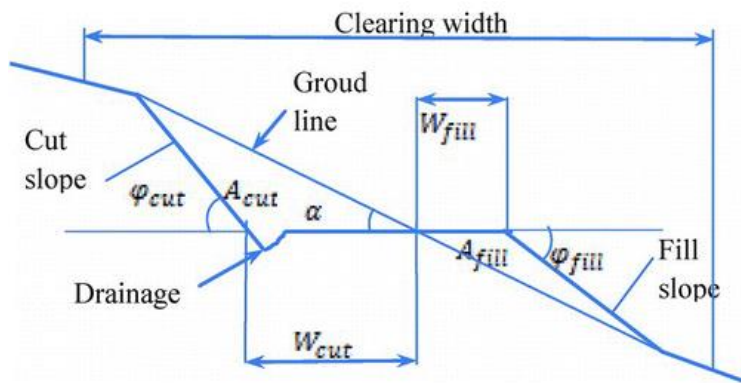
found in Ghajar et al. (2013).

Figure 4. Cross-section of a forest road with variables used in formulae indicated.

Ghajar *et al.* (2013) identified the main costs associated with forest road construction as the cost of excavating or filling earthworks to create a level roadbed; the cost of surfacing the road with aggregate to prevent rutting of the road surface; and the cost of grading the road surface to evenly distribute aggregate across the roadbed. Additionally, as resource roads in Ontario must be adequately drained, a drainage costing model was created (OMNR 2014a).

The cost values were calculated by the following formulae:

Earthworks Cost:

$$A_{cut} = \frac{Width^2 * \tan(\partial cut) * \tan \alpha}{2(\tan(\alpha fill) - \tan(\alpha))}$$

$$Cost_{Earth} = \left(\frac{A_{cut} + \sqrt{A_{cut} * (A_{cut} + 1)} + (A_{cut} + 1)}{3} * \frac{1}{2} \right) * c_{excavate}$$

$$Cost_{Earth} = \left(\frac{A_{cut} + \sqrt{A_{cut} * (A_{cut} + 1)} + (A_{cut} + 1)}{3} * \frac{1}{2} \right) * c_{fill}$$

Surfacing Cost:

$$Cost_{Surfacing} = Width_{Road} * 30m * c_{surf}$$

Grading Cost:

$$Cost_{Grading} = \left(c_{grade} * \left(Width_{Road} + \frac{(W_{cut} + (W_{cut} + 1))}{2} * 30m \right) \right)$$

Drainage Cost:

$$Cost_{Drainage} = \frac{C_{Culvert}}{d} * 30m + (V_{Flow} * c_{excavate})$$

The values represented by $C_{excavate}$ and C_{fill} are the costs, in dollars, to excavate or fill one cubic metre of earth, respectively. As there is no way of knowing which part of the slope a given road through a given cell would cross, it was assumed that there were equal volumes of earth to excavate or fill on either side of the road. The cost of excavating one cubic meter (1 m^3) of earth used was $12.00 /m^3 (Kurulak 2019). The cost of filling one cubic meter (1 m^3) of earth used was $22.50 /m^3 (N. Pawluk in Pers. Comm., Jan. 25 2022).

In regards to the surfacing cost formula, the value of 30 meters is derived from the fact that each cell is 30 meters by 30 meters. This means that areas where the road is not perfectly straight may be sources of differentiation when analyzing the results. The value represented by c_{surf} is the cost to surface one square meter of road bed. The value used for this was $3.70 /m^2, including the cost of machinery, operators' wages, and hauling road aggregate to the site (N. Pawluk in Pers. Comm., Jan. 25 2022).

The value represented by c_{grade} is the cost to grade one square meter of road. The value used for this was $3.70 /m2, including the cost of machinery and operators' wages, (N. Pawluk in Pers. Comm., Jan. 25 2022).

The values for the Cost of Drainage formula were more complex than the other formulas, as this formula required the flow rate (In cubic meters) for each cell to be known, as well as the cost of installing one culvert capable of handling the flow rate. The culvert cost and flow rate capabilities used are seen in Table 2 (Kurulak 2019).

Table 2. Culvert Size, Discharge Rates, and Installation Costs.

Culvert Diameter (mm)	Maximum Discharge Rate (m^3/s)	Average Installation Cost
300	0.040	850.00
400	0.086	1,000.00
450	0.118	1,075.00
500	0.156	1,150.00
600	0.254	1,500.00
700	0.383	1,725.00
800	0.548	2,000.00
900	0.750	3,000.00
1,000	0.993	4,000.00
1,200	1.614	6,000.00
1,400	2.435	8,000.00
1,600	3.477	10,000.00
1,800	4.760	12,000.00
2,000	6.304	14,000.00
2,200	8.128	18,000.00
2,400	10.250	22,000.00
2,600	12.689	26,000.00
2,800	15.462	30,000.00
3,000	18.585	34,000.00

The flow rate for each cell in the Digital Elevation Model was calculated using the Flow Accumulation Tool in ArcGIS Pro, which is a tool that determines the maximum flow rate in cubic meters for a given cell based on the input elevation model (ESRI n.d.(b)). An ArcPy function was then applied to the Flow Accumulation Raster, providing the cost of installing drainage for a road segment in each cell of the raster.

Once the above values had been calculated for the area of interest, the cost raster was created, by calculating the sum of all of the above costs associated with road construction for each cell in the focused study area. To maximize the number of potential routes for the Least-Cost-Path function to consider, the cost surface was re-

sampled to a resolution of 15m, done by dividing each existing cell into four new cells with the same values and overall extent as the parent cell. The raster calculator function was then used to divide the value of all cells in the cost surface by four, to keep the cell costs relative to their extents.

In an attempt to replicate a real-world scenario, the Cost Surface was then 'Clipped' by 'Mask Extent', with all cells that were overlapped entirely or partially by vector features from the layer containing all areas with road restrictions. This resulted in a new dataset showing only the cells where a road could not be built, with the cost surface values still stored in each cell. The raster calculator was then used to set every cell in this dataset to have a value of 0 (Zero), creating a rasterized dataset containing only cells with road restrictions. The raster representing cells with road restrictions was then mosaicked onto the interpolated Cost Surface, with the parameters set so that a cell's value would be taken from the road restrictions dataset if that cell existed in the restriction's dataset, otherwise the value would remain unchanged. In the resultant mosaiced raster, the 'NoData' value was set to be 0, as all cells with that value were identified as having road restrictions, and were considered to be empty. Figure 5, below, shows the finalized Cost Surface within the focused study area, only displaying cells where roads can be located.
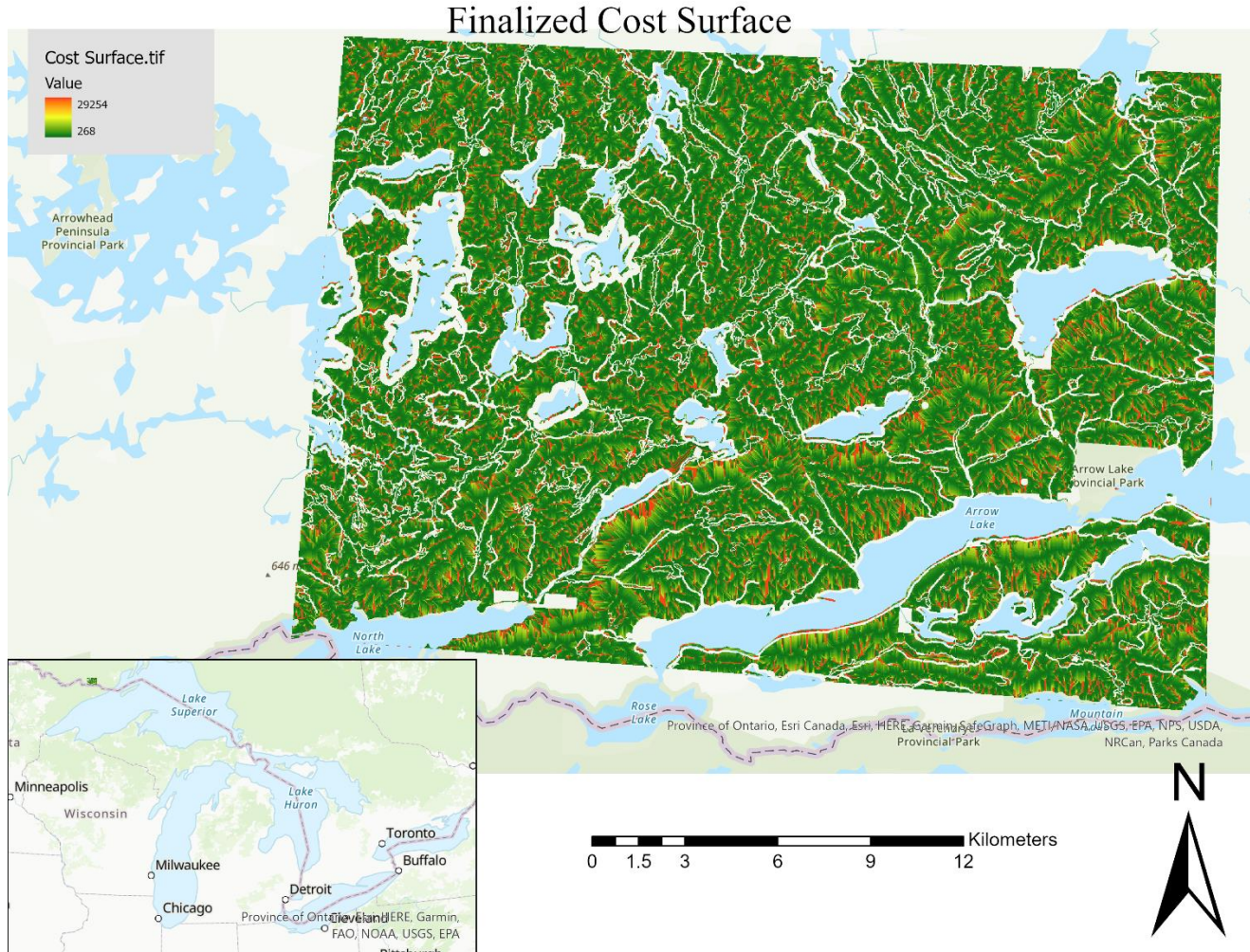
Finalized Cost Surface

Figure 5. Finalized Cost Surface.

<u>Creation of Optimize Roads</u>

For the 42 candidate roads identified, each road was assigned a name, consisting
of one or two letters, beginning with 'Road A', all the way through 'Road AP'. For these
roads, the 'Extract Vertices' tool was used to extract all vertices along the roads
(QGIS.org 2021). All vertices not at a terminal end of a road were manually deleted. The
terminal point on each road within the harvest cutblock was exported to its own
shapefile, named 'RoadName_End', and the other terminal point was exported to a
different shapefile, name 'RoadName_Start'. Initially the ArcGIS Pro 'Least-Cost Path'
tool was used; however, the output from this tool was not delivered in a manner suitable

for further analysis (ESRI 2021). Instead, the 'Least-Cost Path' plugin for QGIS was then used to generate optimal roads between that start and end point shapefiles for a given road (FlowMap Group@SESS-PKU 2020). The resulting line features were saved as separate shapefiles, each titled 'RoadName_Optimized'.

Comparison of Original and Optimized Road Locations

Quantifying the differences in road locations between the original and optimized road pairs, random point sampling was done. In QGIS, the 'Random Points on Lines' tool was utilized to create the maximum possible number of point features for each of the original and optimized roads, with these points at least 60 meters from other point features along the same line. The linear (ellipsoidal) distance between a given point along the optimized route and the analogous point on original point was measured and recorded to the hundredth decimal place (0.xx), with the road name, sample point number, and distance between the points recorded in Microsoft Excel.

As a Null Hypothesis was put forward, stating that no significant differences between the real and modelled roads would be found, any differences between the road datasets must be tested for significance. The most commonly accepted way of testing for significance is a Chi-Square test, where the actual and expected, results are compared using a Chi-Square distribution (Morey and Wagenmakers 2014). A Chi-Square test requires the actual and expected results, the degrees of freedom (Number of results – 1), and an alpha, or significance, level (Morey and Wagenmakers 2014). The significance level represents the probability that a correct null hypothesis would be falsely rejected (Morey and Wagenmakers 2014). The value used for the actual results were the measurements between the real and optimized road locations, as described above.

The Chi-Square test were done with an expected value of 37.50 meters, based

on:

1) All points were randomly sampled within 60-meter segments of road. If two

   routes were exactly identical, these points could still be 60 meters apart.

   Therefore, the median value (30m) of the possible sampling differentiation

   was used.

2) While the Least-Cost-Path route must pass through the centre of any cell

   used for the route, the original line features had no such limitations. If two

   routes passed through the exact same cells for the entire route, the points

   could be up to 7.5 meters apart, which is the distance from the centre of a

   given cell to an adjacent cell.

A Chi-Square test will compare the Sum of Squares for the dataset to the critical

value for the Chi-Square distribution (Morey and Wagenmakers 2014). The Sum of

Squares is calculated by:

$$Sum\ of\ Squares = \sum_{i=1}^{n}(x_i - \bar{x})^2 \text{ (Khan Academy n.d.)}.$$

For each data point, the expected distance (37.50) was subtracted from the

observed distance between the points (O − E). The result of the subtraction was then

squared ([O-E]2), and then divided by the expected value ([O-E]2/E). The Sum of

Squares is the sum of this value for all points in the dataset.

The critical value represents the value that a Sum of Squares can equal or be less

than for a given degrees of freedom and alpha value and represent insignificant results

(Morey and Wagenmakers 2014). A Sum of Squares below the critical value means

there is a 95% probability that the values are not significantly different than expected, while a Sum of Squares greater than this value means there is a 95% probability that these values are significantly different than expected.

RESULTS

Modelled Road Pair Results

After culling non-testable roads, a total of 42 optimal routes were created. Overview maps presenting each mirrored road pair can be found in Appendix IV.

For the generated optimized roads, the average length was 1,435.91 meters, with the real roads having an average length of 1,120.34 meters. The shortest length of an optimized road was 180.4 meters (Road AO; Original 153.98 meters) and the greatest length of an optimized road was 4,877.68 meters (Road B; Original 2,655.48 meters). The greatest length of an original road was Road Y (3198.59 meters; optimized length 3028.72 meters) and the shortest length of an original road was Road AO (153.98 meters; optimized length 180.4 meters). The average cost of the optimized roads was $50,619.44 ($CAD), with the lowest cost of $5,659.76 for Road AC and the greatest cost of $168,593.94 for Road B. Table 3 displays the real and optimized length, and cost of each optimized road.

Table 3. Real length, optimized length, and optimized cost by road pair.

Road Name	Total Cost (CAD$)	Length (m)	Original Length(m)
A	$ 96,498.23	3194.13	3184.76
AA	$ 41,130.97	466.49	313.31
AB	$ 67,507.92	1708.10	936.60
AC	$ 5,659.76	242.32	220.47
AD	$ 37,314.81	798.69	779.22
AE	$ 56,335.65	1769.13	774.90
AF	$ 10,490.87	467.25	751.53
AG	$ 39,761.11	1050.33	724.24
AH	$ 97,858.10	1894.28	1711.84
AI	$ 16,957.46	661.94	692.40
AJ	$ 57,773.43	1247.39	667.27
AK	$ 11,028.60	278.61	188.97
AL	$ 36,648.23	1384.96	980.78
AM	$ 31,181.74	1139.93	636.76
AN	$ 29,589.98	802.12	592.80
AO	$ 11,142.27	180.40	153.98
AP	$ 35,120.16	632.46	540.53
B	$ 168,583.94	4877.68	2655.48
C	$ 56,220.12	2096.24	2511.70
D	$ 81,758.83	1400.28	525.80
E	$ 42,816.05	919.08	1976.00
F	$ 42,961.29	1349.57	1935.76
G	$ 10,419.15	469.90	454.91
H	$ 105,535.16	3955.78	2604.54
I	$ 51,088.08	1879.80	1664.61
J	$ 17,091.98	586.84	445.48
K	$ 48,465.92	1534.56	1482.34
L	$ 37,002.64	1476.36	1457.82
M	$ 27,358.99	973.04	1439.82
N	$ 10,701.44	487.80	474.47
O	$ 45,517.75	678.23	438.88
P	$ 108,177.83	3360.08	1326.13
Q	$ 54,448.59	2406.57	2290.13
R	$ 26,808.51	504.08	431.38
S	$ 20,358.17	594.38	393.06
T	$ 46,081.93	1507.00	1057.28
U	$ 60,209.45	976.06	1051.75
V	$ 17,691.88	515.03	378.57
W	$ 150,058.46	3949.42	1014.91
X	$ 95,661.43	2022.28	1011.98
Y	$ 89,205.02	3028.72	3198.59
Z	$ 29,794.68	840.84	982.58

Figure 6, on the following page, displays an overview map for both the original and optimized routes of Road A. The original route is shown in black and the optimized in red. Bodies of water are shown in blue, areas with road restrictions in purple, forest reserves in green, and stands harvested post-2016 are shown in orange. An inset map is also provided, showing the location of Road A within the study area.
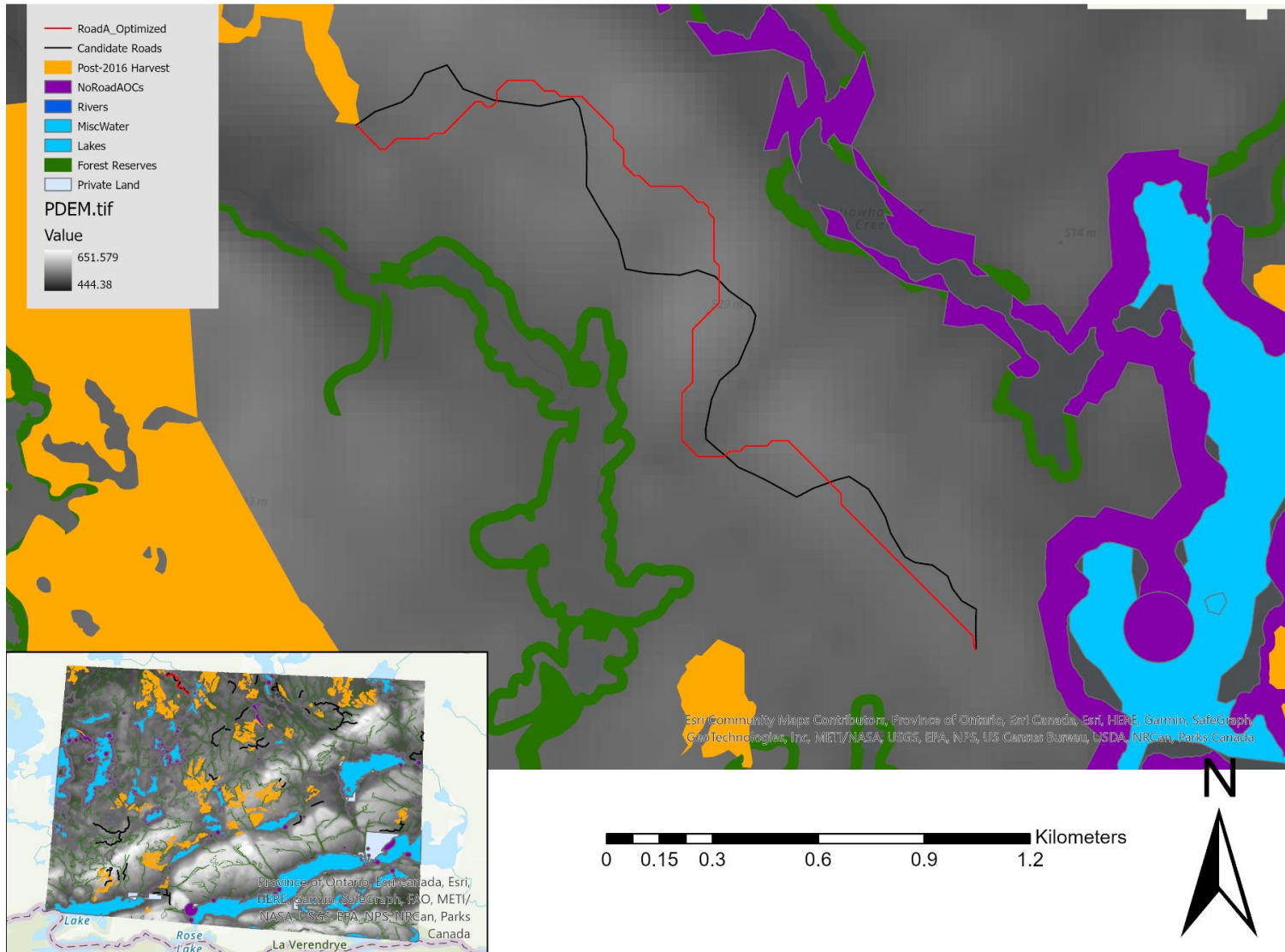
Results: Road Pair A

Figure 6. Overview of Road pair A, showing the modelled route in red and the actual route in black. Also shown are areas incompatible with road construction, as well as the Digital Elevation Model. With compass rose, legend, scale, and inset map.

Testing of the Null Hypothesis

Across the 42 pairs of road locations compared, there were a total of 701 points recorded. Road 'B' had the greatest number of sampled points with 52, while Road's 'AS' and 'AO' had the lowest number of sampled points with 3 each. Appendix V contains a table displaying the number of sampled points recorded for each road.

To test the Null Hypothesis, a Chi-Square test was performed. For the Chi-Square test, 701 data points at the 0.05-alpha (significance) level were tested to determine whether the spatial differences between the road locations were significant. The Chi-Square had 700 degrees of freedom (701-1 = 700). At the 0.05-alpha (significance) level, this gives a right-tail critical value (Also called Chi-Square X^2) of 762.66. The calculated Sum of Squares was 2,887,706.07, much greater than the critical value of 762.66. Therefore, the Null Hypothesis is rejected, meaning that the optimized network of roads was found to significantly differ from the actual network of roads with a 95% probability.

A Chi-Square test was then performed for each individual road-pair at the 0.1 and 0.05-alpha levels. These results are presented in Table 4. Also shown is the original road length, optimal route length, and the number of sampled points. The Chi-Square results column identifies whether the Null Hypothesis is accepted or rejected for a given road pair and alpha-level.

35

Table 4. Chi-Square results for each road at the 0.1 and 0.05-alpha levels.

Road Name	Road Length (m) Original	Optimal	Sampled Points	Chi-Square Result Alpha 0.1	Alpha 0.05
A	3,185	3,194	38	Reject	Reject
AA	313	466	5	Reject	Reject
AB	937	1,708	21	Reject	Reject
AC	220	242	3	Reject	**Accept**
AD	779	799	9	Reject	Reject
AE	775	1,769	9	Reject	Reject
AF	752	467	6	Reject	Reject
AG	724	1,050	12	Reject	Reject
AH	1,712	1,894	27	Reject	Reject
AI	692	662	9	Reject	Reject
AJ	667	1,247	13	Reject	Reject
AK	189	279	4	Reject	Reject
AL	1,641	1,385	21	Reject	Reject
AM	637	1,140	14	Reject	Reject
AN	593	802	11	Reject	Reject
AO	154	180	3	Reject	Reject
AP	541	632	7	Reject	Reject
B	2,655	4,878	52	Reject	Reject
C	2,512	2,096	25	Reject	Reject
D	526	1,400	15	Reject	Reject
E	971	919	12	Reject	Reject
F	1,936	1,350	16	Reject	Reject
G	455	470	6	Reject	Reject
H	2,605	3,956	40	Reject	Reject
I	1,665	1,880	21	Reject	Reject
J	445	587	12	Reject	Reject
K	1,482	1,535	19	Reject	Reject
L	1,458	1,476	16	Reject	Reject
M	1,440	973	12	Reject	Reject
N	474	488	7	Reject	Reject
O	439	678	9	Reject	Reject
P	1,326	3,360	35	Reject	Reject
Q	2,290	2,407	28	Reject	Reject
R	431	504	6	Reject	Reject
S	393	594	8	Reject	Reject
T	1,057	1,507	18	Reject	Reject
U	1,052	976	12	Reject	Reject
V	379	515	7	Reject	Reject
W	1,015	3,949	41	Reject	Reject
X	1,012	2,022	23	Reject	Reject
Y	3,199	3,029	43	Reject	Reject
Z	983	841	10	Reject	Reject

As seen above, the only road pair where the original and optimal routes were not found to be significantly different was Road AC, and only at the 0.1-alpha level, meaning there is a 10% probability that the acceptance of the null hypothesis is erroneous (Khan Academy n.d.).

As the Null Hypothesis was accepted for only one road pair, the Chi-Square critical value was calculated for each road pair using Microsoft Excel. Table 5, below, shows the results of this for all roads with significance values greater than 0.

Table 5. Significance level by road pair.

Road Name	Significance Level	Road Length (m)	
		Original	Optimal
AC	0.08	220.47	242.32
AO	3.66E-05	153.98	180.40
G	1.15E-09	454.91	469.90
V	2.74E-18	378.57	515.03
AI	2.90E-24	692.40	661.94
AK	1.27E-30	188.97	278.61
AP	1.67E-32	540.53	632.46
R	6.08E-48	431.38	504.08
AA	3.61E-52	313.31	466.49
AN	2.43E-69	592.80	802.12
L	4.77E-73	1457.82	1476.36
N	7.22E-80	474.47	487.80
K	2.61E-110	1482.34	1534.56
AF	3.91E-133	751.53	467.25
E	1.45E-167	1976.00	919.08
AG	2.24E-242	724.24	1050.33
J	1.34E-271	445.48	586.84
AM	6.06E-297	636.76	1139.93
A	2.40E-297	3184.76	3194.13

DISCUSSION

Analysis of results.

A total of 42 real roads were mirrored using the optimization methodology described above. As seen in Table 5, there were 19 road pairs with differences significant at an alpha level greater than 0.00. Of those roads, only 4 of the mirrored original roads were greater than 1000 meters in length. For the 23 roads with significance values of 0.00, 14 were greater than 1000 meters in length. As 77.78% of roads greater than 1000 meters in length had significance values of exactly 0, this suggests that the greater the distance between the terminal points of a road, the more significant the differences would be. The road with the greatest significance level overall was Road AC, with the greatest significance level for a road longer than 1000 meters belonging to Road L. The road with the greatest sum of squares with a significance value of exactly 0.00 (ad infinitum) was Road B. Maps of these roads and their real-world counterparts are shown on the next three pages.

Road AC
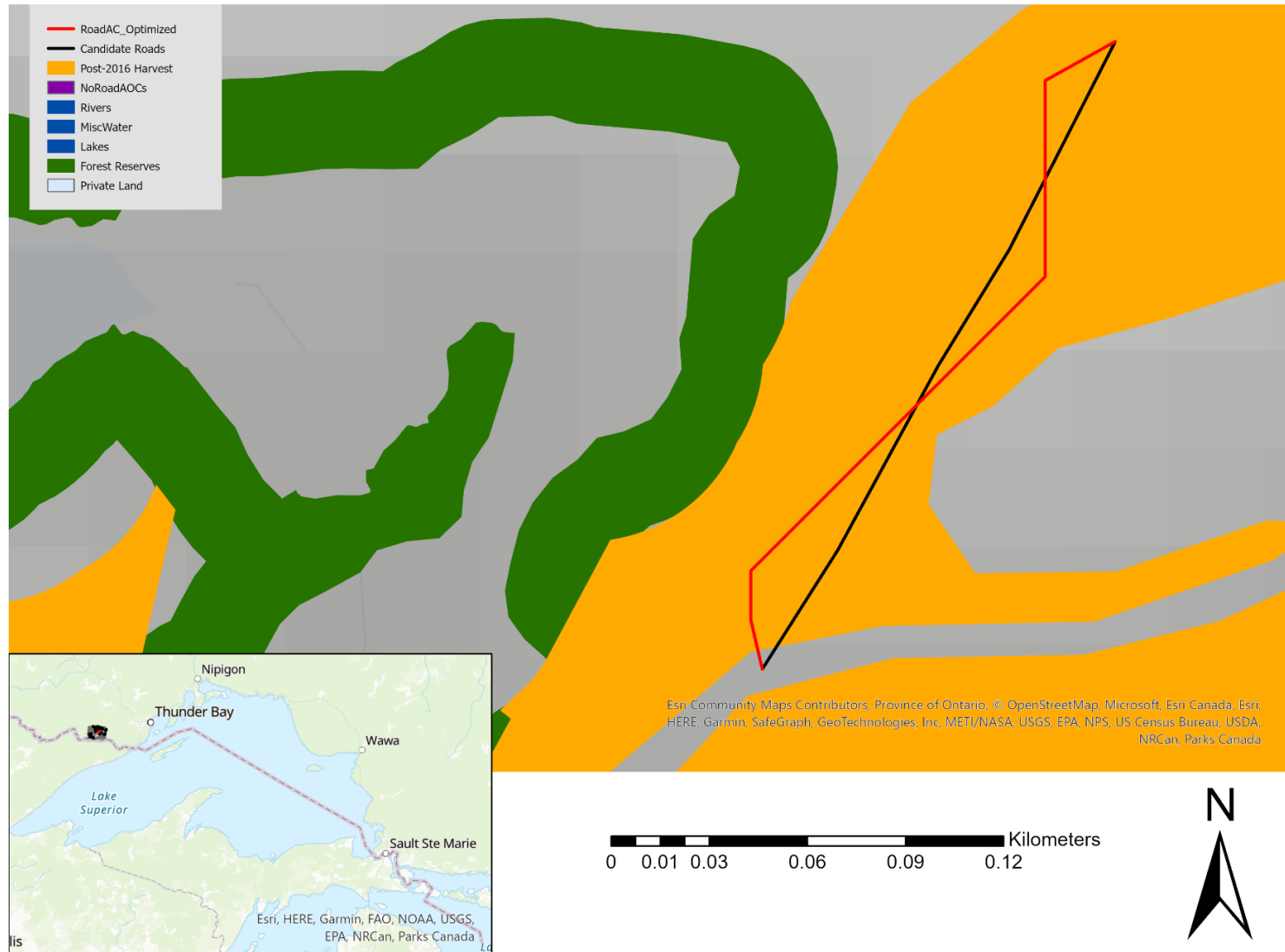
Figure 7. Comparison of Road AO, showing the modelled route in red and the actual route in black. Also shown are areas incompatible with road construction, as well as the Digital Elevation Model. With compass rose, legend, scale, and inset map.
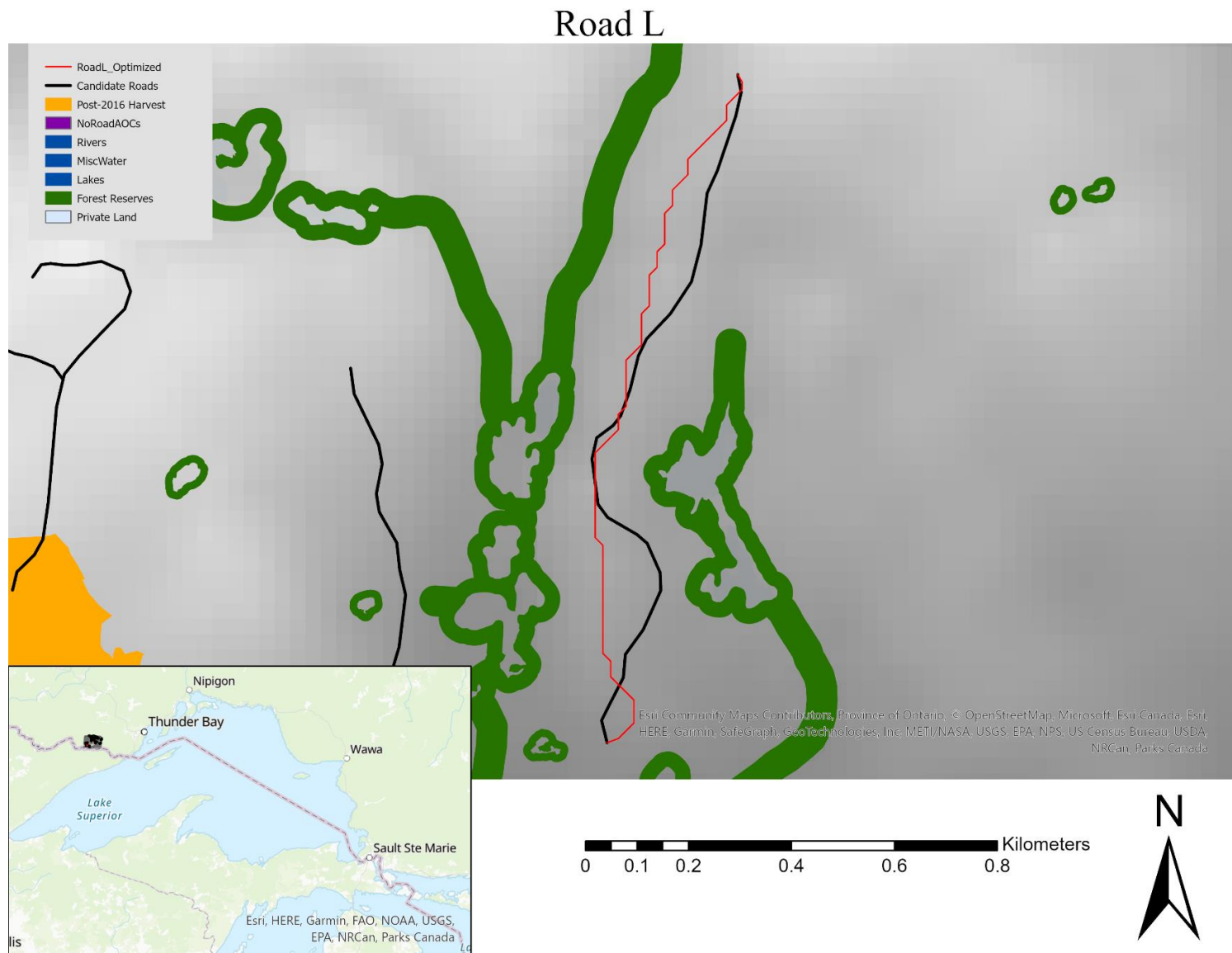
Road L

Figure 8. Comparison of Road L showing modelled route in red and the actual route in black. Also shown are areas incompatible with road construction, as well as the Digital Elevation Model. With compass rose, legend, scale, and inset map.

Road B
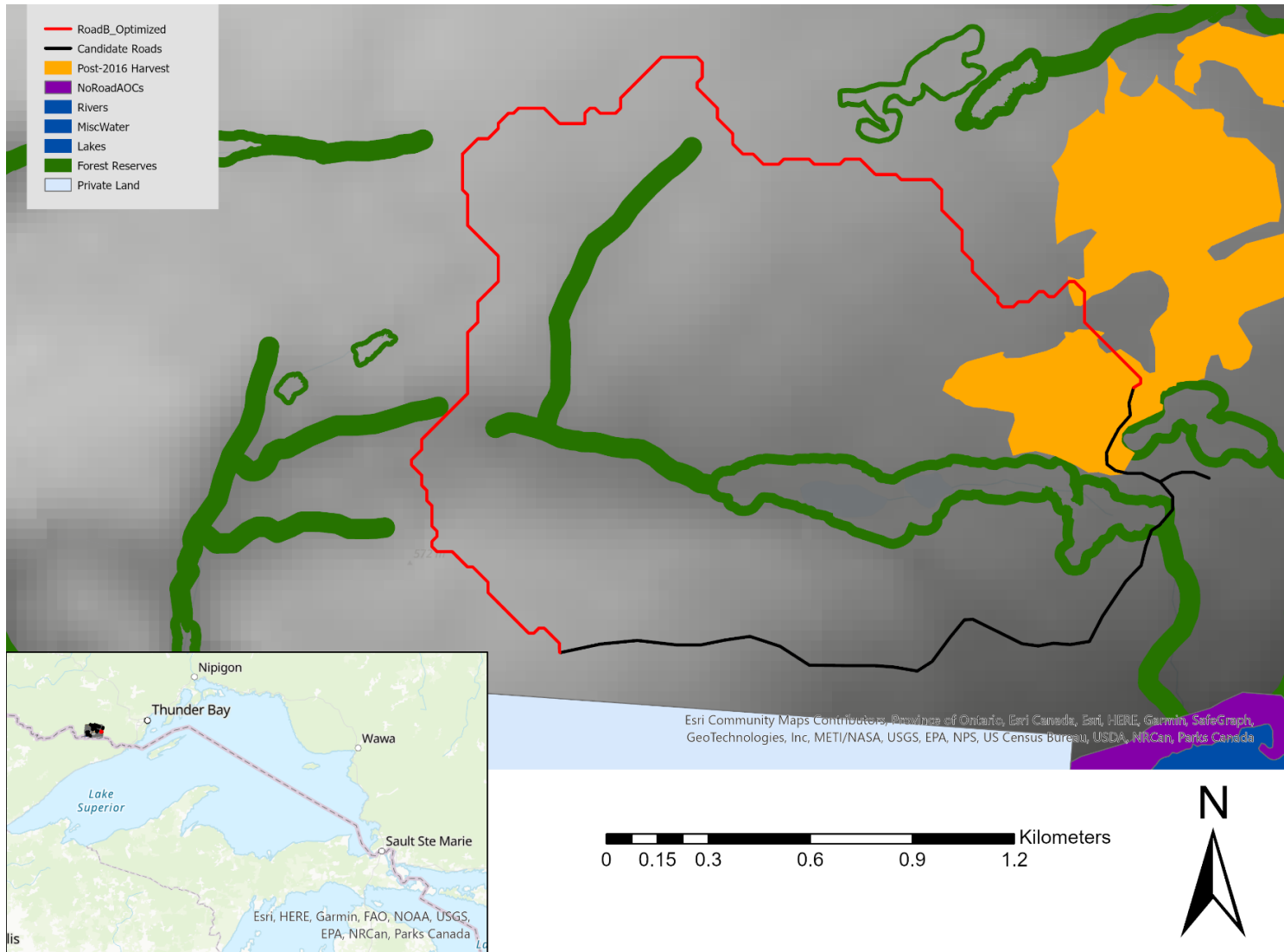
Figure 9. Comparison of Road B showing modelled route in red and the actual route in black. Also shown are areas incompatible with road construction, as well as the Digital Elevation Model. With compass rose, legend, scale, and inset map.

As seen in Figure 9, above, the original route for Road B passes through an area identified as a forest reserve. In the methodology described above, these areas were removed from the cost surface to prevent any optimized roads from being located here. As a result, the optimized route for Road B must travel a significant difference to avoid the forest reserve. The spatial results for many of the road pairs indicate that the created road network was modelled with different parameters than the real-world roads, in particular the disallowance of trespasses in the modelled road, causing significant differences. This was a shortcoming of the methodology used to create the modelled roads, as opposed to a shortcoming of the Least-Cost Path analysis itself.

Reasons for differences.

There are several possible factors identified as plausible explanations for this. Factors causing the differences between the road-pairs include the limitations of the software and data used, as well as assumptions made when designing the workflow. Additionally, the coarse spatial scale of the input DEM is hypothesized as a contributor to the significant differences.

Limitations of Software Used

One of the possible factors causing the differences between the original and optimized routes is the limitations of the software used. The Least-Cost Path plugin used evaluated the most cost-efficient route using Dijkstra's algorithm, which only considered the cost of road construction as a factor to optimize (Antikainen 2013; FlowMap Group@SESS-PKU 2020). However, the cost of hauling harvested volumes of wood to the mill along these roads was a factor not considered when optimizing routes. This limited the scenario in which the roads were being optimized as the hauling cost

(Ignoring the cost of road construction) is a significant factor in the cost of bringing wood to market (Grebner *et al.* 2013). Two key factors identified by Grebner *et al.* (2013) for hauling costs on resource roads were the length and slope of the road. While the formulas used to create the cost surface incorporated the slope perpendicular to the road centre into the calculations of the earthwork's costs, the cost surface itself did not consider the slope of the road when determining cost (Ghajar *et al.* 2013). Additionally, the Least-Cost Path plugin is not sufficiently complex as to incorporate minimum curve radii or to force the use of switchbacks on slopes greater than a given angle, both of which are identified as factors that must be considered when planning a forest road (FlowMap Group@SESS-PKU 2020; Ghajar *et al.* 2013). Furthermore, the Least-Cost Path tool output was a line feature, connecting the centre of one cell along the optimized route to the centre points of the subsequent and previous cells, resulting in all roads existing as straight lines (FlowMap Group@SESS-PKU 2020). The Greenmantle roads were not constricted by the locations of the cells in the cost surface, instead being located wherever specified by their planning team. These are only a few of the factors considered when planning the original roads, leading to a fundamentally different set of parameters and limitations for road network creation between the methodology used here and the methodology used by Greenmantle.

It is these reasons that cause the Least-Cost Path methodology of resource road optimization to be inferior in this exercise, to the results of RoadEng (Kurulak 2019). RoadEng is capable of incorporating the attributes listed above as limiting the results of both the ArcGIS Pro and QGIS Least-Cost Path analyses (Kurulak 2019; ESRI 2022;

FlowMap Group@SESS-PKU 2020). The implication of this is that the results of Least Cost Path analysis for forest road planning are inferior to those of RoadEng.

<u>Assumptions made in workflow</u>

Included in the output of the Least-Cost Path analysis was a value, in Canadian dollars ($CAD) representing the cumulative cost of road construction in all cells traversed by a given optimized road (FlowMap Group@SESS-PKU 2020). The most expensive road to construct was Road B, with an optimized route of 4,877.7 meters, compared to a length of 2,644.5 meters. The second, third, and fourth most expensive optimized roads were also found to be longer than their original counterparts, those being Roads P, W, and H (Appendix IV). In the cases of these four roads, their real-world routes were identified as having traversed areas that were assumed as incompatible with forest road construction in the model design, effectively preventing the resulting optimized routes from being spatially similar.

As seen in Figure 9, the original route for Road B utilized cells which were identified as areas where roads could not be located, therefore resulting in the optimized route taking a circuitous route in order to avoid the area with road restrictions. For Road Pairs W, P, and H, the original routes also traversed areas identified as forest retention reserves. Since the cost surface assumed that forest roads could not traverse these areas, cells overlapping, partially or fully, forest retention patches were removed from the set of traversable cells. To quantify the impact this erroneous assumption had on the results, all other road pairings were examined in order to identify all original roads where this had occurred. Across the 42 original roads, only roads B, H, P, and W traversed forest retention patches, and no other routes traversed any other areas with road restrictions.

Forest roads are permitted to cross retention patches when the road location, use, and mitigation measures in place are consistent with directions provided in Ontario's stand and site guide (OMNR 2010). As these parameters could not be adjusted accurately within the scope of the QGIS Least-Cost Path tool, or during the creation of the cost surface, forest retention patches were instead treated as barriers (FlowMap Group@SESS-PKU 2020). If this methodology were modified to be used in the future, identifying areas where trespasses are allowed and applying an additional cost factor during the creation of the cost surface may be a viable work-around to incorporate this.

Additionally, two factors identified by Ghajar *et al.* (2013) as impacting the cost of forest road construction were soil type and vegetation land cover. Neither of these factors were included in this methodology due to constraints in available data, and thus may have impacted results. In much of the road optimization literature, soil type and soil depth were parameters incorporated into the cost surface creation (Kurulak 2019; Ghajar *et al.* 2013; Akay 2006; Antikainen 2013; Aguiar *et al*. 2021). This is relevant, as the depth of the soil and the soil type will modify the volume of earthworks, and the cost, necessary to construct a roadbed on that site (Aguiar *et al*. 2021; Kurulak 2019). Much of the literature also included the density, size, and species of trees within a given cell when creating the cost surfaces (Ghajar *et al.* 2013; Antikainen 2013; Aguiar *et al.* 2021). Information on site vegetation is relevant as the revenue from any merchantable trees cleared from the road corridor can help offset the cost of constructing the road (Aguiar *et al.* 2021). The exclusion of these factors influencing road construction cost is expected to have reduced the accuracy of the cost surface, and therefore decreased the accuracy of the optimized road locations (Antikainen 2013). As Ghajar *et al.* (2013), and

others, have incorporated soil and forest resource data into their methodologies, the

results shown above are not representative of Least Cost Path optimization for road

planning. In the future, if data is available, these must be incorporated into the creation

of the cost surface. One possible solution could be modelling the earthworks cost with

no soil modifiers across the future area of interest, before applying cost modifiers based

on soil data through the "raster calculator' function (QGIS.org 2021). Additionally, if

forest data is known wall-to-wall for the area of interest, the cost of clearing one area of

the same size as a cost surface cell could be calculated for each polygon storing forest

resource data, and then rasterized and mosaicked onto the cost surface (QGIS.org 2021).

Spatial Scale of Inputs relative to Output accuracy

In the 25 years since Dean (1997) described a methodology for optimizing forest

road locations using digital terrain models, the technology has advanced significantly.

Dean (1997) was able to optimize routes in a raster containing 14,500 cells (121 by 121)

at a 30-meter resolution in time frames ranging from seconds to minutes using the

newest technologies. In this exercise, routes were optimized across a raster containing

12,844,352 cells (4138 by 3104) at a 15-meter resolution, with no route taking more than

3 seconds to be created and saved as a new vector layer. While the processing time and

the size of datasets that can be utilized have advanced significantly, the accuracy of this

modelling is much more important to non-academic users. The spatial resolution of the

DEM data used in constructing a given model has been found to have a significant

impact on the accuracy of any results generated by that model (Schoorl *et al.* 2000;

Chow and Hodgson 2009). It has been found that the raster cell size in DEM models has

a significant impact on the accuracy of those models, with finer spatial resolutions

resulting in reduced deviation between the mean slope and the modelled mean slope
(Chow and Hodgson 2009). Additionally, other findings have shown that model
accuracy in topographical indices modelling is affected by spatial resolution, with finer
spatial resolutions leading to increased model accuracy (Sorenson and Seibert 2007). As
a result, it can be theorized that the accuracy of this model may have increased if the
scale of the DEM utilized was finer. The latest PDEM data for the Lakehead Forest, at
time of writing, was a 30-meter resolution dataset, published in 2019 (OMNRF 2019a).
In contrast, LiDAR data is capable of generating DEM data at resolutions as low as 1
meter, greatly refining the accuracy of any models made with the data (Kurulak 2019).

CONCLUSION

The current limitations with Least-Cost Path analysis preclude this method from
being feasible for widespread use for road planning with the limited input parameters of
this study. The created road network was found to be significantly different than the real
road network, with the same being true for all individual road pairs except for road pair
AC. Assuming that existing roads already in place are the optimal layout, this shows that
the roads modelled in this methodology are inferior to those planned by Greenmantle
under current methods, precluding this methodology from being viable for real-world
use. Causes for the significant differences between the real and modelled roads include
the exclusion of distance optimization, lack of soil depth and type consideration, lack of
forest resource consideration, and the scale of the DEM used to determine slope
(Grebner *et al.* 2013; Ghajar *et al.* 2013; Akay 2006; Schoorl *et al.* 2000). However,
with further refinements it is possible that this method of Least-Cost Path analysis can
be used to generate road networks comparable to real-world road networks (Antikainen

2013). Additionally, by refining the scale of elevation data used to build the cost surface in future iterations of this methodology, it is expected that the accuracy of results will increase (Schoorl *et al.* 2000; Chow and Hodgson 2009). As a result of these limitations, specialized software, such as RoadEng, is superior to this method of Least-Cost Path analysis for road planning (Kurulak 2019).

LITERATURE CITED

Abdi, E., B. Majnounian, A. Darvishsefat, Z. Mashayekhi, J. Sessions. 2009. A GIS-
MCE based model for forest road planning. Journal of Forest Science 55(4) pp.
171-176. https://bit.ly/3NmAXE5.

Aguiar, M.O., G. Fernandes da Silva, G.R. Mauri, A. Ribeiro de Mendonca, C.J. de
Oliveira Santana, G.E. Marcatti, M.L. Marques da Silva, E.F. da Silva, E.O.
Figueiredo, J.P. Silva, R. Freitas Silva, J. Silva-Santos, G.L. Lavagnoli, C.C
Leite. 2021. Optimizing Forest Road planning in a sustainable forest
management area in the Brazilian Amazon. Journal of Environmental
Management 288(112332).

Akay, A.E. Minimizing total costs of forest roads with computer-aided design model.
Sadhana 31 pp. 321-633. https://doi.org/10.1007/BF02715918.

Antikainen, H. 2013. Comparison of Different Strategies for Determining Raster-Based
Least-Cost Paths with a Minimum Amount of Distortion. Transactions in GIS
17(1) pp. 96-108.

Berges, L., R. Chevalier, C. Avon. 2013. Influence of forest road, road surfacing
material, and stand age on floristic diversity and composition in a nutrient-poor
environment. Applied Vegetation Science 16(3) pp. 470-479.

Brunson, A. 1842. A Western Pioneer: Or, Incidents of the life and times of Reverend
Alfred Brunson embracing a period of over seventy years. Hitchcock and
Walden Publishing, Cincinnati. 32 pp.

Bryant, R.C. 1913. Logging: The principles and general methods of operation in the

    Unite States. F.H. Wilson Company, Boston, Massachusetts. Accessed online

    October 2021 from https://bit.ly/3pS9dht.

Burke, D. 1974. An automated analysis of timber access road alternatives. US. Dept. of

    Ag. For. Serv. PNW-27.

Cahskan, E. 2013. Planning of Forest Road Network and Analysis in Mountainous Area.

    Life Science Journal 10(2) pp. 2456-2465.

Chow, T.E., M.E. Hodgson. 2009. Effects of LiDAR post-spacing and DEM resolution

    to mean slope estimation. Internation Journal of Geographical Information

    science 23(10) pp. 1277-1295. https://doi.org/10.1080/13658810802344127.

Dean, D.J. 1997. Finding optimal routes for networks of harvest site access roads using

    GIS-based techniques. Can. Jour. For. Res. 27(1) pp. 11-22.

Dijkstra, E.W. 1959. A Note on Two Problems in Connexion (sic) with Graphs.

    Numerische Mathematik 1 pp. 569-271.

Durmaz, A.I., E.O. Unal, C.C. Aydin. 2019. Automatic Pipeline Route Design with

    Multi-Criteria Evaluation Based on Least-Cost Path Analysis and Line-Based

    Cartographic Simplification: A Case Study of the Mus Project in Turkey. ISPRS

    International Journal of Geo-Information 8(4) pp. 173.

Engstrom, O., G.L. Tigerstrom. 2017. Improving usability of land warfare simulator:

    pathfinding and adaptive speed based on geographic data. Exanebsarbete Inom

    Teknik, Grundniva, Stockholm, Sverige (Sweden) 15pp. Original in Swedish and

    English.

EPSG. n.d. EPSG:26916. ESPG Coordinate Systems Worldwide. Accessed from
epsg.io.

ESRI. 2021. ArcGIS Pro 2.9.1. ESRI Inc. https://bit.ly/364UbwY.

ESRI (a). n.d. ArcGIS Pro: Creating the least-cost path. ESRI Help. Accessed from
https://bit.ly/3rGt9TI.

ESRI (b). n.d. ArcGIS Pro Spatial Analyst Tool Reference. ESRI Help. Accessed from
pro.arcgis.com/en/pro-app/latest/tool-reference.

Etherington, T.R. 2011. Python based GIS tools for landscape genetics: Visualizing
genetic relatedness and measuring landscape connectivity. Methods in Ecology
and Evolution 2 pp. 52-55.

FlowMap Group@SESS-PKU. 2020. Least-Cost Path plugin for QGIS. Installed from
the QGIS Plugin Repository January 27, 2022.

Ghajar, I., A. Najafi, A.M. Karimimajd, K. Boston, S.A. Torabi. 2013. A program for
cost estimation of forest road construction using engineer's method. Forest
Science and Technology 9(3) pp. 111-117.

Grebner, D.L., L.A. Grace, W. Stuart, D.P. Gilliland. 2013. A Practical Framework for
Evaluating Hauling Costs. International Journal of Forest Engineering 16(2) pp.
115-128.

Greenmantle Forest Incorporated. n.d. About the Lakehead Forest. Viewed October
2021 from greenmantle.ca

Gucinski, H., M.J. Furniss, R.R. Ziemer, M.H. Brookes. 2001. Forest Roads: A
    Synthesis of Scientific Information. Gen. Tech. Rep. PNW-GTR-509. Portland,
    OR. US Dept. of Agriculture, Forest Service, Pacific Northwest Research
    Station. 103 pp.

Harrison, J.L. 1955. The kay-out and construction of forest roads. Empire Forestry
    Review 34(1) pp. 42-48.

Hutson, H.P. 1953. Low-cost roads: Their design and construction for timber extraction.
    Empire Forestry Review 32(4) pp. 316-329.

Irwin, J.C. 1947. The Canadian Forest and Its Future. Pp. 52-58 in Features of Present-
    Day Canada. Sage Publishing, Thousand Oaks, California. 266 + viii pp.

Jones, H.R. 1942. Planning for Forest Transportation. Journal of Forestry 40(4) pp. 296-
    300.

Kallio, M., A. Propoi, R. Seppala. 1986. A Model for the Forest Sector. Management
    Sciences 21 pp. 89-112.

Kamarudin, N., M.H. Ismail, K. Jusoff. 2014. Quantification of least cost path analysis
    for best forest road planning. Malaysian Forester 77(2) pp. 101-110.

Khan Academy. n.d. Analysis of variance (ANOVA): ANOVA 1: Calculating SST.
    Khan Academy. Accessed online March 2022 from https://bit.ly/3vUkJMs.

Knapp, F.M. 1921. Motor Truck Logging Methods. Engineering Experiment Station,
    University of Washington, Seattle. Accessed online October 2021 from
    https://bit.ly/2ZyJBuT.

Kurulak, A. 2019. Exploring the potential to minimize forest road cost in Ontario with LiDAR and RoadENG. Undergraduate thesis, Faculty of Natural Resources Management, Lakehead University, Thunder Bay, ON. 105 PP.

Laschi, A., F. Neri, N.B. Montorselli, E. Marchi. 2016. A Methodological Approach Exploiting Modern Techniques for Forest Road Network Planning. Croatian Journal of For. Eng. 37(2) pp. 319-331.

Lepoglavec, K. I. Potocnik, T. Pentek, Z. Tomasic, A. Poje, M. Mihelic. 2011. "RoadEng" software package for designing forest roads. Nova Mehanizacija Sumarstva 32 pp. 39-51. https://bit.ly/36JC6F1.

McManus, J.H. 1919. A forgotten trail. The Wisconsin Magazine of History 3(2) pp. 139-192. https://www.jstor.org/stable/4630211.

Morey R.D., E.J. Wagenmakers. 2014. Simple relation between Bayesian order-restricted and point-null hypothesis tests. Statistics & Probability Letters 92 pp. 121-124. https://doi.org/10.1016/j.spl.2014.05.010.

Murray, A.T., R.L. Church. 1997. Optimizing the location of harvesting equipment and access roads. pp. 361-363 in Seventh Symposium on Systems Analysis in Forest Resources. US. Dept. of Ag., For. Ser. NC-205. 470 + viii pp.

Murray, A.T. 1998. Route planning for harvest site access. Canadian Journal of Forest Research 28(7) pp. 1084-1087.

Nasiri, M., B. Askari. 2020. Improving drainage conditions of forest roads using the GIS and forest road simulator. Journal of Forest Science 66(9) pp. 361-367.

Norcross, T.W., R.F. Grefe. 1931. Transportation Planning to Meet Hour-Control

  Requirements. Journal of Forestry 29(7) pp. 1019-1033.

[OMNR] Ontario Ministry of Natural Resources. 2009. Lakehead Forest Management

  Unit Forest Resources Inventory in Forest Resources Inventory – Version 2.

  Ontario Ministry of Natural Resources and Forestry, Peterborough, Ontario.

  Accessed via Ontario Geohub, September 2021.

[OMNR] Ontario Ministry of Natural Resources. 2010. Forest Management Guide for

  Conserving Biodiversity at the Stand and Site Scales. Queen's Printer for

  Ontario, Toronto. 223 pp.

[OMNR 2014a] Ontario Ministry of Natural Resources and Forestry. 2014. Forest

  Compliance Handbook. Queen's Printer for Ontario, Toronto. 222 pp.

[OMNR 2014b] Ontario Ministry of Natural Resources. 2014. Forest Management

  Guide for Boreal Landscapes. Queen's Printer for Ontario, Toronto. 104 + viii

  pp.

[OMNRF 2019a] Ontario Ministry of Natural Resources and Forestry. 2019. Provincial

  Digital Elevation Model (PDEM). Ontario Ministry of Natural Resources and

  Forestry, Provincial Mapping Unit, Peterborough, Ontario.

[OMNRF 2020a] Ontario Ministry of Natural Resources and Forestry. 2020. Forest

  Management Planning Manual. Queen's Printer for Ontario, Toronto. 318 pp.

[OMNRF 2020b] Ontario Ministry of Natural Resources and Forestry. 2020. Forest

  Resources Inventory – Version 2. Ontario Ministry of Natural Resources and

  Forestry, Provincial Mapping Unit, Peterborough, Ontario.

[OMNRF] Ontario Ministry of Natural Resources and Forestry. 2021. Ministry of
Natural Resources and Forestry Road segments. Ontario Ministry of Natural
Resources and Forestry, Provincial Mapping Unit, Peterborough, Ontario.

Peterson, L.L., B.S. Davie. 2012. Internetworking pp. 169-305 *in* Computer Networks
(Fifth Edition). Morgan Kaufmann Publishers, Burlington, Massachusetts. 884
pp.

Prouty, A.M. 1985. More Deadly than War: Pacific Coast Logging, 1827-1981. Garland
Publishing, New York.

QGIS.org. 2021. QGIS Geographic Information System. QGIS Association. Available
from qgis.org

Ramos-Scarron, C.E., M.C. LeFevor. 2018. Effects of Forest Roads on Runoff Initiation
in Low-Order Ephemeral Streams. Water Resources Research 54(11) pp. 8613-
8631.

Rogers, L. P. Schiess. 2001. PEGGER and ROADVIEW – A new GIS tool to assist
engineers in operations planning pp.171-182 *in* Schiess, P. and F. Krogstad (eds.)
The International Mountain Logging and 11th Pacific Northwest Skyline
Symposium 2001; Proceedings of the meeting held in Seattle, Washington,
U.S.A., December 10-12, 2001. Gen. Tec. Rep. International Union of Forestry
Research Organizations, Vienna, Austria. 284 pp.

Schoorl, J.M., M.P. Sonnevald, A. Veldkamp. Three-dimensional landscape process
modelling: The effects of DEM resolution. Earth Surface Processes and
Landforms 28(9) pp. 1025-1034. https://bit.ly/34KTjNS.

Softree. 2021. Softree Optimal for Forestry Industry. Softree, North Vancouver, B.C., Canada. Accessed March 25, 2022 from https://bit.ly/3NmS88D.

Sorenson, R., J. Seibert. 2007. Effects of DEM resolution on the calculation of topographical indices: TWI and its components. Journal of Hydrology 347(1-2) pp. 79-89.

Talebi, M., A. Nickabadi, B. Majnounian, E. Abdi, R. Safabakhsh, N. Izadyar, and A. Laschi. 2022. Forest Road planning to improve tourism accessibility: A comparison of different methods applied in a real case study. Geocarto International: Ahead of Print. 20pp.

Weintraub, A., D. Navon. 1976. A Forest Management Planning Model Integrating Silvicultural and Transportation Activities. Management Science 22(12) pp. 1299-1309. https://doi.org/10.1016/j.jhydrol.2007.09.001.

Yu, C., J. Lee, M.J. Munro-Stasiuk. Extensions to least-cost path algorithms for roadway planning. International Journal of Geographical Information Science 17(4) pp. 361-376.

(This page intentionally left blank)

APPENDICES

<u>Appendix I. Greenmantle Forest Incorporated Operating Areas and location within</u>

<u>Ontario.</u>
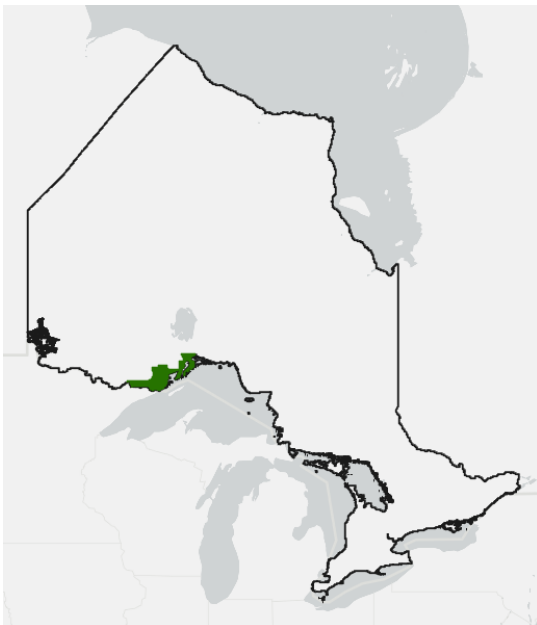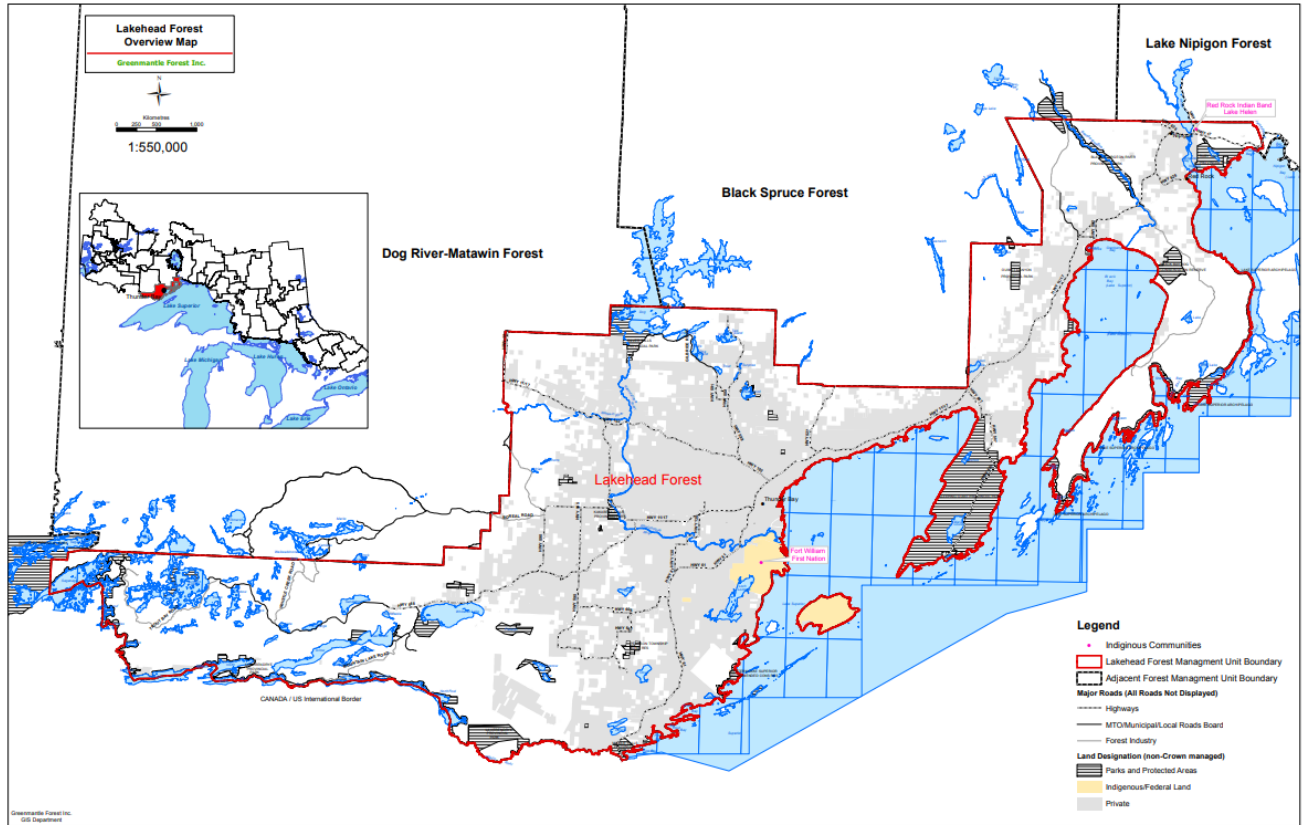
Appendix II: Study Area within the Lakehead SFL.

Study Area and Immediate Vicinity
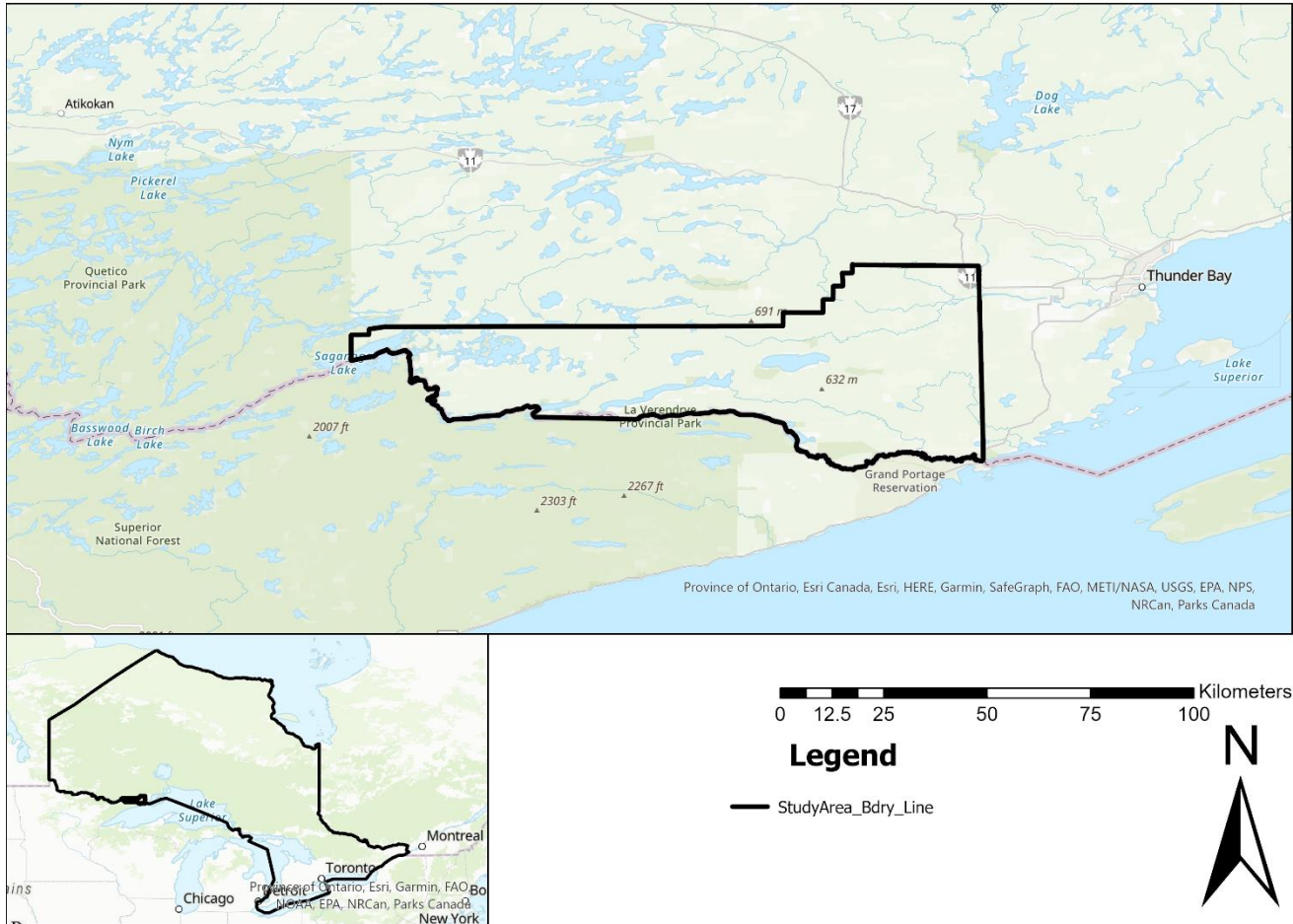
Appendix III: Annotated ArcPy Script for Cost Raster

```
import arcpy

import os

import cmath

from arcpy.sa import *

arcpy.env.workspace = r"C:\...\Create_CostRaster.gdb"

workspace = arcpy.env.workspace

rasters = arcpy.ListRasters()

for raster in rasters:

    print(raster)

global slope_Raster

slope_Raster = arcpy.Raster("Slope_Clipped")

slope_Raster.readOnly = False

global flow_Raster

global boundary

boundary = "StudyArea_BDRY"

flow_Raster = "Flow_Accumulation"
```

##These are the known values as they will be the same for all operational roads, assuming the road is located along the centre of the slope

```
global road_Width

road_Width = 5

global clearing_Width

clearing_Width = 6.8

global road_Fill

road_Fill = 2.5

global fill_Diff

fill_Diff = 0.9

global road_Cut

road_Cut = 2.5
```

global cut_Diff

cut_Diff = 0.9

##These values are needed to create multiple cost raster layers but are calculated on a pixel-by-pixel basis.

global slope

global corrected_Slope

global sigma_Cut

global sigma_Fill

c_Earth = 17.5 ##Cost per cubic meter of earth filled removed; assumption is that these values are equal along this road as scale is too coarse to be more specific

c_Grade = 0.04 ##Cost to grade on square meter of road surface, assuming road is already surface and there is no additional aggregate needed

c_Surf = 3.70 ##cost per square meter of road surface, assuming 15cm depth of aggregate to surface road. Included in this figure is the cost of materials; cost of hauling materials; and cost of grading the finished road

outPath = workspace

outName = "Actual_EarthworksCost"

cellSize = "30,30"

pixelType = "16_BIT_UNSIGNED"

bands = "1"

pyramids = "NONE"

arcpy.management.CreateRasterDataset(outPath,outName,cellSize,pixelType,"",bands," ",pyramids,"","","")

##Clip all layers to the new boundaries

CulvertCost = r r"C:\...\Create_CostRaster.gdb\CulvertCosts"

arcpy.management.Clip(CulvertCost,"-90.574787 48.110933 -90.177149 48.296909 ", os.path.join(workspace,"CulvertCost_Clipped"),boundary,"#","ClippingGeometry","NO _MAINTAIN_EXTENT")

arcpy.management.Clip(slope_Raster,"-90.574787 48.110933 -90.177149 48.296909" , os.path.join(workspace,"Slope_Clipped"),boundary,"#","ClippingGeometry","NO_MAI NTAIN_EXTENT")

##Create the slope rasters for each RasterCellIterator:

```
arcpy.management.CopyRaster(slope_Raster,"Earthworks_Cost")

arcpy.management.CopyRaster(slope_Raster,"Surfacing_Cost")

arcpy.management.CopyRaster(slope_Raster,"Grading_Cost")

##Create the cost raster for culverts

in_Raster = flow_Raster

range_Values =
RemapRange([[0,0.04,510],[0.041,0.086,600],[0.087,0.118,645],[0.119,0.156,690],[0.15
7,0.254,900],[0.255,0.383,1035],[0.384,0.548,1200],[0.549,0.750,1800],[0.751,0.993,24
00],[0.994,1.614,3600],[1.615,2.435,4800],[2.436,3.477,6000],
[3.478,4.760,7200],[4.761,6.304,8400],[6.305,8.128,10800],[8.129,10.250,13200],[10.2
51,12.689,15600],[12.690,15.462,18000],[15.463,18.585,20400],[18.586,300,50000]])

CulvertCost = Reclassify(in_Raster, "VALUE", range_Values )

CulvertCost.save(r"C:\...\Create_CostRaster.gdb\CulvertCosts")

Convert Culvert Costs per one culvert to an actual value for the road:

CulvertCost_Clipped = Raster(r"C:\...\Create_CostRaster.gdb\CulvertCosts_Clipped")

DrainageCosts = Raster(r"C:\...\Create_CostRaster.gdb\CulvertCosts\DrainageCosts")

CulvertCost_Clipped.readOnly = False

DrainageCosts.readOnly = False

culvert_Info = CulvertCost_Clipped.getRasterInfo()

with arcpy.sa.RasterCellIterator({"rasters":[CulvertCost_Clipped, DrainageCosts],
"skipNoData":[CulvertCost_Clipped]}) as rci:

    for r,c in rci:

        v = int(CulvertCost_Clipped[r,c])

        DrainageCosts[r,c] = (int(v+(v/1250)*18))

DrainageCosts.save((r"C:\...\Create_CostRaster.gdb\CulvertCosts\DrainageCosts_Calc")

 print("The cost raster for Drainage Costs has been calculated")


##Calculate the cost of grading

grade_Cost = Raster("Grading_Cost")

grade_Cost.readOnly = False

with arcpy.sa.RasterCellIterator({"rasters":[slope_Raster,grade_Cost],
"skipNoData":[slope_Raster]}) as rci:
```

```
    for r,c in rci:

        v = int(slope_Raster[r,c])

        grade_Cost[r,c] = (int(c_Grade * (road_Width + ((fill_Diff + fill_Diff + 1)/2))*30))

grade_Cost.save("Grading_CalculatedCost")

print("The Grading Cost has been calculated")


##Calculates the cost of surfacing

surf_Cost = Raster("Surfacing_Cost")

surf_Cost.readOnly = False

with arcpy.sa.RasterCellIterator({"rasters":[slope_Raster,surf_Cost],
"skipNoData":[slope_Raster]}) as rci:

    for r,c in rci:

        v = int(slope_Raster[r,c])

        surf_Cost[r,c] = (int(204 * c_Surf ))

surf_Cost.save("Surfacing_CalculatedCost")

print("The Surfacing Cost has been calculated")


##Convert Slope value to the earthworks cost of the road in pixel r,c

earth_Cost = arcpy.Raster("Slope_Clipped_1")

earth_Cost.readOnly = False

with arcpy.sa.RasterCellIterator({'rasters':[slope_Raster,earth_Cost],
'skipNoData':[slope_Raster,earth_Cost]}) as rci:

    for r,c in rci:

        v = (slope_Raster[r,c])

        corrected_Slope = ((road_Fill+fill_Diff)*v)

        sigma_Cut = cmath.atan(corrected_Slope/0.9)

        sigma_Fill = cmath.atan(corrected_Slope/0.9)

        a_Cost = ((((road_Width - road_Fill)**2) *
((cmath.tan(sigma_Fill))*(cmath.tan(v)))))/(2*(cmath.tan(sigma_Fill))-
(cmath.tan(corrected_Slope))))

        b_Cost = a_Cost+1
```

```
        c_Cost = cmath.sqrt(a_Cost*b_Cost)

        d_Cost = a_Cost + c_Cost + b_Cost

        e_Cost = abs((d_Cost/3)*c_Earth)

        earth_Cost[r,c] = (e_Cost.real)

earth_Cost.save("Earthworks_Cost")

print("The Earthworks Cost has been calculated")
```

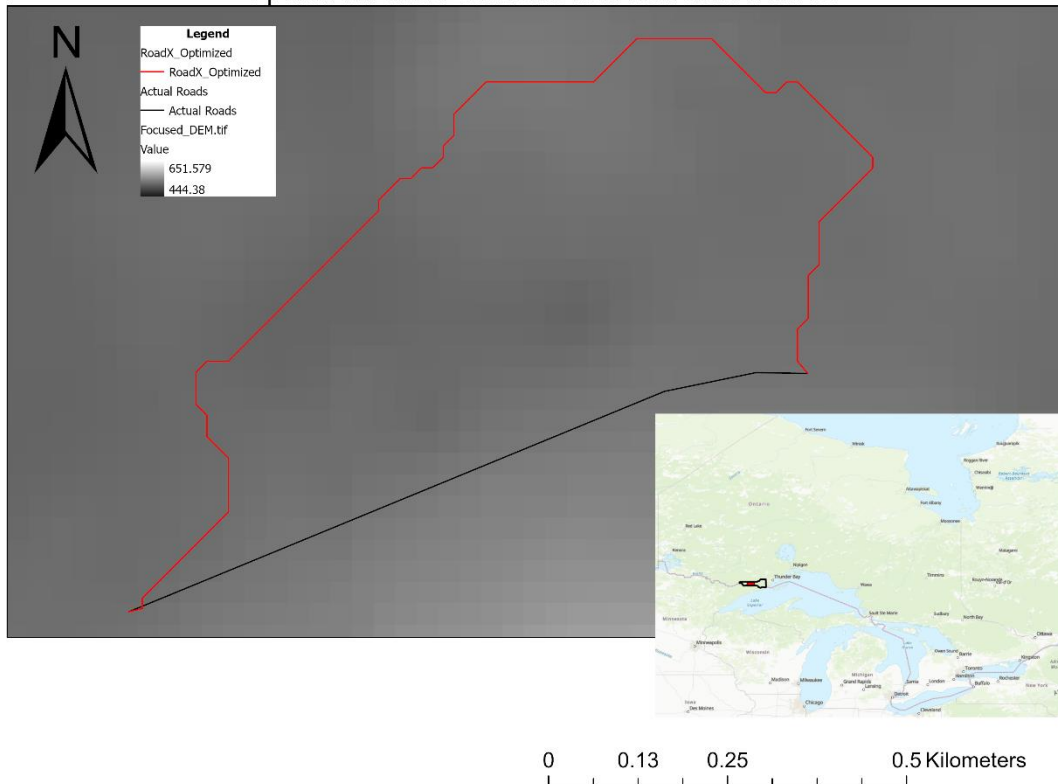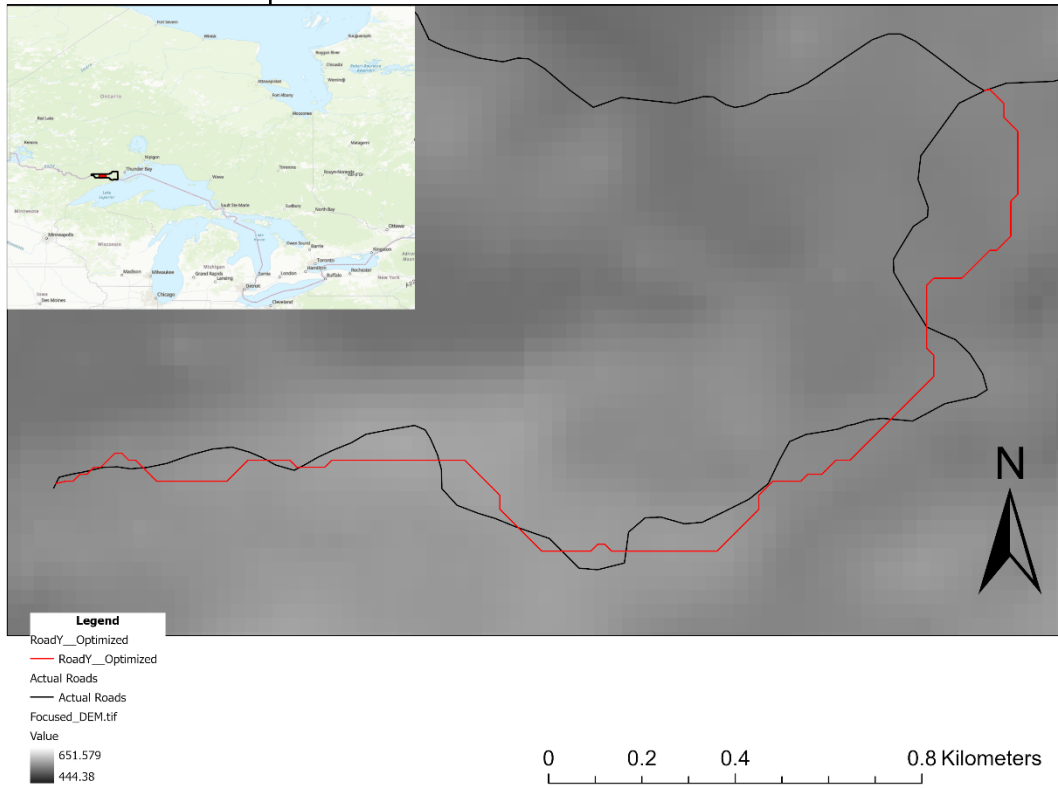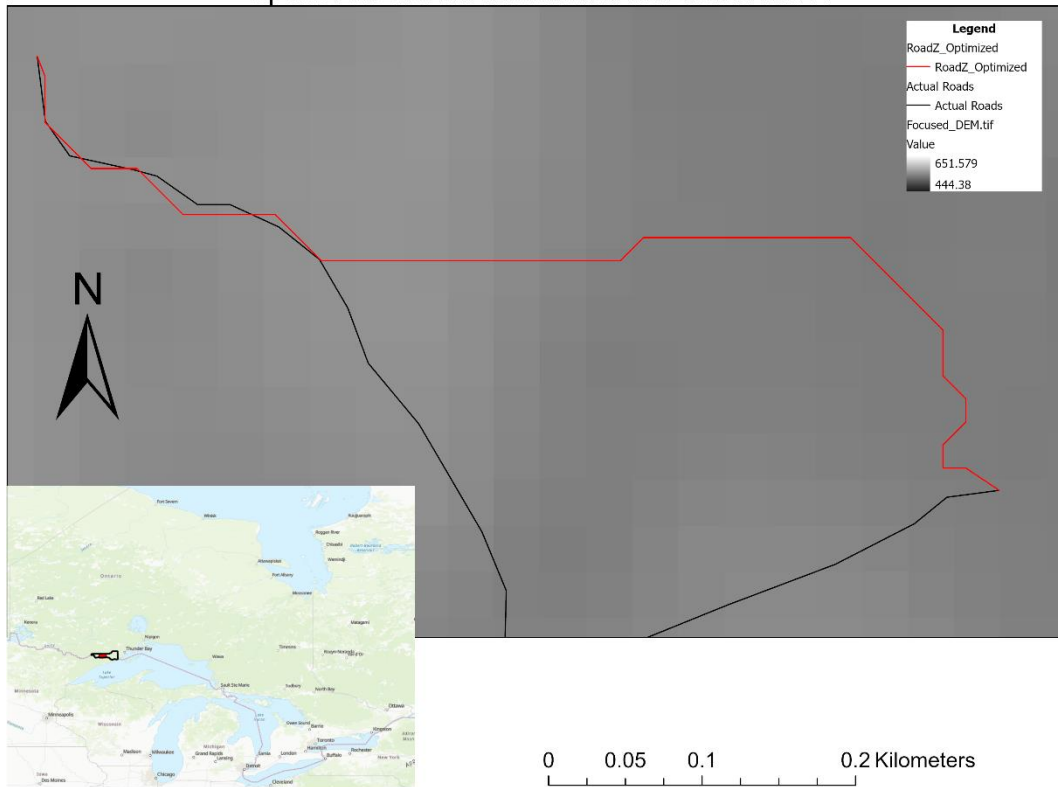Appendix IV: Visual Comparison between actual and optimized road locations.

Overview of Optimized and Actual Routes
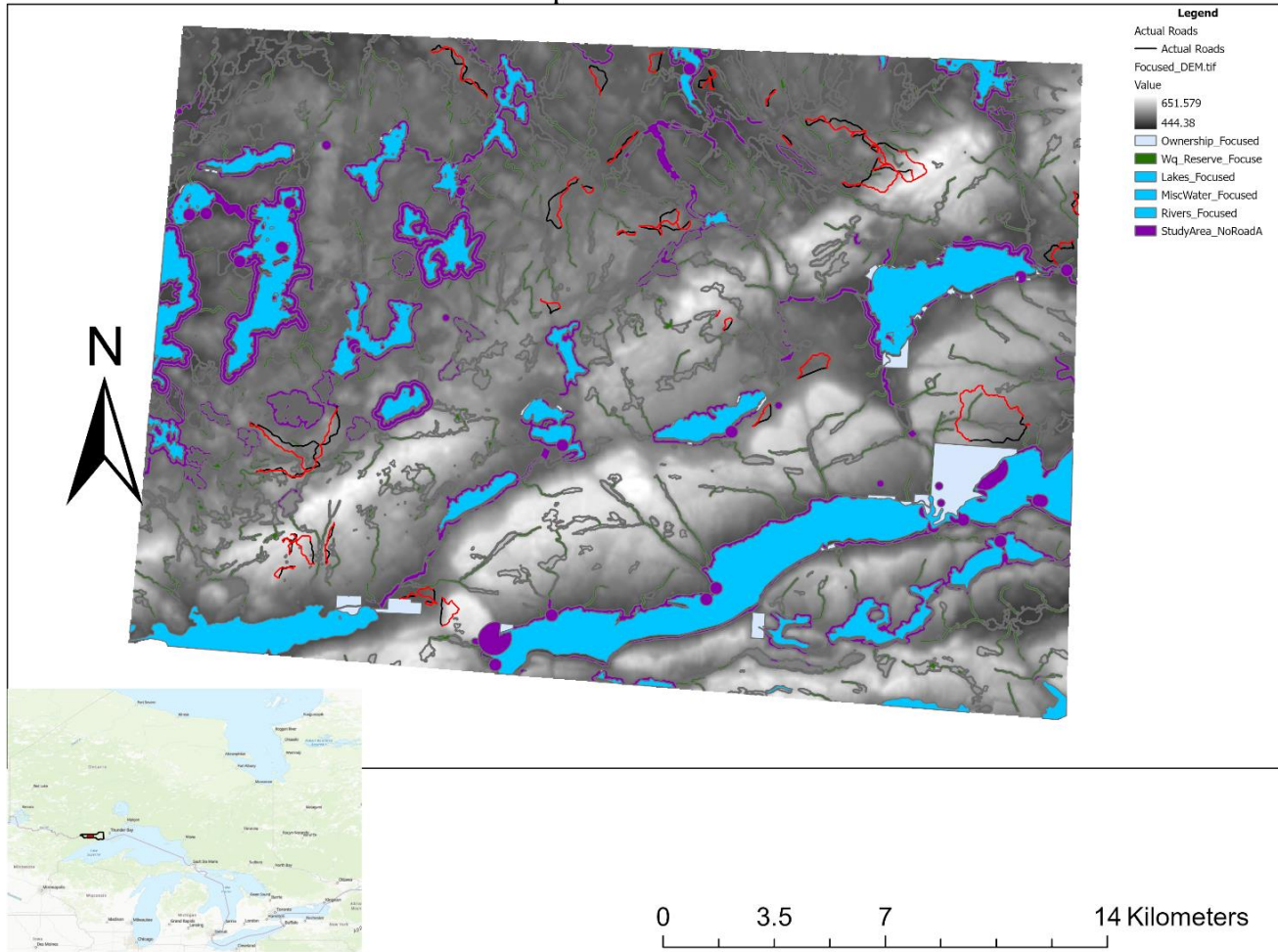
Optimized and Actual Routes for Road Pair A
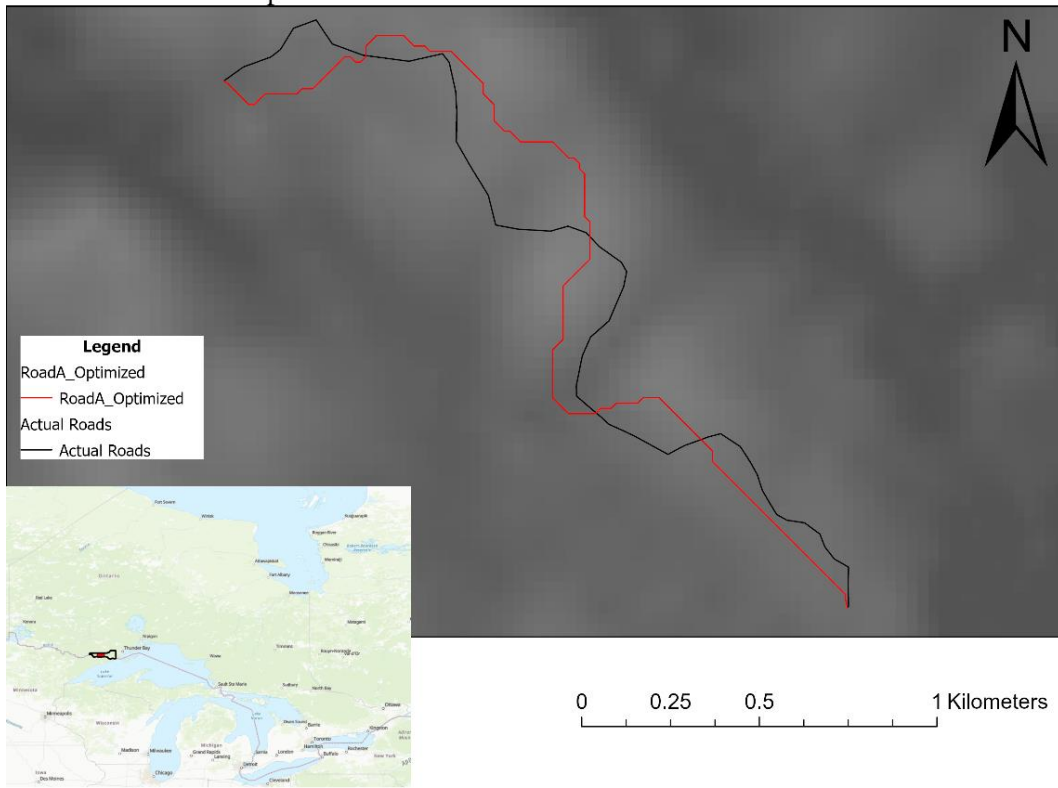
Optimized and Actual Routes for Road Pair B
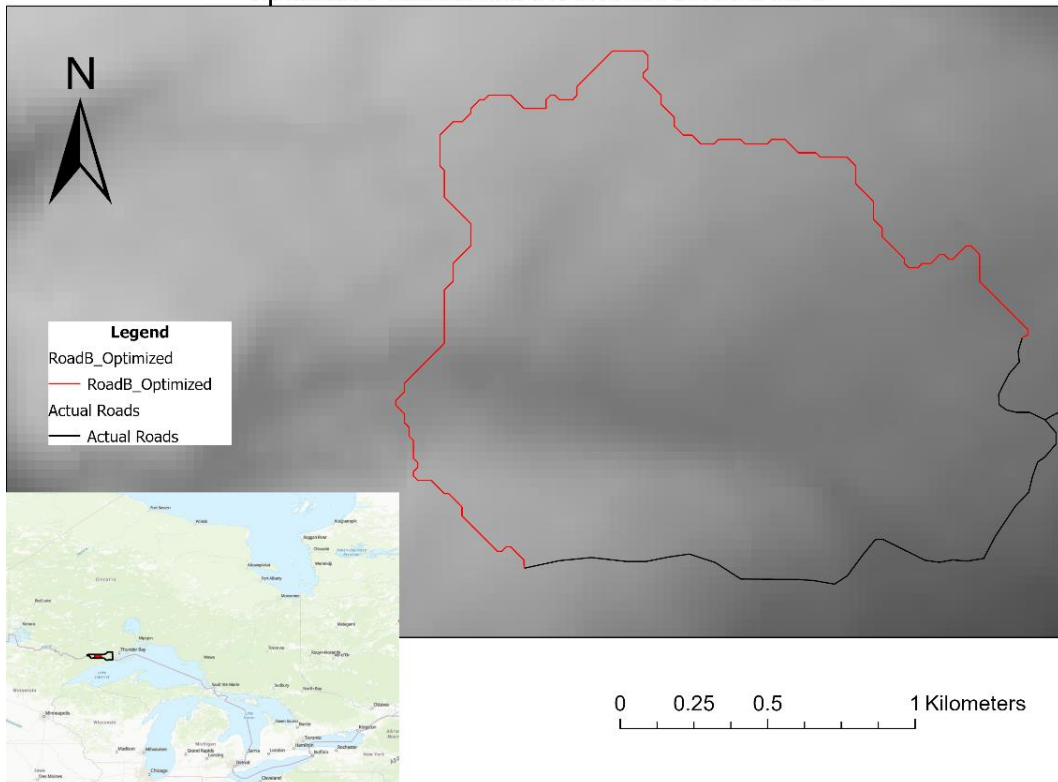
Optimized and Actual Routes for Road Pair C
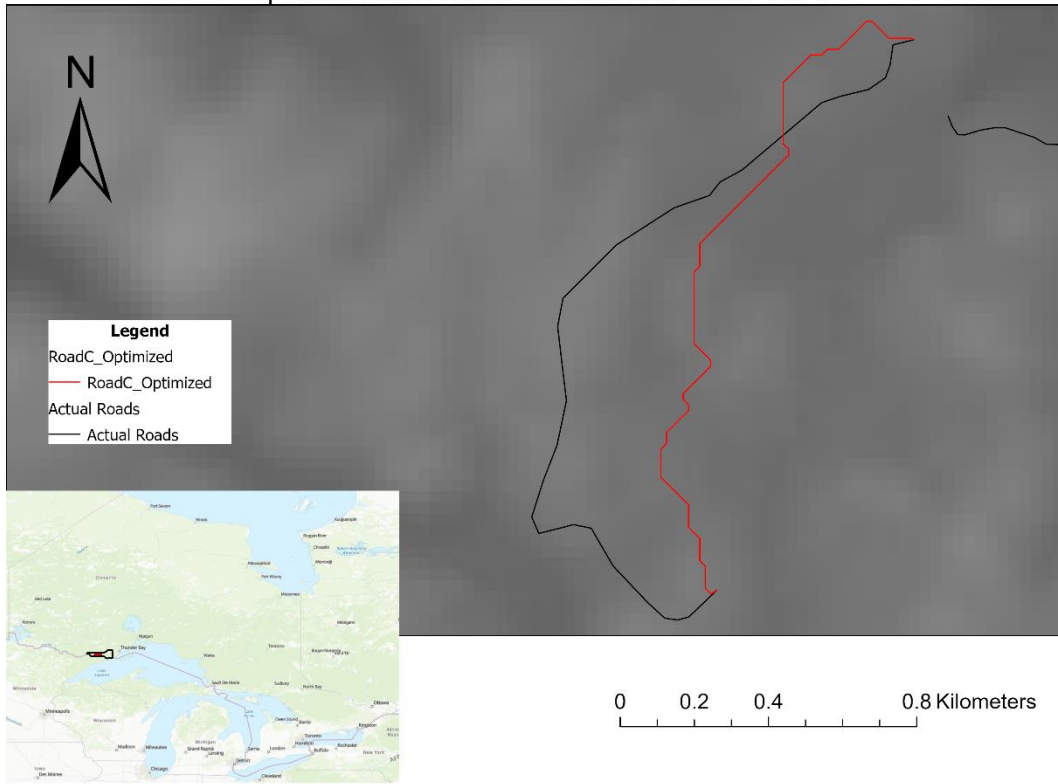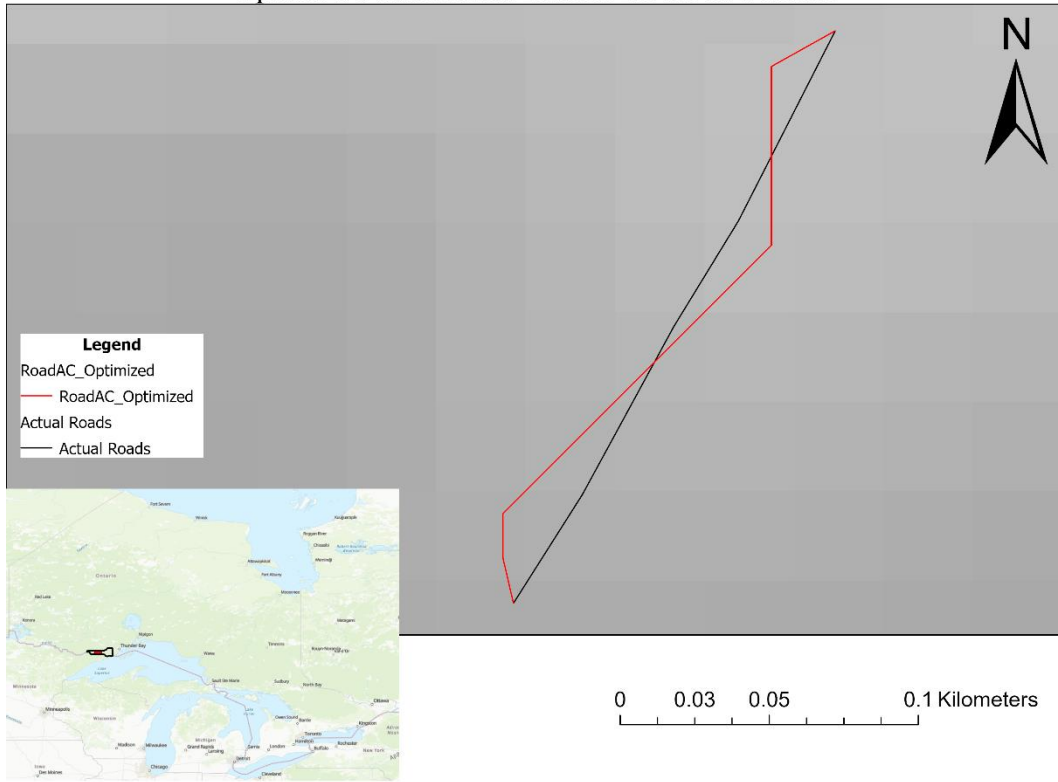

Optimized and Actual Routes for Road Pair D
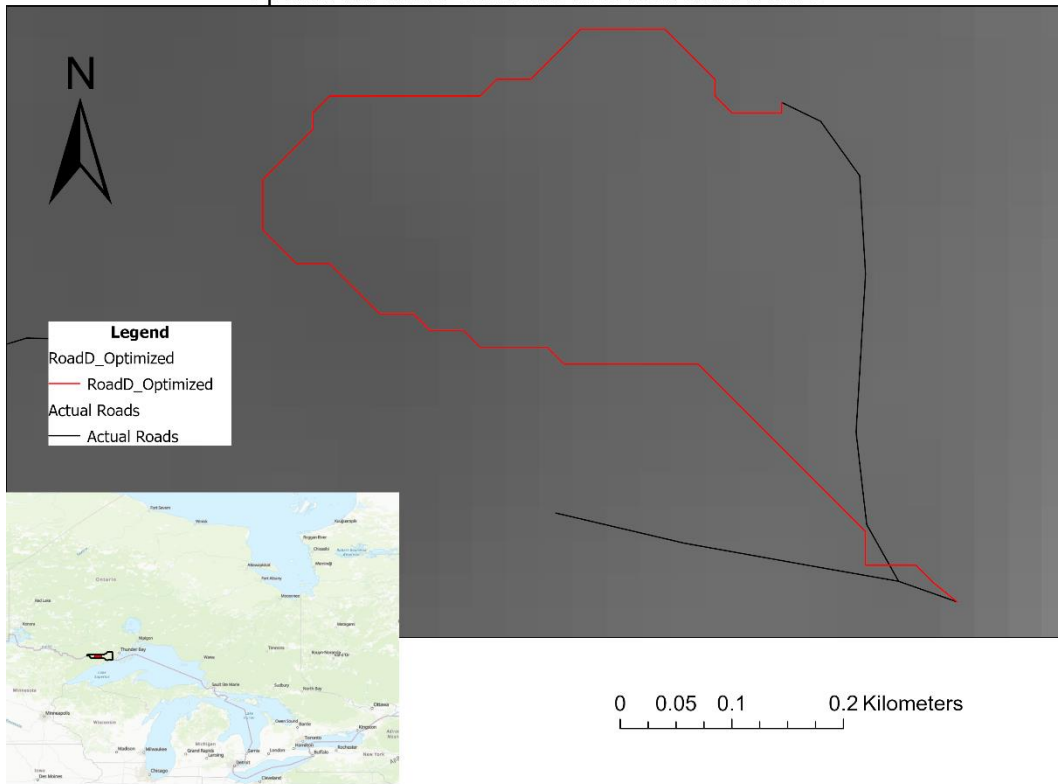
Optimized and Actual Routes for Road Pair E
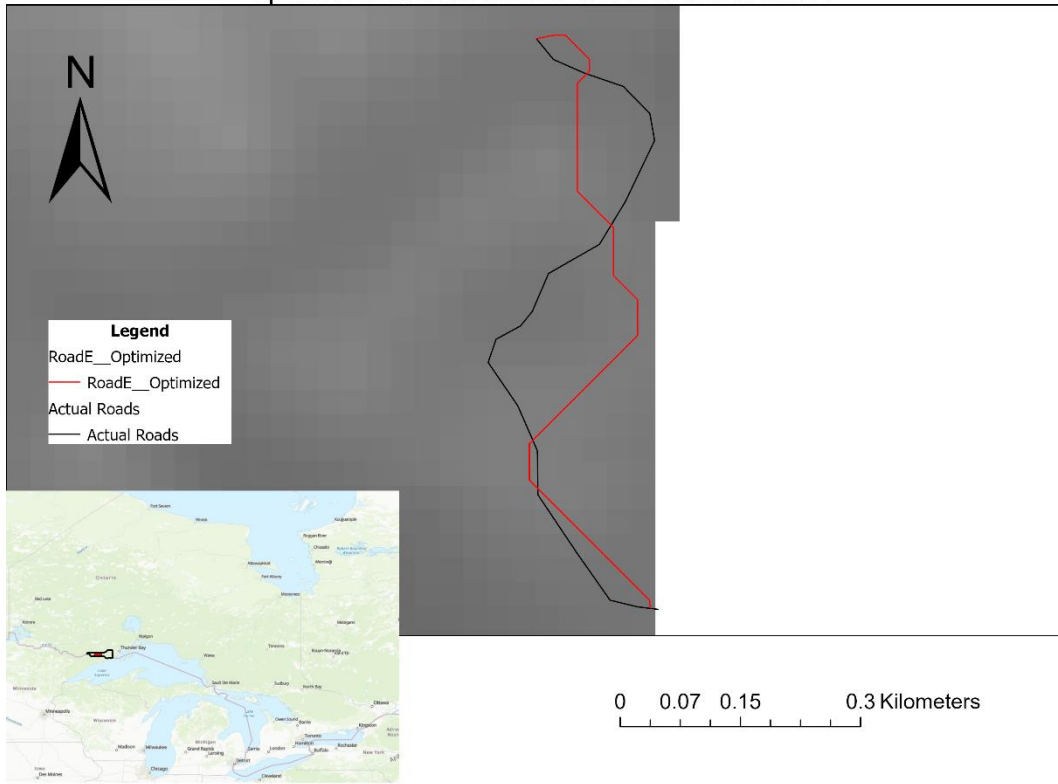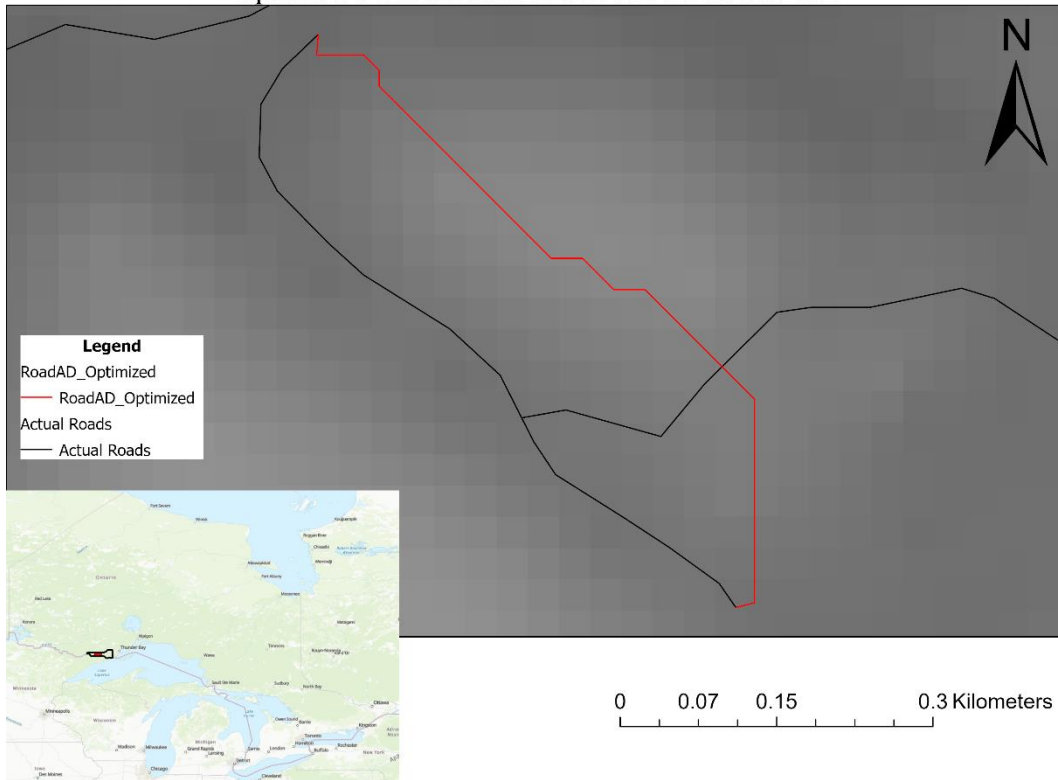

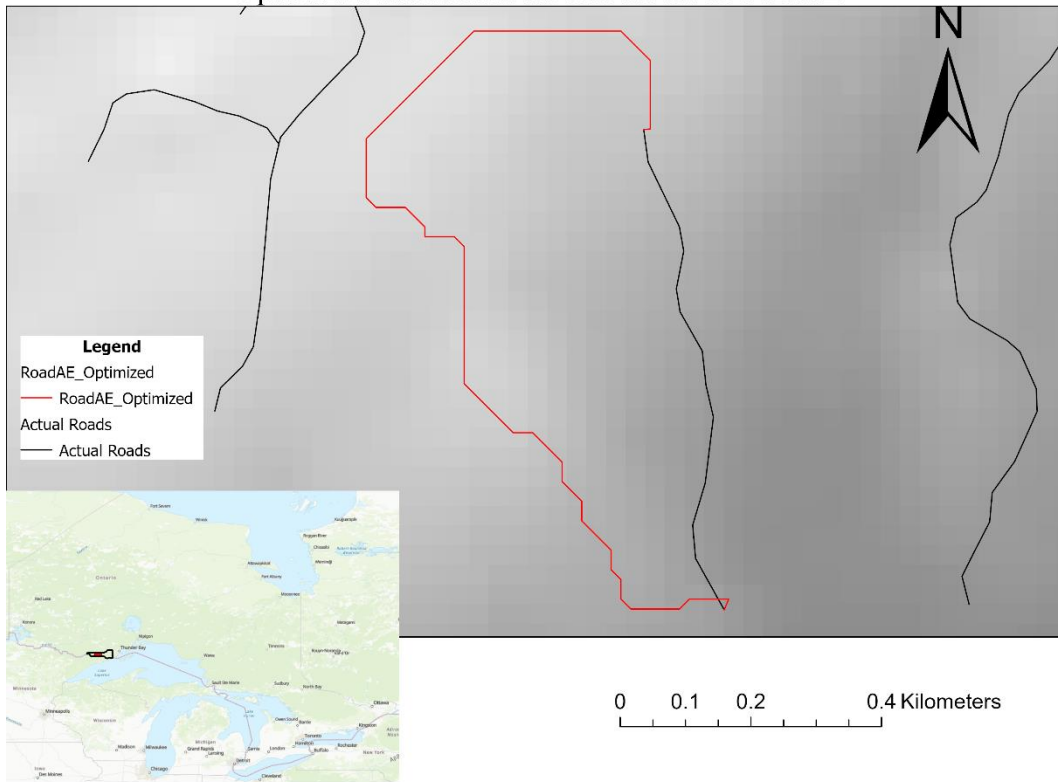## Optimized and Actual Routes for Road Pair E

Optimized and Actual Routes for Road Pair G
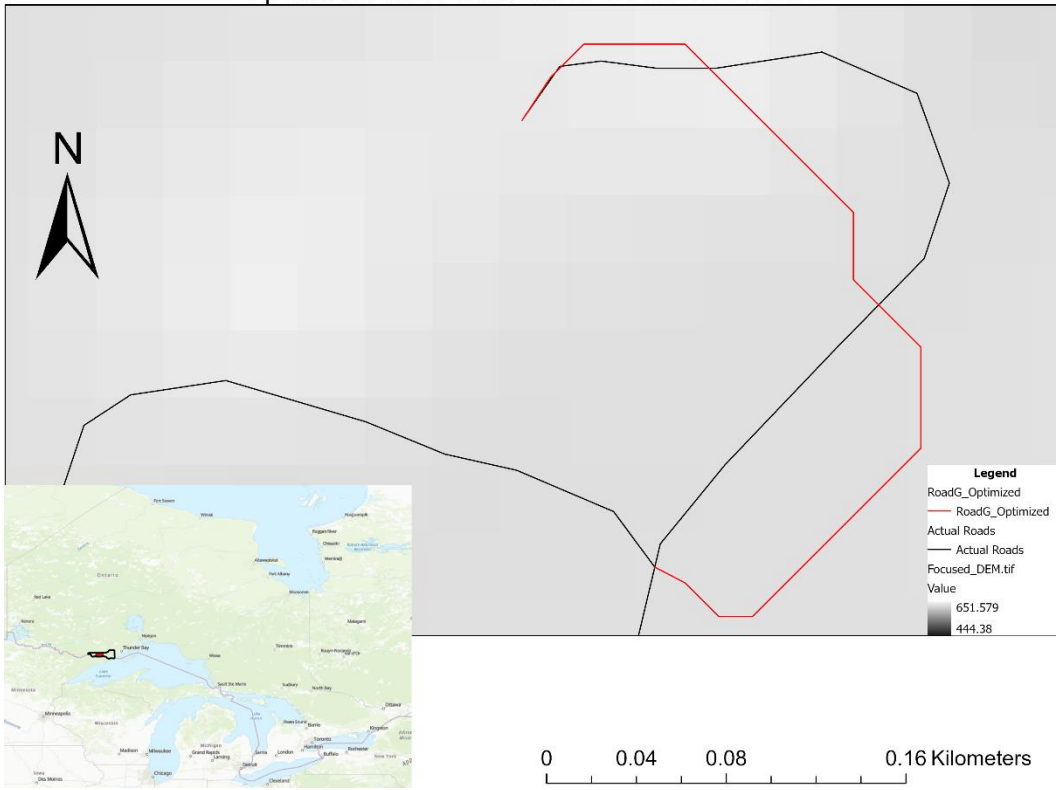
Optimized and Actual Routes for Road Pair H
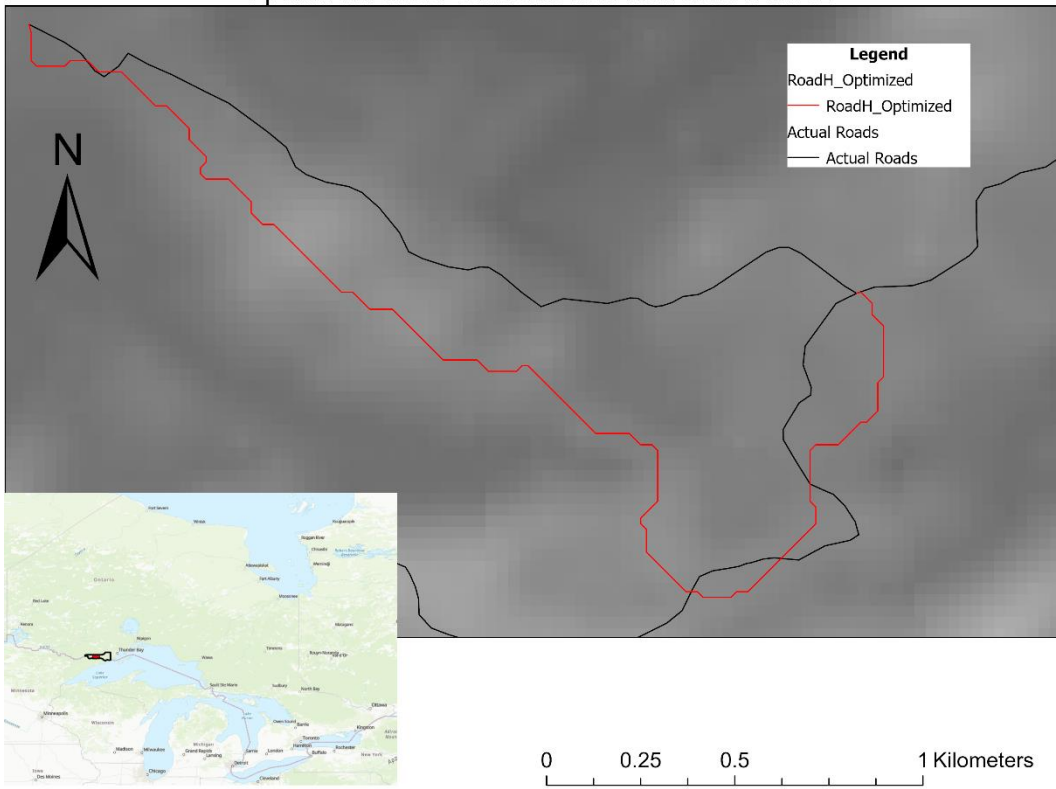
Optimized and Actual Routes for Road Pair I
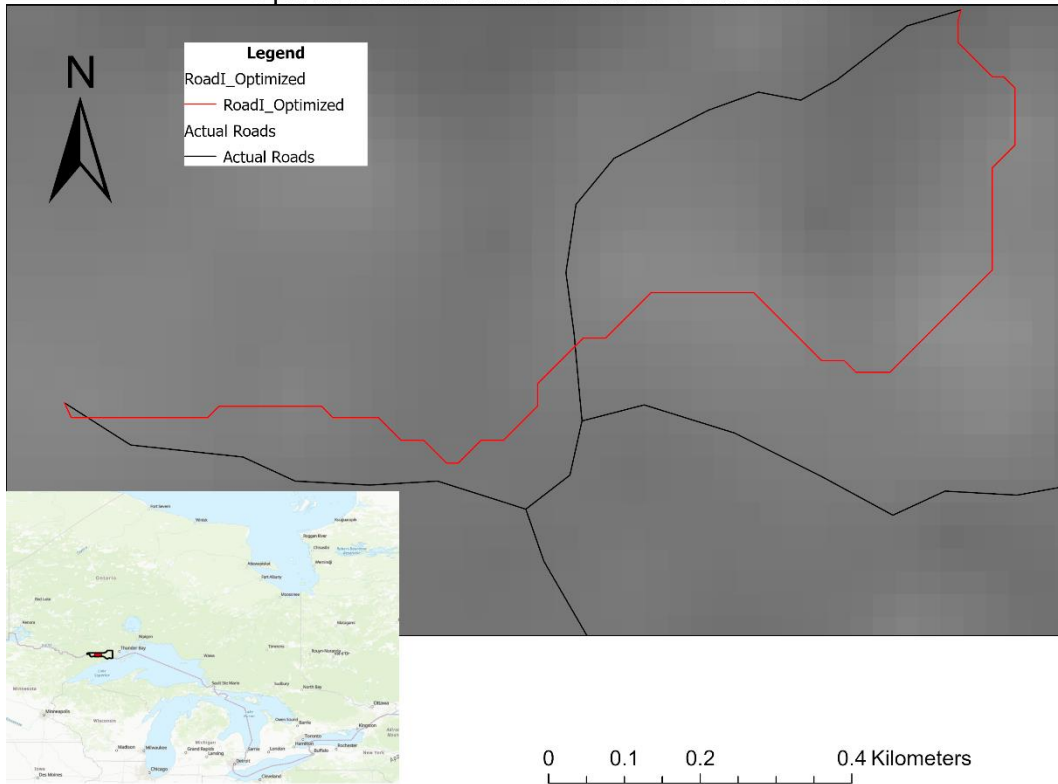
Optimized and Actual Routes for Road Pair J
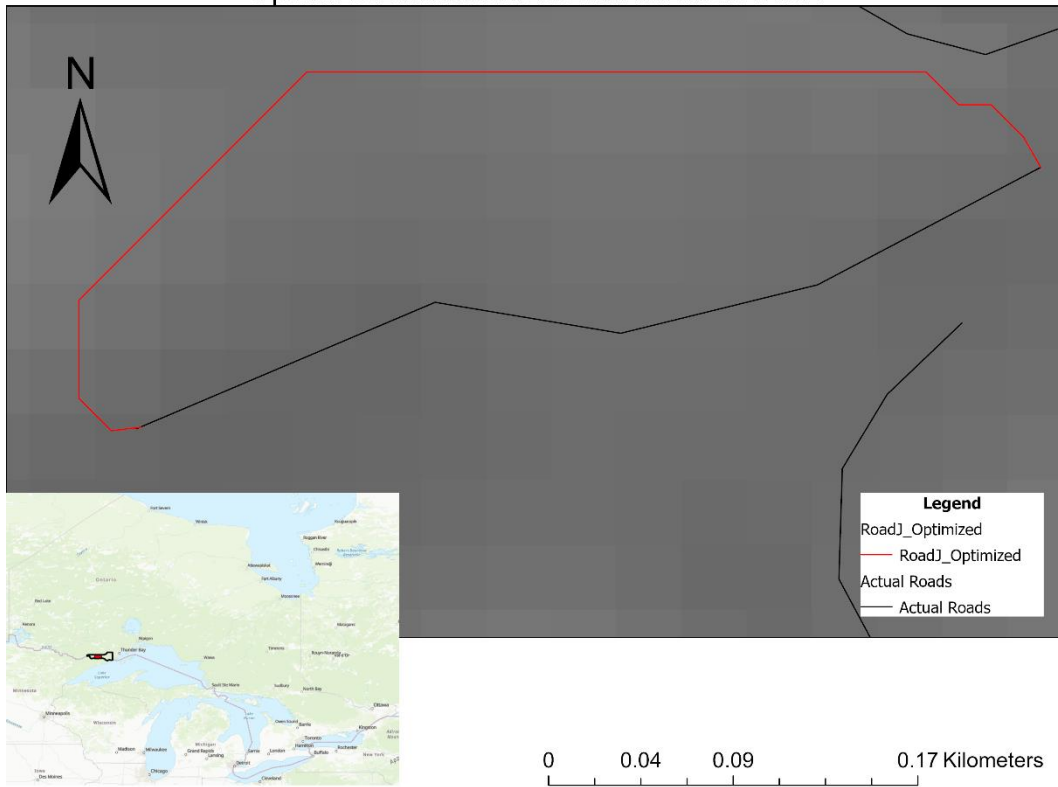
Optimized and Actual Routes for Road Pair K
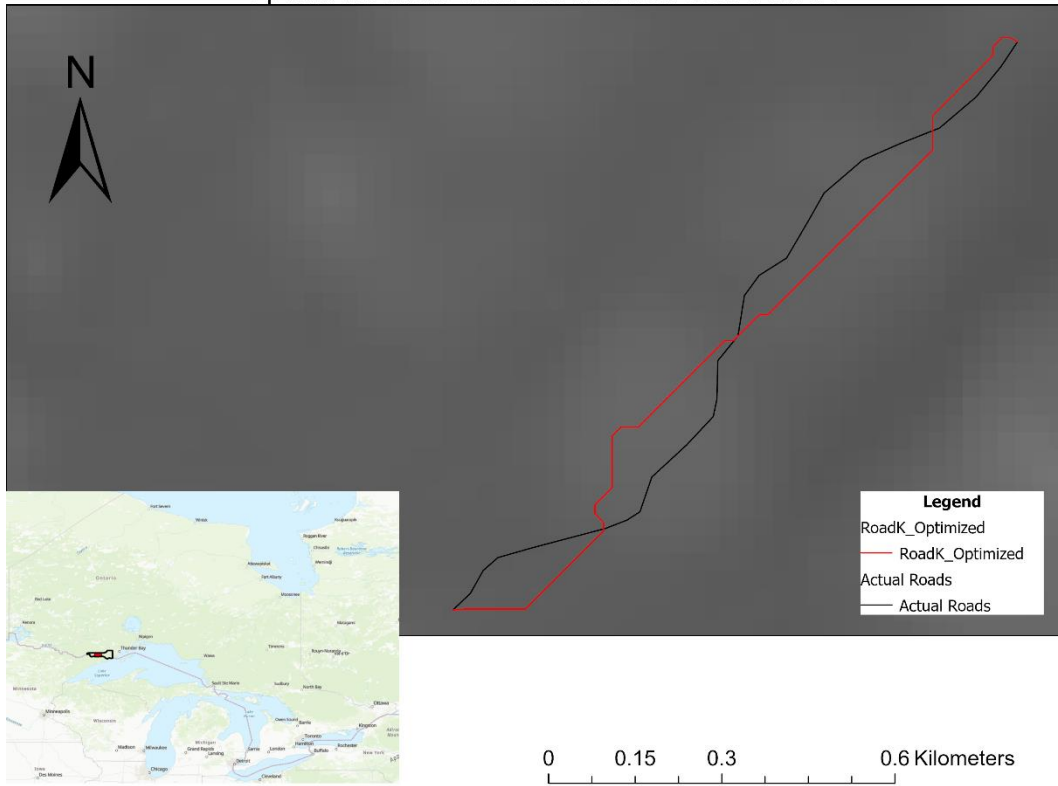
Optimized and Actual Routes for Road Pair L
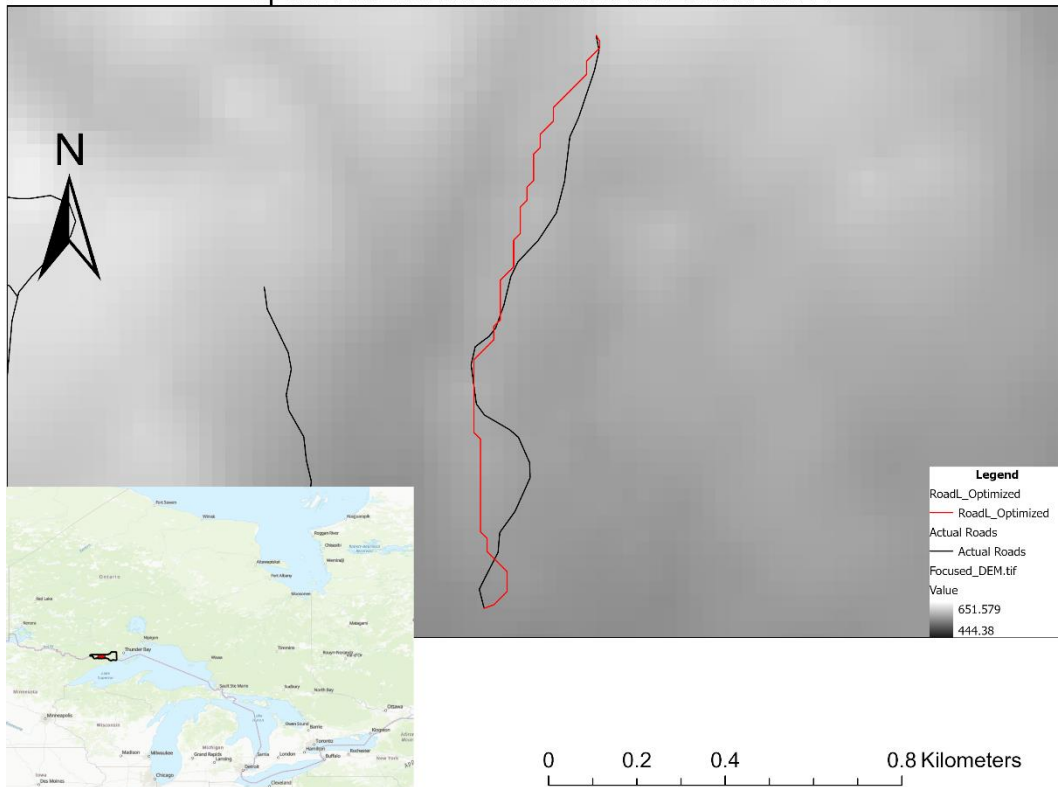
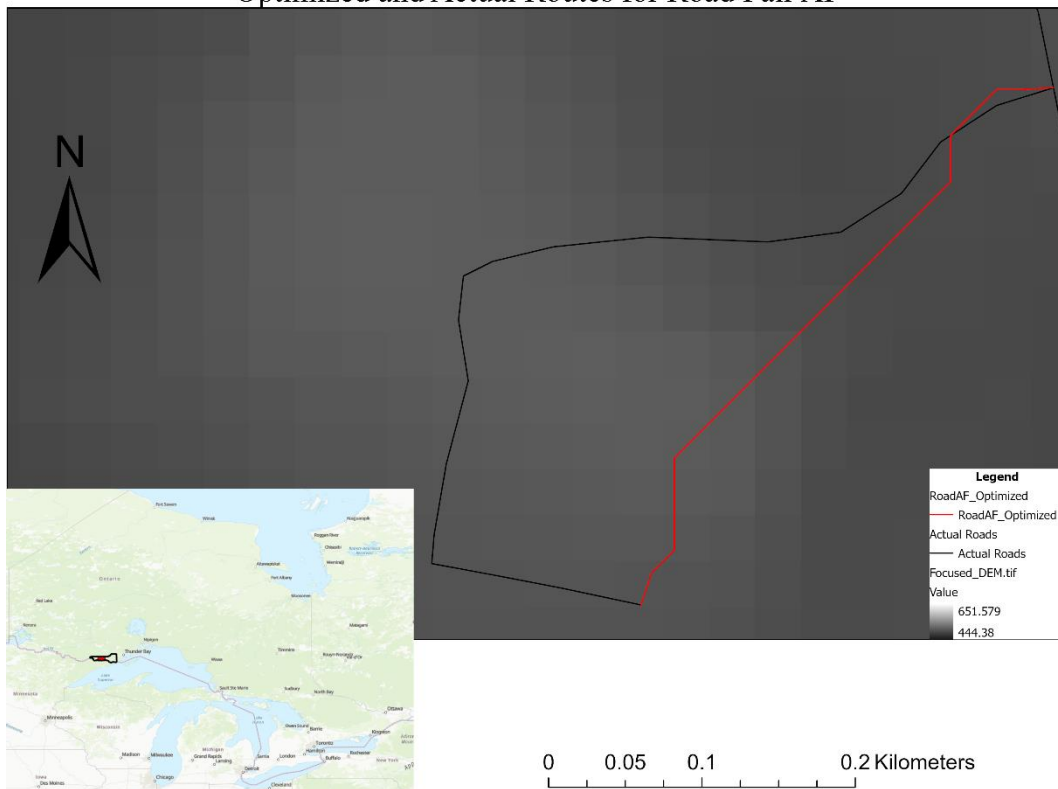Optimized and Actual Routes for Road Pair M
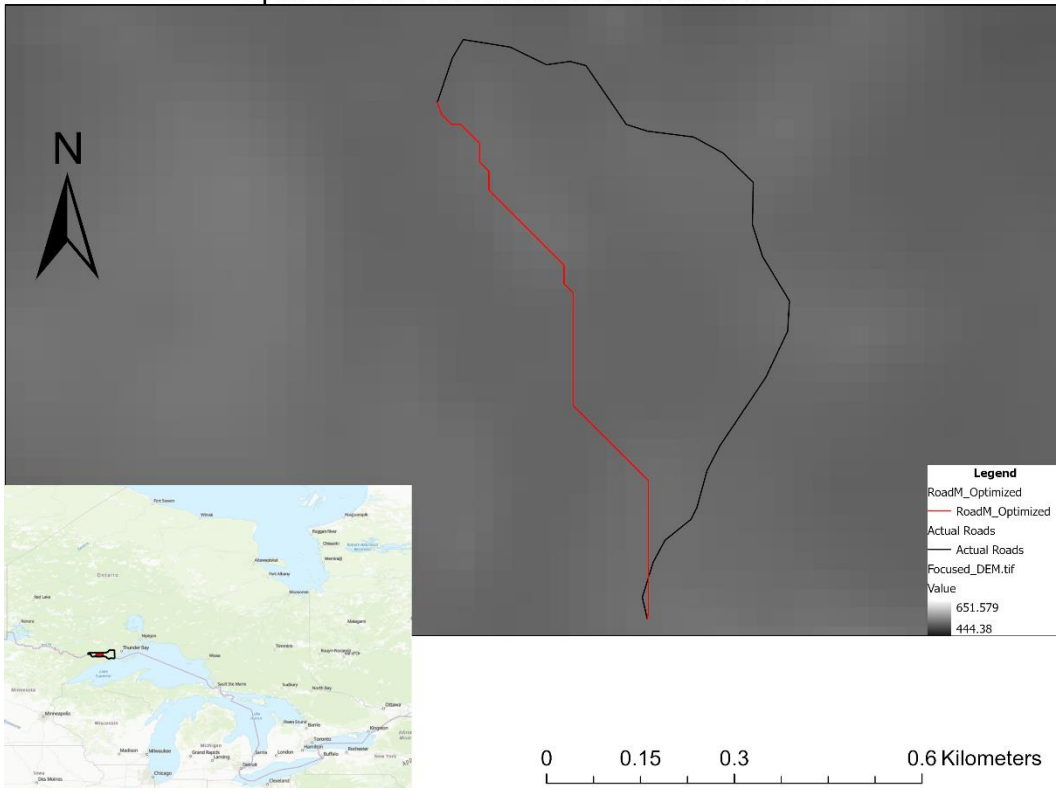
Optimized and Actual Routes for Road Pair N
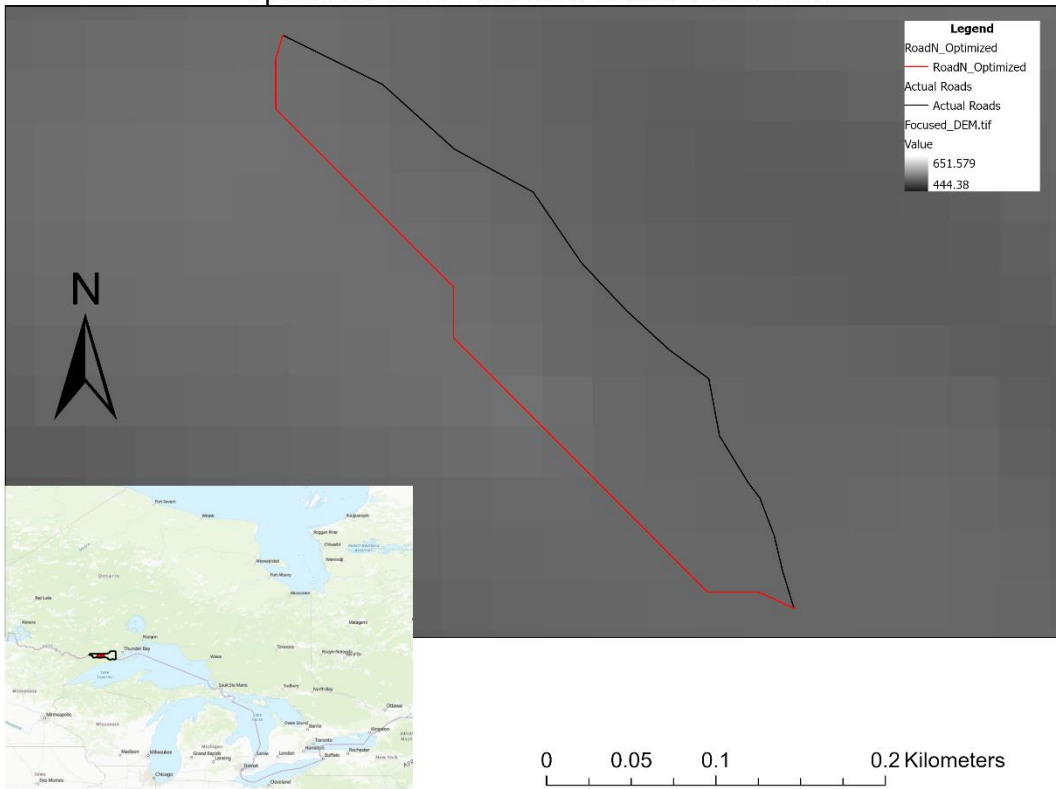
Optimized and Actual Routes for Road Pair O
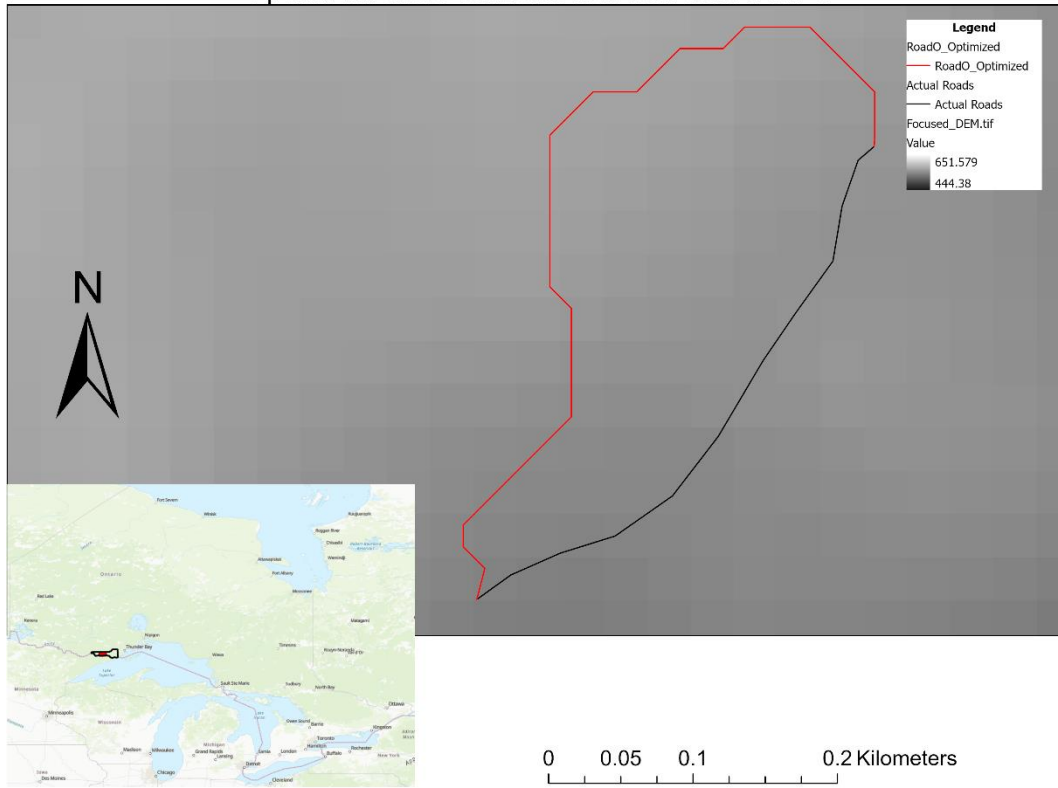
Optimized and Actual Routes for Road Pair P
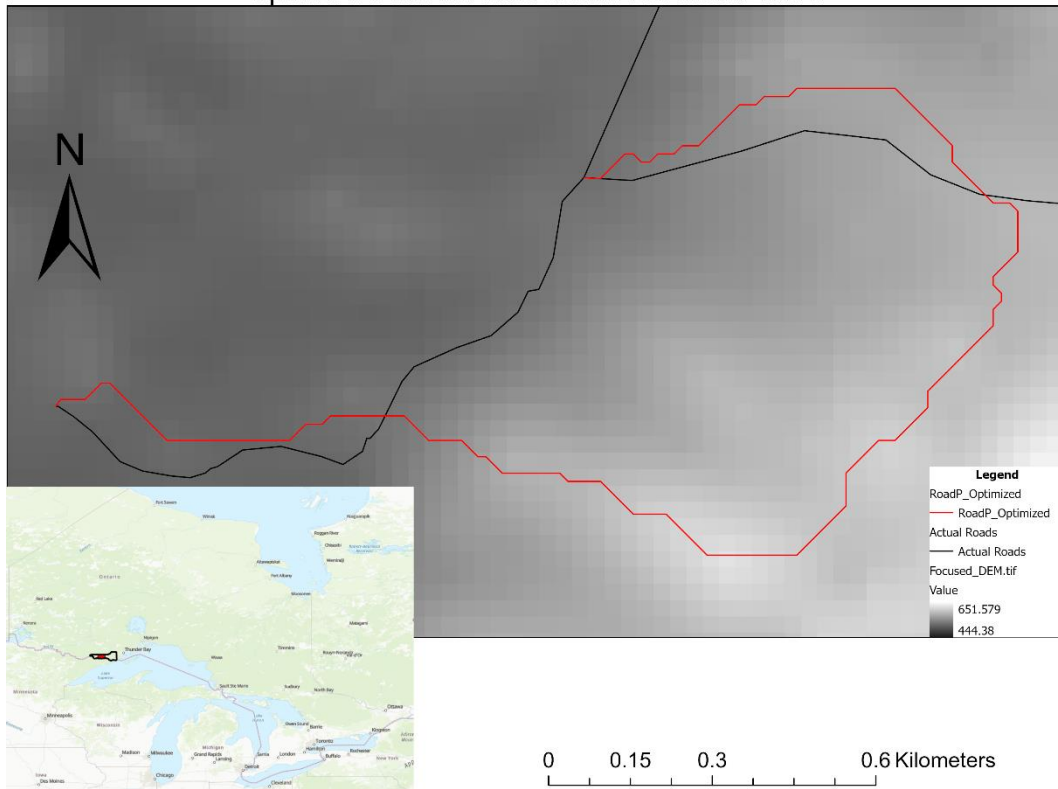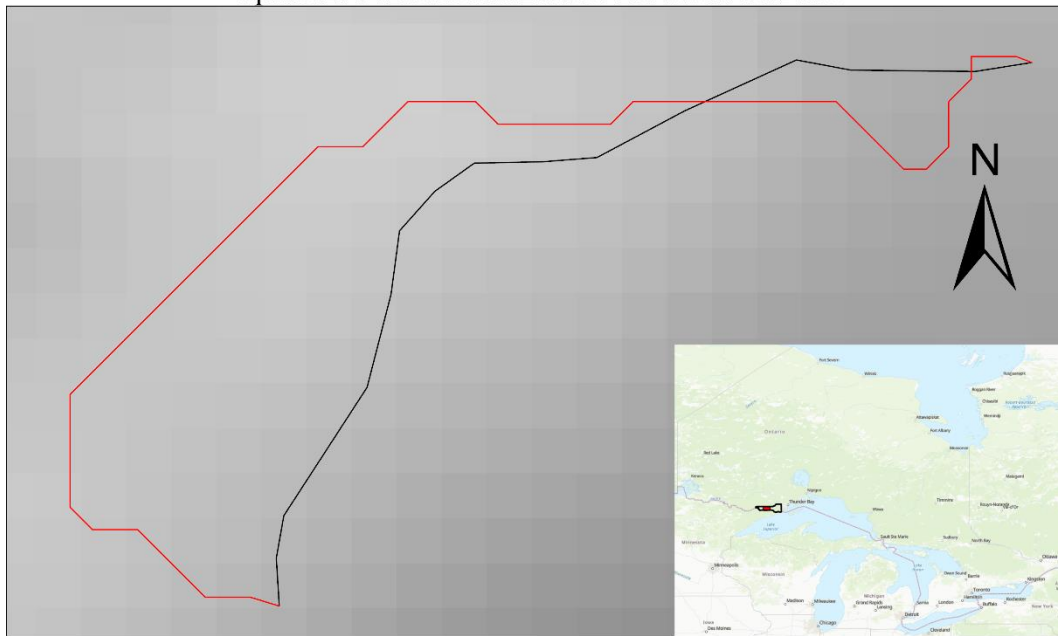
Optimized and Actual Routes for Road Pair Q
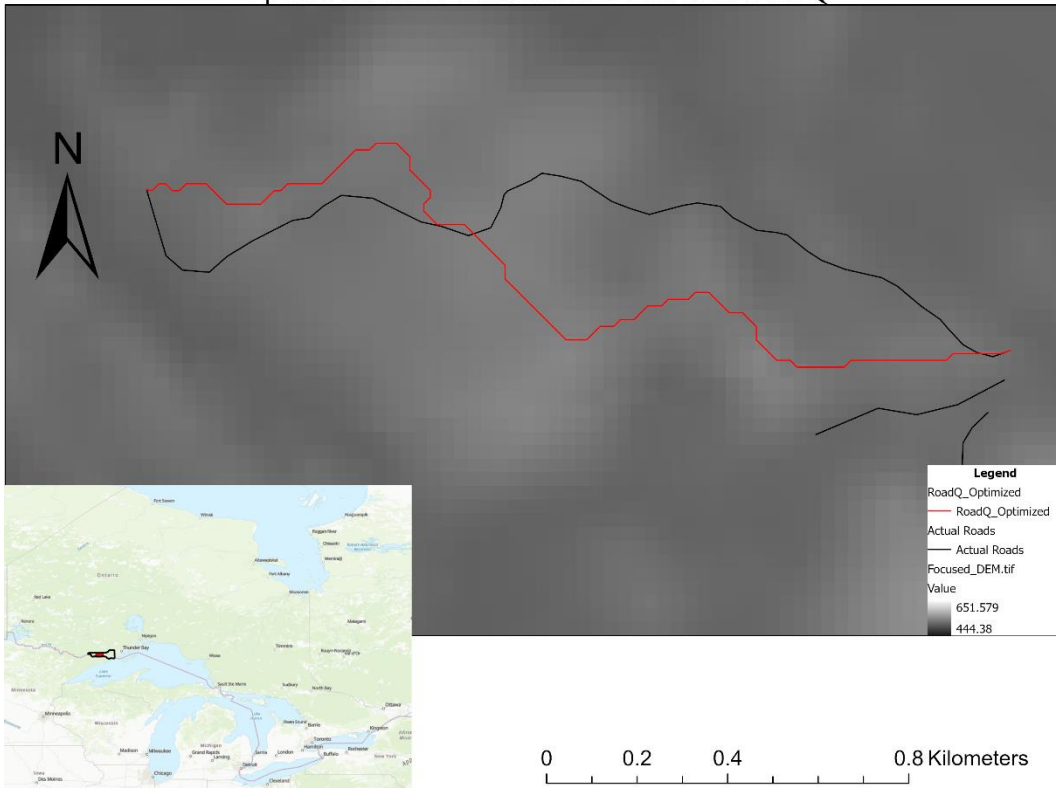
Optimized and Actual Routes for Road Pair R
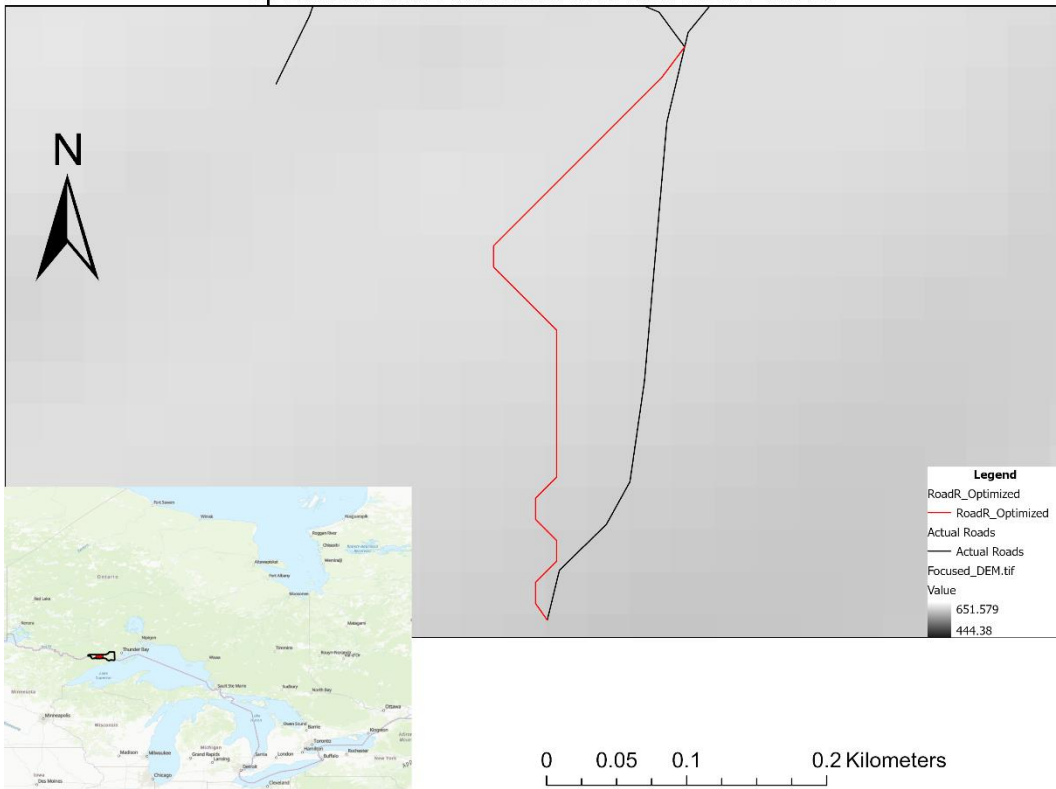
Optimized and Actual Routes for Road Pair S
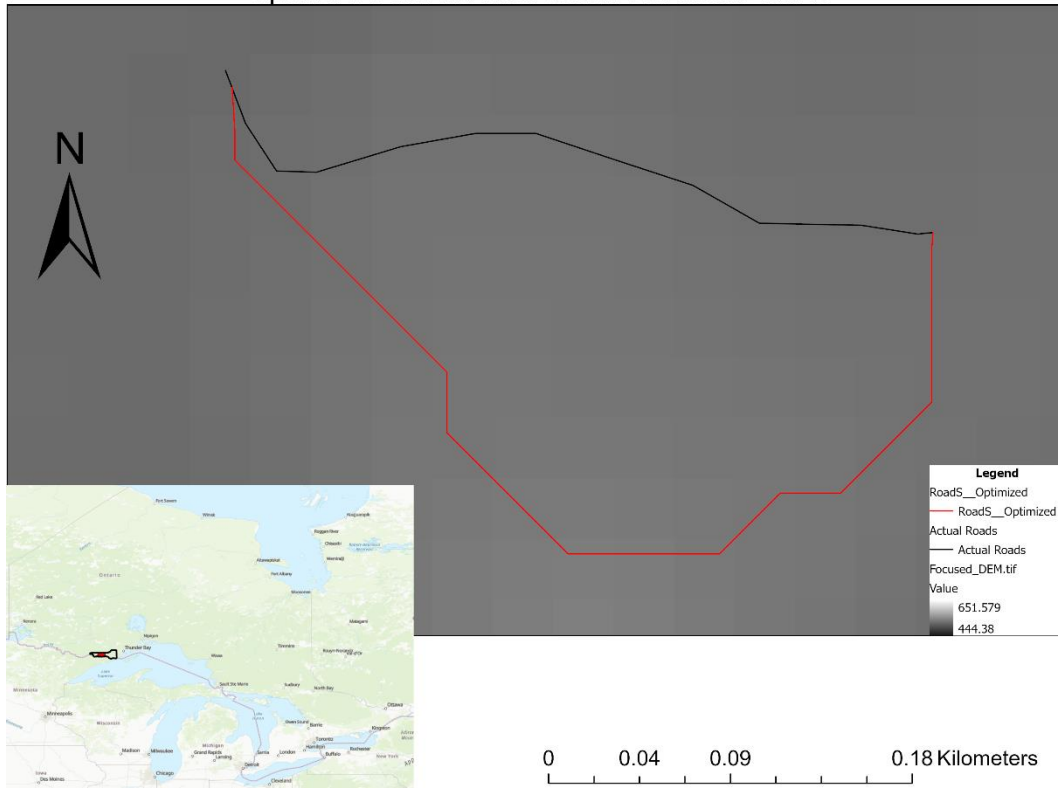
Optimized and Actual Routes for Road Pair T
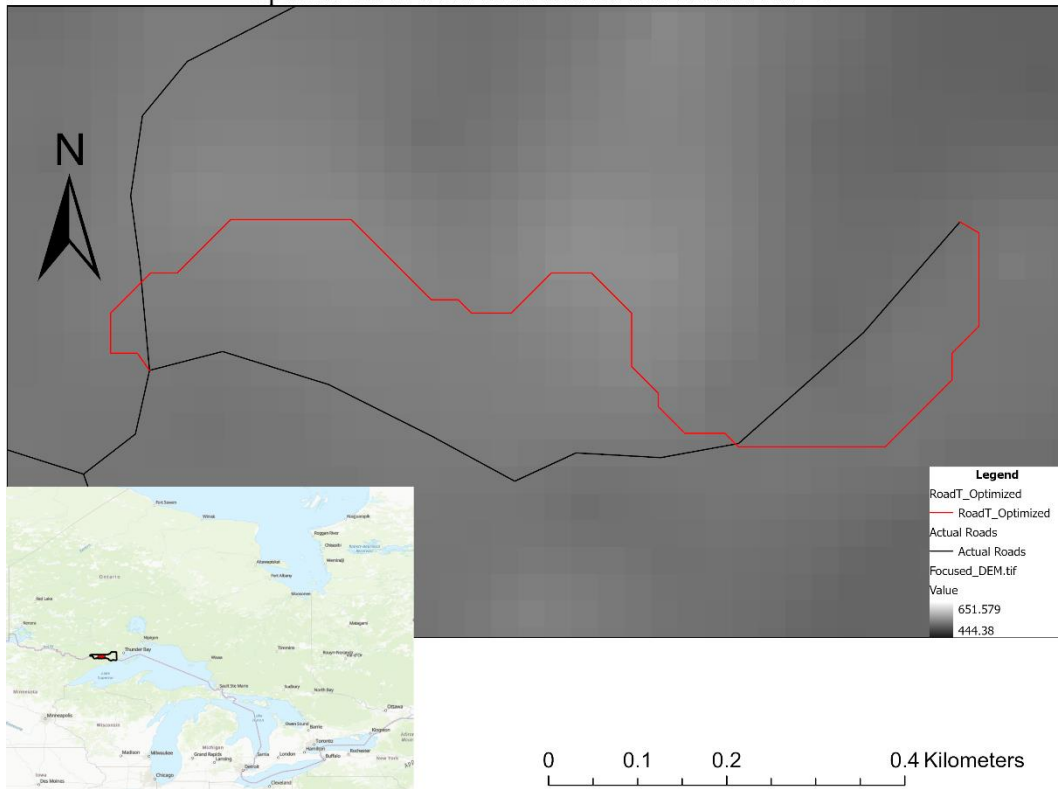
Optimized and Actual Routes for Road Pair U
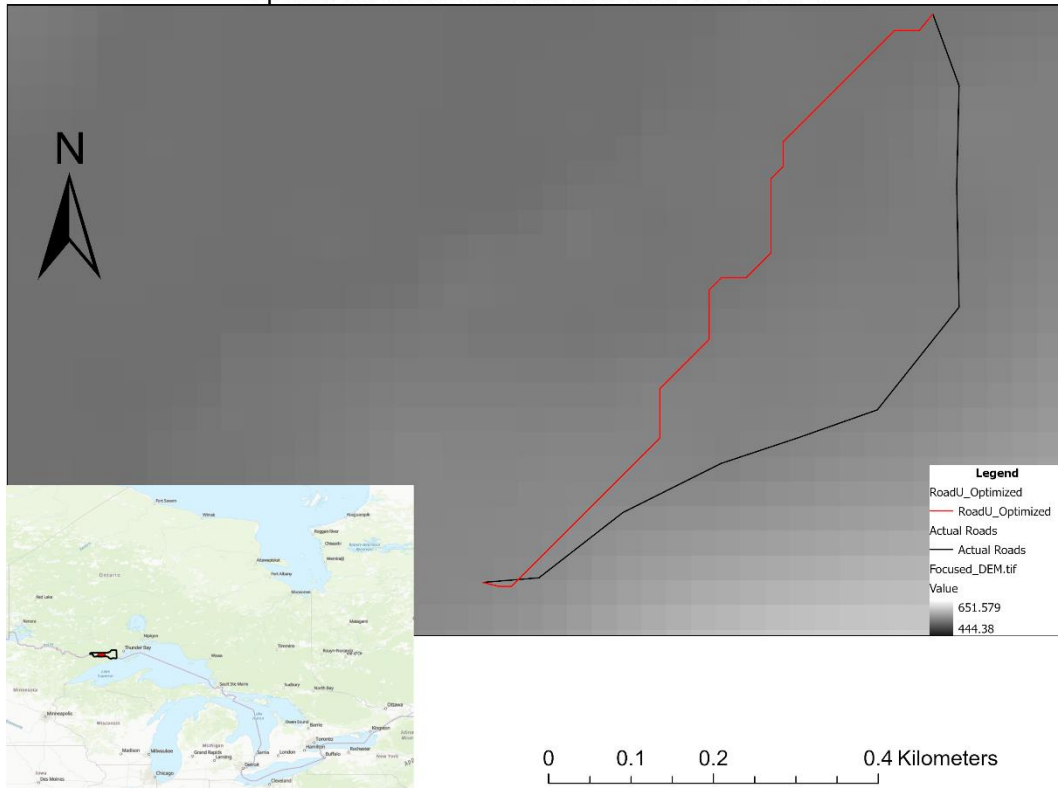
Optimized and Actual Routes for Road Pair V
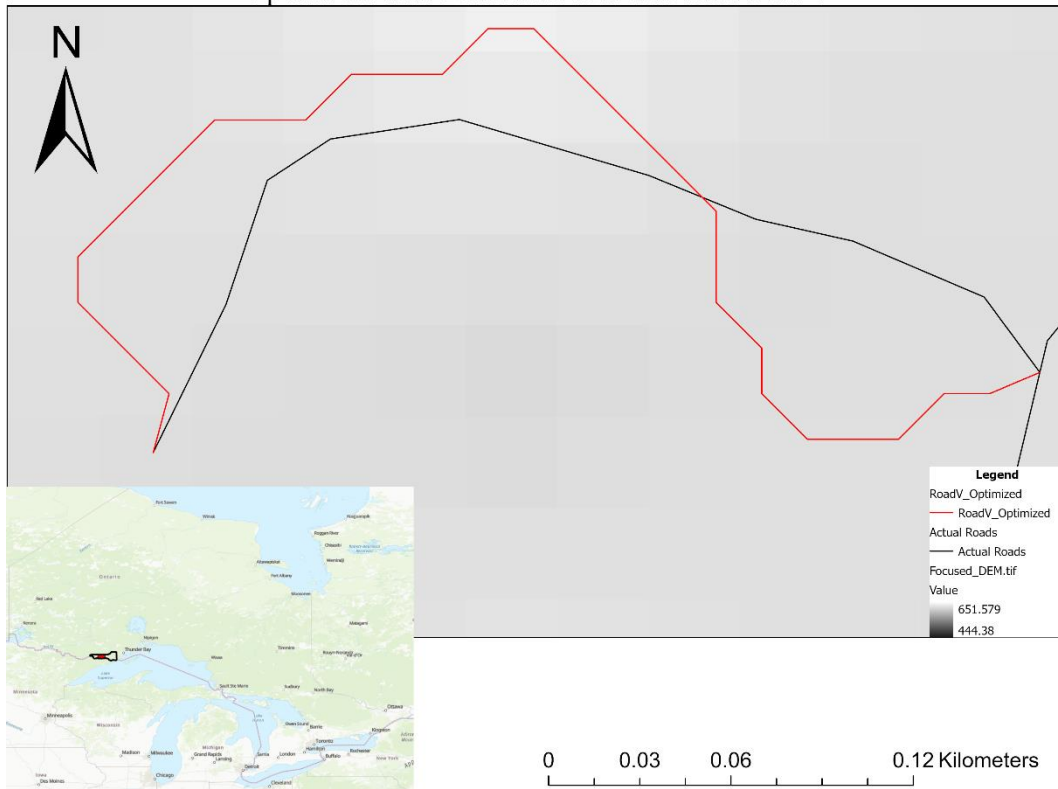
Optimized and Actual Routes for Road Pair W
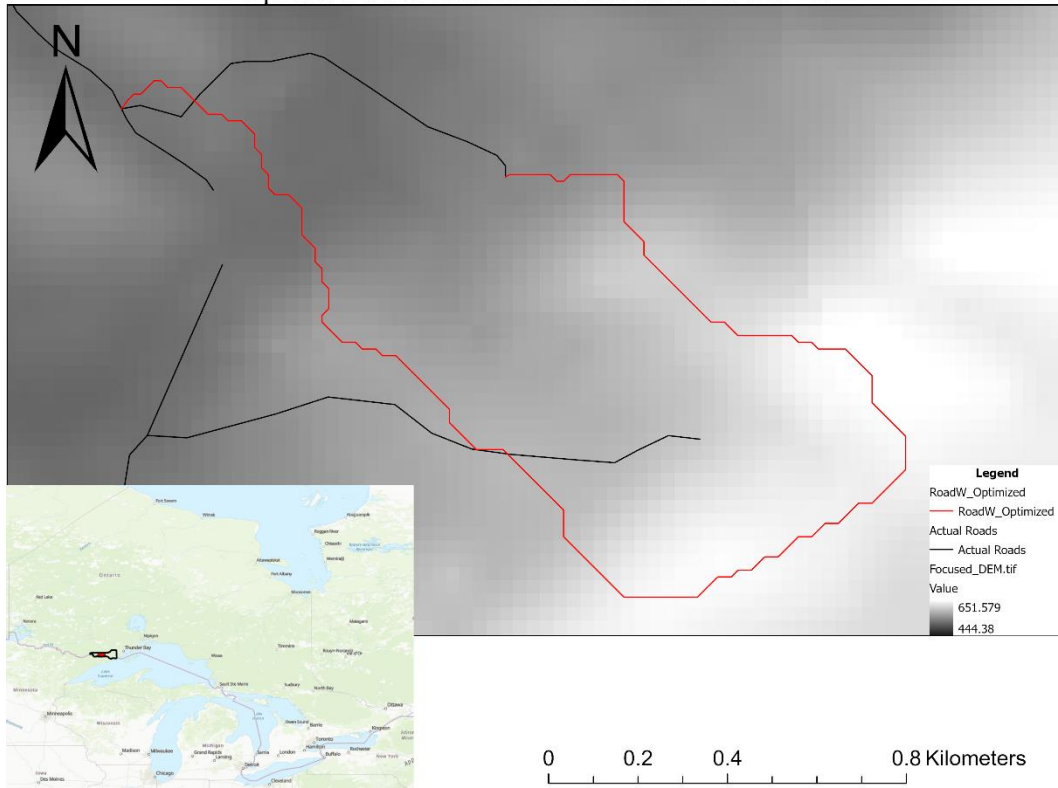
Optimized and Actual Routes for Road Pair X
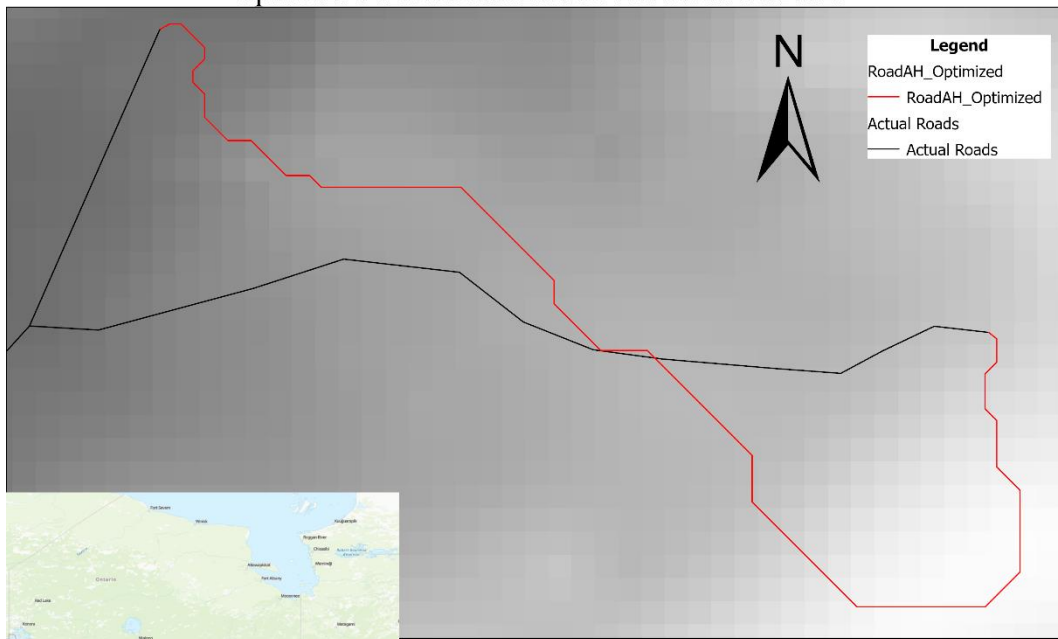
Optimized and Actual Routes for Road Pair Y

Legend

RoadY__Optimized
— RoadY__Optimized

Actual Roads
— Actual Roads

Focused_DEM.tif
Value
651.579
444.38

0   0.2   0.4   0.8 Kilometers

Optimized and Actual Routes for Road Pair Z

Legend

RoadZ_Optimized
— RoadZ_Optimized

Actual Roads
— Actual Roads

Focused_DEM.tif
Value
651.579
444.38

0   0.05   0.1   0.2 Kilometers

Optimized and Actual Routes for Road Pair AA
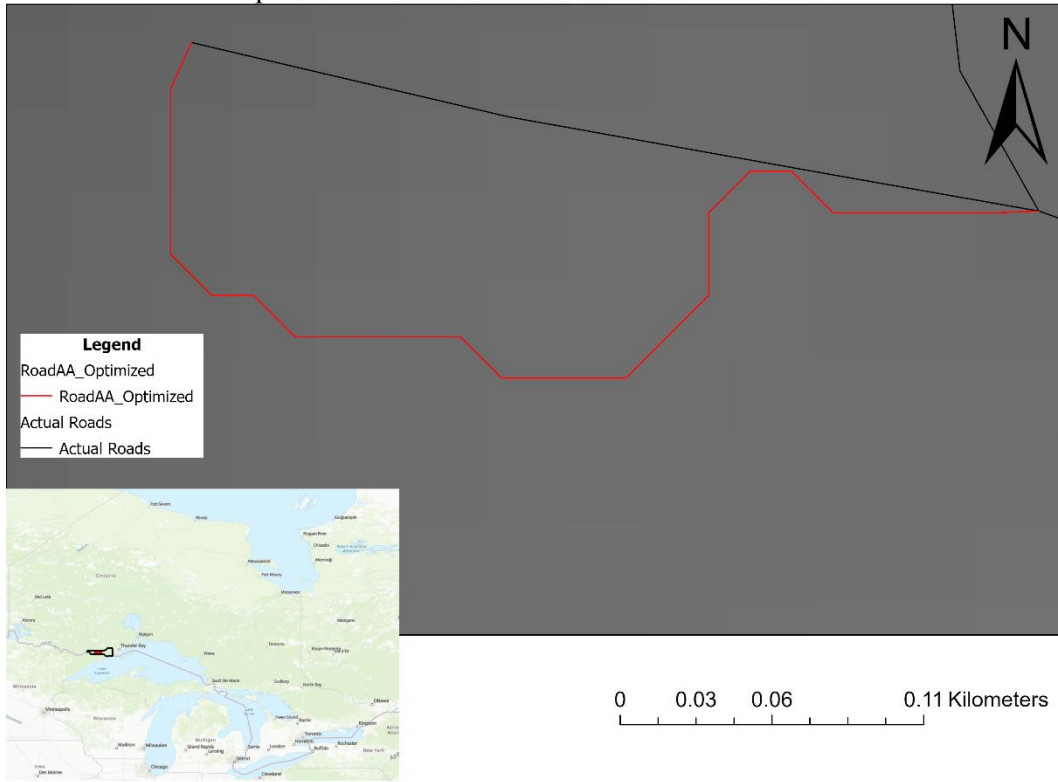
Optimized and Actual Routes for Road Pair AB
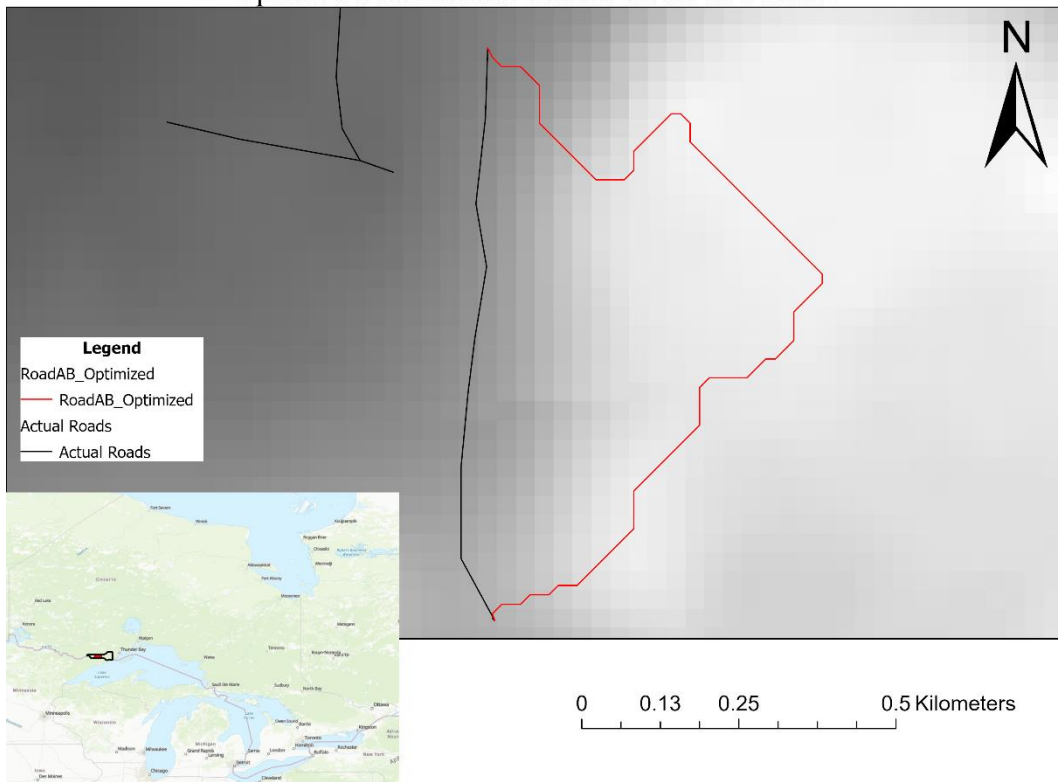
Optimized and Actual Routes for Road Pair AC
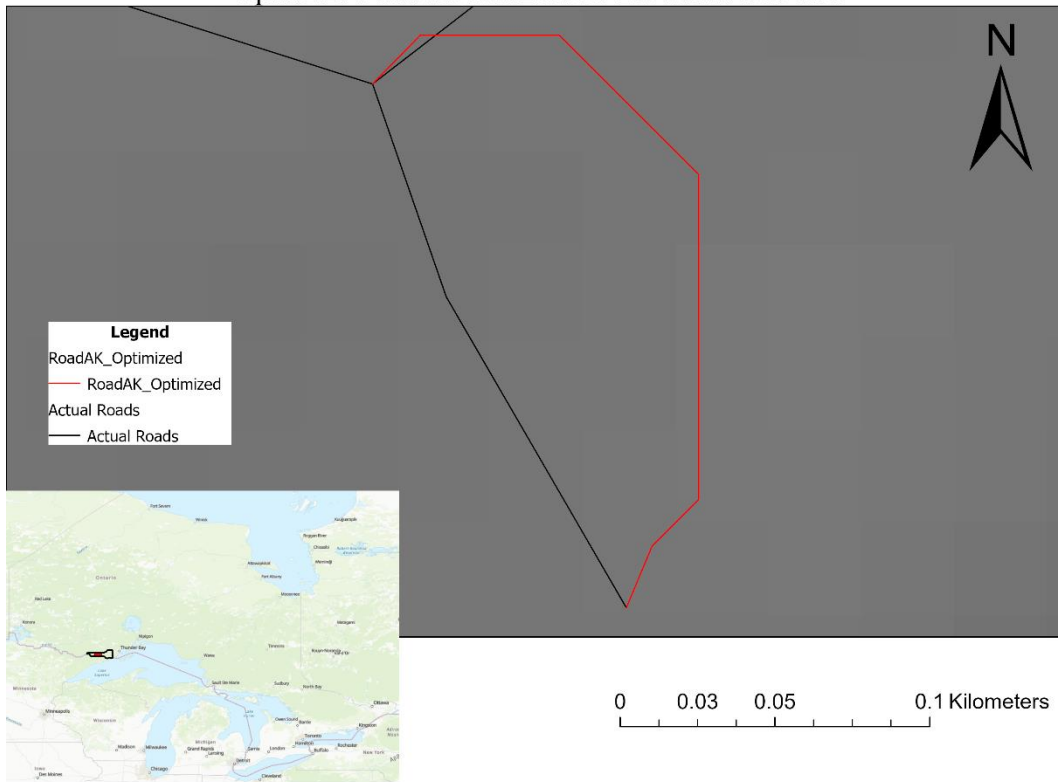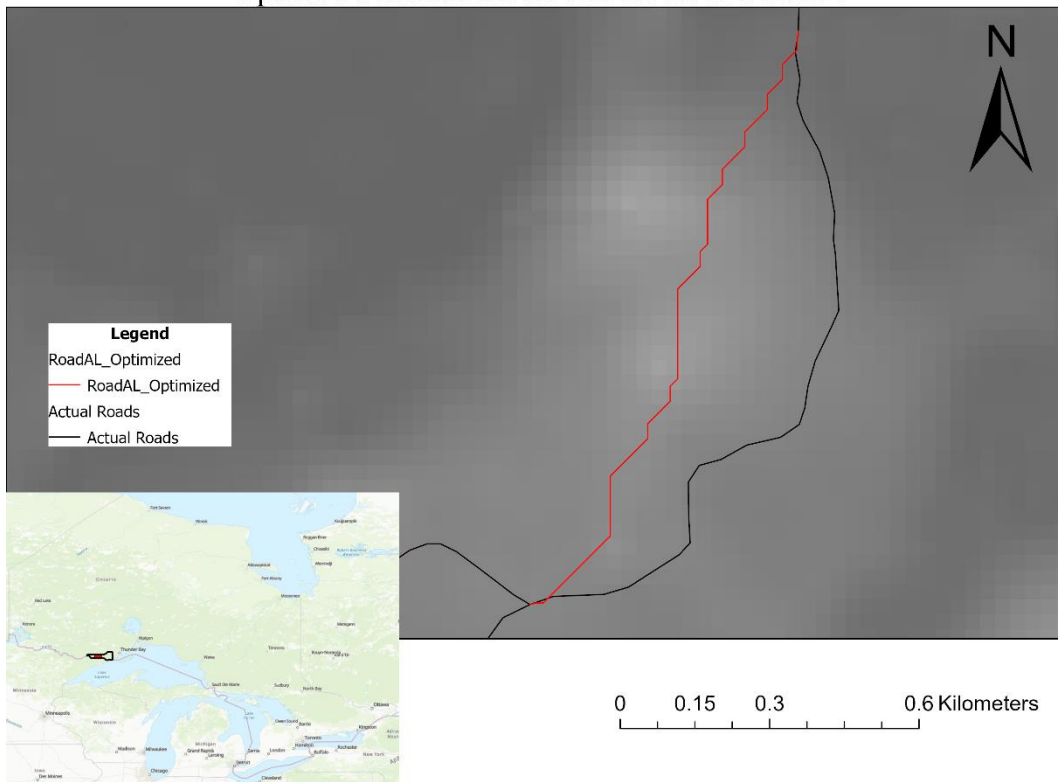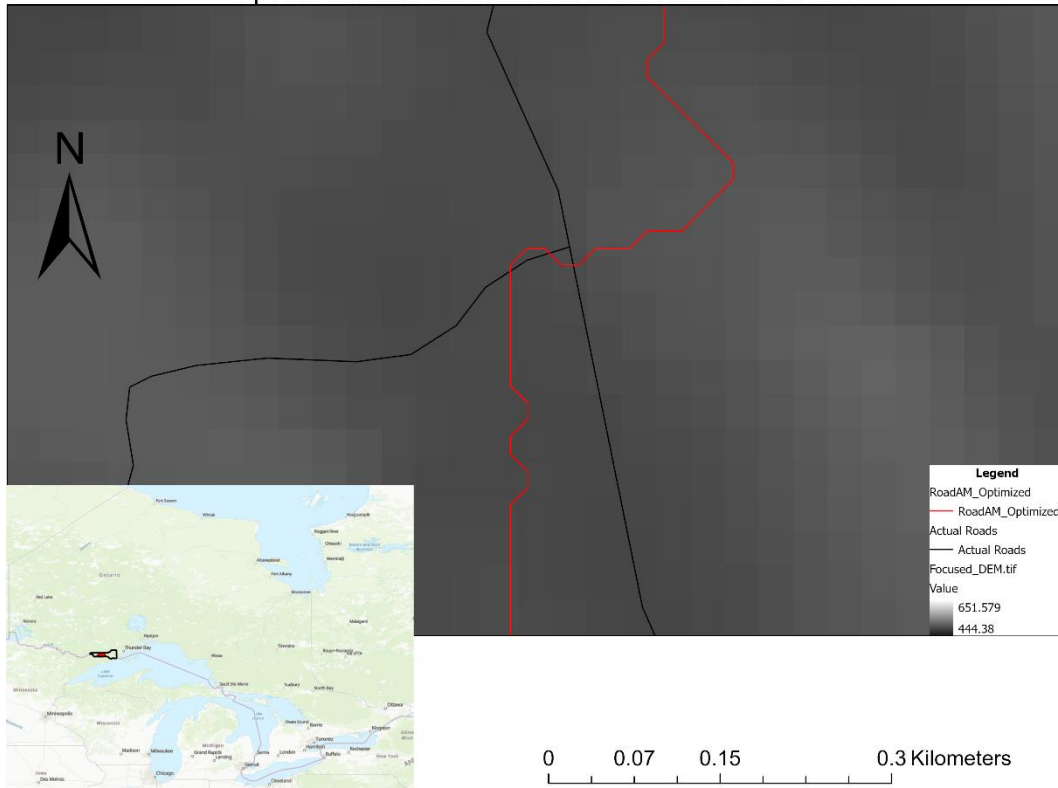

Optimized and Actual Routes for Road Pair AD

Optimized and Actual Routes for Road Pair AE

Optimized and Actual Routes for Road Pair AF

Optimized and Actual Routes for Road Pair AG

Legend

RoadAG_Optimized
— RoadAG_Optimized
Actual Roads
— Actual Roads

0   0.05   0.1   0.2 Kilometers

Optimized and Actual Routes for Road Pair AH

Legend

RoadAH_Optimized
— RoadAH_Optimized
Actual Roads
— Actual Roads

0   0.1   0.2   0.4 Kilometers

Optimized and Actual Routes for Road Pair AI
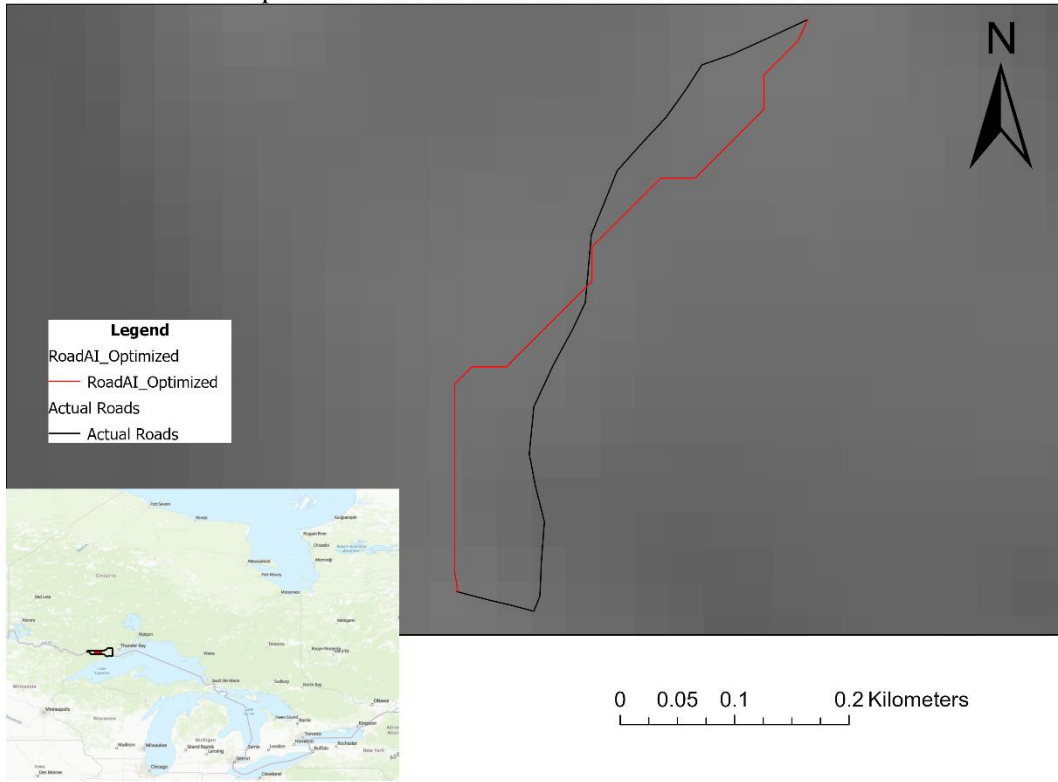
Optimized and Actual Routes for Road Pair AJ
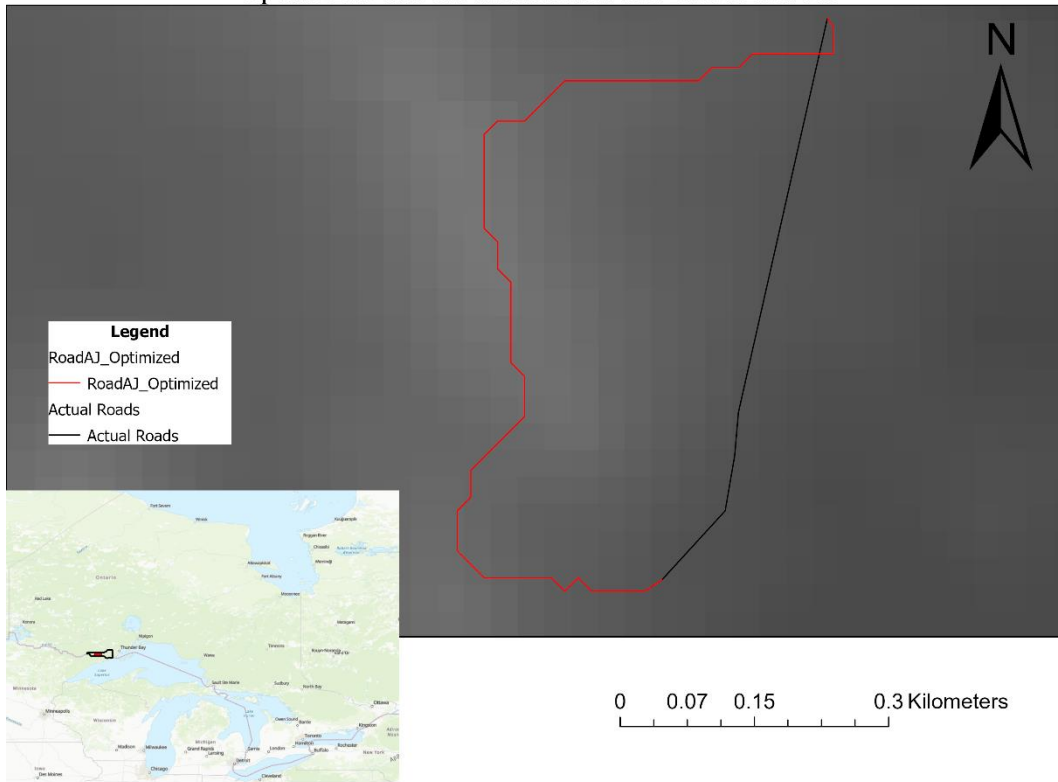
Optimized and Actual Routes for Road Pair AK

Optimized and Actual Routes for Road Pair AL

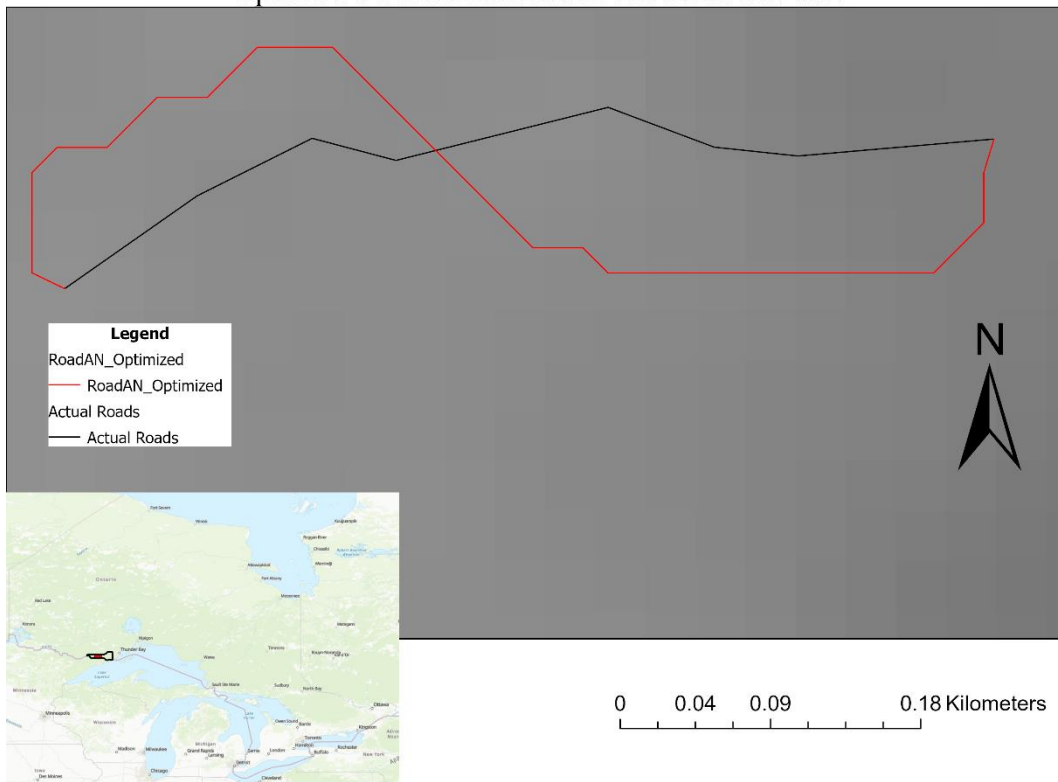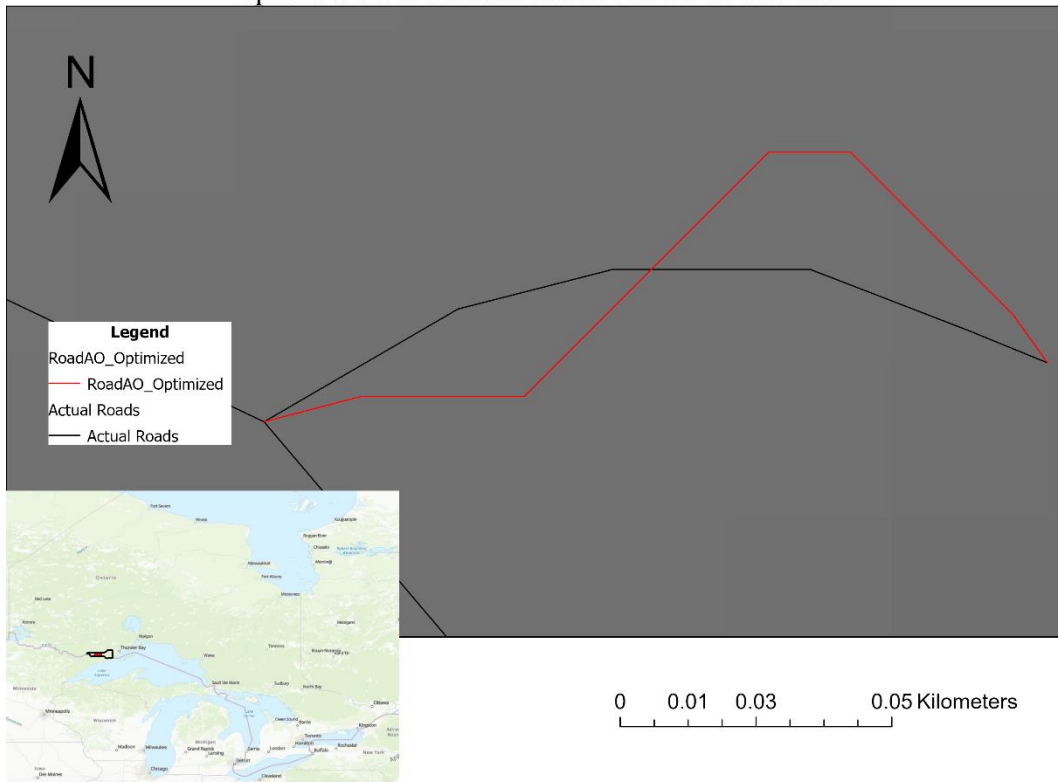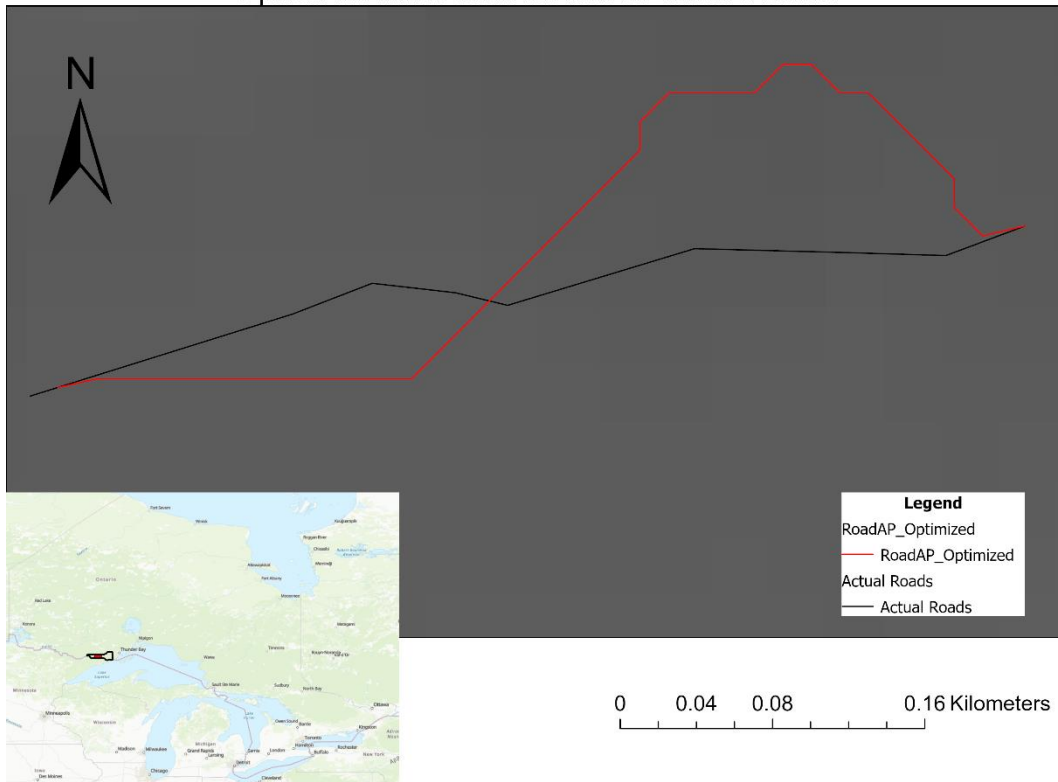## Optimized and Actual Routes for Road Pair AM

Optimized and Actual Routes for Road Pair AN

Optimized and Actual Routes for Road Pair AO

Optimized and Actual Routes for Road Pair AP

Appendix V: Sampled Point Count by Road

Road Name	# of Points
A	38
AA	5
AB	12
AC	3
AD	9
AE	9
AF	6
AG	12
AH	27
AI	9
AJ	13
AK	4
AL	19
AM	14
AN	11
AO	3
AP	7
B	52
C	25
D	15
E	12
F	16
G	6
H	40
I	21
J	11
K	19
L	16
M	12
N	7
O	9
P	35
Q	28
R	6
S	8
T	18
U	12
V	7
W	41
X	23
Y	43
Z	10